



Durham E-Theses

Extracting MS from experiment

Reader, Matthew Thomas

How to cite:

Reader, Matthew Thomas (1994) *Extracting MS from experiment*, Durham theses, Durham University. Available at Durham E-Theses Online: <http://etheses.dur.ac.uk/5363/>

Use policy

The full-text may be used and/or reproduced, and given to third parties in any format or medium, without prior permission or charge, for personal research or study, educational, or not-for-profit purposes provided that:

- a full bibliographic reference is made to the original source
- a [link](#) is made to the metadata record in Durham E-Theses
- the full-text is not changed in any way

The full-text must not be sold in any format or medium without the formal permission of the copyright holders.

Please consult the [full Durham E-Theses policy](#) for further details.

Extracting
 $\Lambda_{\overline{MS}}$
From Experiment

Matthew Thomas Reader
Department of Physics
University of Durham

The copyright of this thesis rests with the author.
No quotation from it should be published without
his prior written consent and information derived
from it should be acknowledged.

A thesis submitted to the University of Durham
for the Degree of Doctor of Philosophy
March 1994



10 AUG 1994

Acknowledgements

Firstly, I would like to wholeheartedly thank Chris Maxwell for his supervision and patience over the last three years.

Thanks also go to Nigel Glover and to Mike Pennington for their help and guidance throughout my time here in Durham.

I would like to extend my gratitude to Andrew Morgan and Mark Oakden (in alphabetical order) for being great friends and putting up with me in the confined space of room 301.

I am grateful to SERC for financing this research.

Finally, I am indebted to my parents and to my fiancée, Heather, for their continued support and encouragement. Hence, I would like to dedicate this Ph.D. thesis to them.

Declaration

I declare that no material in this thesis has previously been submitted for a degree at this or any other university.

All the research in this thesis has been carried out in collaboration with Dr. C.J.Maxwell, part of which has appeared in the paper

“Extracting $\Lambda_{\overline{MS}}$ from Experiment”, D.T.Barclay, C.J.Maxwell, and M.T.Reader, Phys.Rev. **D49** (1994).

“The artist is the creator of beautiful things.

To reveal art and conceal the artist is art’s aim. The critic is he who can translate into another manner or a new material his impression of beautiful things.

The highest, as the lowest, form of criticism is a mode of autobiography.

Those who find ugly meanings in beautiful things are corrupt without being charming. This is a fault.

Those who find beautiful meanings in beautiful things are the cultivated. For these there is hope. They are the elect to whom beautiful things mean only Beauty.

There is no such thing as a moral or an immoral book. Books are well written, or badly written. That is all.

The nineteenth century dislike of Realism is the rage of Caliban seeing his own face in a glass.

The nineteenth century dislike of Romanticism is the rage of Caliban not seeing his own face in a glass.

The moral life of man forms part of the subject-matter of the artist, but the morality of art consists in the perfect use of an imperfect medium.

No artist desires to prove anything. Even things that are true can be proved.

No artist has ethical sympathies. An ethical sympathy in an artist is an unpardonable mannerism of style.

No artist is ever morbid. The artist can express everything.

Thought and language are to the artist instruments of an art.

Vice and virtue are to the artist materials for an art. From the point of view of form, the type of all the arts is the art of the musician. From the point of view of feeling, the actor’s craft is the type.

All art is at once surface and symbol.

Those who go beneath the surface do so at their peril.

Those who read the symbol do so at their peril.

It is the spectator, and not life, that art really mirrors.

Diversity of opinion about a work of art shows that the work is now, complex, and vital.

When critics disagree the artist is in accord with himself.

We can forgive a man for making a useful thing as long as he does not admire it. The only excuse for making a useless thing is that one admires it intensely.

All art is quite useless.”

Oscar Wilde.

To Mum, Dad and Heather.

Contents

1 Particle Physics - An Introduction	3
1.1 Thesis Outline	5
2 Towards Renormalization	6
2.1 Gauge Theory	6
2.2 Quantization and Perturbation Theory	9
2.3 Calculating Observables	15
2.4 Everything is Infinite!!	16
2.5 Dimensional Transmutation	16
2.6 Renormalization	19
2.7 Extension to the Standard Model	23
2.8 The MS and \overline{MS} Subtraction Procedures	24
3 Measuring $\Lambda_{\overline{MS}}$ at LEP	26
3.1 Introduction	26
3.2 Definitions: The Observables	31
3.2.1 Jet Fractions.	31
3.2.2 Thrust	34
3.2.3 Energy-Energy Correlation	35
3.2.4 Asymmetry In The Energy-Energy Correlation Function	36
3.2.5 The Total Hadronic Cross-Section, R_Z	36
3.3 Review of the Scheme Dependence Problem	37

3.3.1	Parametrizing RS Dependence	37
3.3.2	The RS dependence of $R^{(1)}(\tau)$	39
3.3.3	RS dependence of $r_n(\tau, c_2, \dots, c_n)$	43
3.3.4	NLO extraction of $\alpha_s(M_Z)$	45
3.4	The Effective Charge Formalism	54
3.4.1	The Q dependence of $R(Q)$	54
3.4.2	EC formalism in NLO - the $\Delta\rho_0$ plot.	60
3.4.3	$\Delta\rho_0$ from NNLO calculations and Q-dependence.	73
4	Resumming Leading and Next-to-Leading Logarithms	79
4.1	Introduction	79
4.2	Exponentiation	79
4.3	What Has Been Done To Date?	83
4.4	The Effective Charge Scheme	83
4.5	An Expression For ρ^{DLL}	84
4.6	The Double Leading Logarithm Approximation For $\Delta\rho_0$	86
4.7	The 2-jet Fraction In The Durham Algorithm, $R_2(D)$	88
4.8	Thrust	96
4.9	Energy-Energy Correlation	100
4.10	The 3-jet Fraction In The Durham Algorithm, $R_3(D)$	104
4.11	The Breakdown of the Resummation	109
5	The Renormalization Group Equation Estimates of Perturbative Coefficients	110
5.1	Introduction	110
5.2	The First Attempt	111
5.3	The Pole Approximation	116
6	Summary and Conclusions	123

Chapter 1

Particle Physics - An Introduction

High-energy physics deals basically with the study of the ultimate constituents of matter and the nature of the interactions between them. Experimental research in this field of science is carried out using giant particle accelerators which smash particles together at enormous energies. High energies are necessary for two reasons: First, in order to localise the investigations to the very small scales of distance associated with the elementary constituents, one requires radiation of the smallest possible wavelength and highest possible energy; second, many of the fundamental constituents have large masses and require correspondingly high energies for their creation and study.

Only fifty years ago the only known 'elementary' particles were the proton, the neutron, the neutrino, and the photon. Since then the number of particles discovered has proliferated with the discovery of unstable particles in cosmic rays and the subsequent building of the accelerators.

Out of this seemingly chaotic situation has emerged a rather simple picture

i. All matter is composed of fundamental spin- $\frac{1}{2}$ fermion constituents - the quarks, with fractional electric charges ($+\frac{2}{3}e$ and $-\frac{1}{3}e$), and the leptons, like the electron and the neutrino, carrying integral electric charges. Neutrons and protons are both composed of three quarks.

ii. These components of matter can interact by the exchange of various fundamental

bosons (integral spin particles) which are the carriers or quanta of four distinct types of fundamental interactions or field. Gravity is familiar to everyone, yet on the scales of mass and distance involved in particle physics, it produces an insignificant effect compared to the other three forces. The electromagnetic interaction accounts for most phenomena outside the nucleus, since electromagnetic forces have the longest range, and lead to the bound states of atoms and molecules. Weak interactions are exemplified by the extremely slow process of β -decay of nuclei. Strong interactions are postulated to hold quarks together in a proton, and their residual effects apparently account for the interactions between neutrons and protons, that is, for the nuclear binding force. Both weak and strong interactions are of short range (less than or of the order of one fermi or femtometre, $1\text{fm}=10^{-15}$ metres).

There are many unusual aspects to this picture. The quarks have never been observed as free particles and seem to be permanently confined within hadrons. Quarks come in a variety of types or flavours (six are believed to exist) as do leptons (three types of charged and neutral leptons). We neither understand the mechanism of confinement, nor the reason for the apparent symmetry between the quark and lepton flavours, when the universe, on the basis of what we see today, seems to be constructed predominantly from just two types of quark and one neutral and one charged lepton.

The study of particle physics is considered to be intimately connected with the evolution of the universe. We believe the universe originated in a 'big bang' explosion of an energy bubble, from which all types of particles - quarks, leptons, and quanta - were created. Today, we are left with the expanded, cooled remnant. So, our search towards high energies is also a look backward in time to the very earliest stages of creation, which determined the characteristics of the universe which we find ourselves in today.

Obviously, this Ph.D. thesis will only be able to consider a very small section of this vast and fundamental area of physics. Hence, in it we shall concentrate on a very small area of Quantum Chromodynamics (QCD), the field theory that lies behind the strong interaction. We shall also touch upon the topic of Quantum Electrodynamics

(QED) in Chapter 5.

1.1 Thesis Outline

Chapter 2 presents a brief review of the relevant aspects of the standard model. This review begins by investigating gauge theories, and then by using the path integral formalism will motivate perturbation theory. A discussion of renormalization and the fundamental parameter, Λ follows. This chapter concludes by demonstrating how such principles can be extended to QCD and QED.

Initially chapter 3 investigates the so called renormalization scale problem, and whilst this is being done the notation which will be followed throughout this thesis is introduced. In the second half of this chapter we investigate a possible solution, namely the Effective Charge formalism, and from this an attempt is made to estimate a value of Λ_{QCD} using the LEP data that we have to hand.

In chapter 4 we will try to extend this formalism so that we can determine the usefulness of attempts to resum the leading and next-to-leading logarithms in the perturbative expansion for various QCD observables in e^+e^- annihilation.

Chapter 5 discusses a method for estimating the higher order coefficients in the QED anomalous magnetic moment of the electron, and also demonstrates that the two loop calculation for the R-ratio can be estimated by developing an expansion around the non-trivial fixed point of QCD, $N_c = \frac{2}{11}N_f$.

Finally, a few concluding remarks will be given.

Chapter 2

Towards Renormalization

2.1 Gauge Theory

All of the quantum field theories that have been successful in describing the fundamental interactions of nature are ‘gauge theories’, that is to say they are invariant under gauge transformations of the field potentials. This property has long been recognized in classical electromagnetism and so was built into QED from the start. It also turned out to be the key to the development of QCD for the strong colour interaction, and, albeit with symmetry breaking, to the formation of the unified electroweak theory, too.

It has long been known that a Lagrangian density, commonly referred to simply as a Lagrangian, can be constructed to be invariant under a group of transformations. To see this consider a set of M Dirac four component spinor fields, which for convenience will be written in a column vector and denoted by ψ . For the sake of simplicity we shall use the group $SU(N)$, with the fields transforming under an M -dimensional irreducible representation of $SU(N)$:

$$\psi(x) \rightarrow U(\alpha_a)\psi(x) \tag{2.1}$$

where $U(\alpha_a)$, which is an $M \times M$ matrix, can be written

$$U(\alpha_a) = \exp(i\alpha_a T_a), \tag{2.2}$$

with $a = 1, \dots, N^2 - 1$. The α_a are arbitrary real constants, and the T_a are traceless, hermitian matrices which form an M -dimensional irreducible representation of the generators of $SU(N)$. The T_a may be chosen such that

$$\text{Tr}(T_a T_b) \propto \delta_{ab}. \quad (2.3)$$

The implied constant of proportionality fully specifies the structure constants, f_{abc} , of the Lie algebra of the group that the T_a must obey:

$$[T_a, T_b] = i f_{abc} T_c \quad (2.4)$$

The Lagrangian

$$\mathcal{L} = i \bar{\psi} (\gamma_\mu \partial^\mu) \psi \quad (2.5)$$

is invariant under the above transformation. This is known as a global symmetry because each of the group parameters, α_a , is the same at every space-time point.

If we now make the group parameters functions of space-time, then the latter Lagrangian will not be invariant under such a transformation since the derivative will now act on $U(\alpha_a(x))$. In order to proceed we must define a new operator, namely the covariant derivative, to replace the ordinary derivative, so that the invariance of the Lagrangian is restored. This new operator must obey the following transformation for invariance to be preserved.

$$D_\mu \psi \rightarrow U(\alpha_a(x)) D_\mu \psi. \quad (2.6)$$

The only way to construct such a quantity is to introduce vector gauge fields $G_{a\mu}$ - in fact one for each generator of the group. It turns out that if we write D_μ as

$$D_\mu = \partial_\mu + ig G_\mu \quad (2.7)$$

where $G_\mu = G_{a\mu}T_a$. By requiring that this transformation holds we are requiring that the fields must transform as

$$G_\mu(x) \rightarrow G'_\mu(x) = U(\alpha_a(x)) \left(G_\mu(x) - \frac{i}{g} \partial_\mu \right) U^{-1}(\alpha_a(x)). \quad (2.8)$$

A kinetic term for the gauge fields can be constructed by first defining the tensor

$$\begin{aligned} F_{a\mu\nu}T_a \equiv F_{\mu\nu} &\equiv -\frac{i}{g}[D_\mu, D_\nu] \\ &= \partial_\mu G_\nu - \partial_\nu G_\mu + ig[G_\nu, G_\mu] \\ &= (\partial_\mu G_{a\nu} - \partial_\nu G_{a\mu} - gf_{abc}G_{b\mu}G_{c\nu})T_a \end{aligned} \quad (2.9)$$

which transforms as

$$F_{\mu\nu}(x) \rightarrow F'_{\mu\nu}(x) = U(\alpha_a(x))F_{\mu\nu}(x)U^{-1}(\alpha_a(x)). \quad (2.10)$$

The kinetic term,

$$-\frac{1}{4}F_{a\mu\nu}F_a^{\mu\nu} \propto Tr(F_{\mu\nu}F^{\mu\nu}), \quad (2.11)$$

is clearly invariant, due to the cyclic properties of a trace. The full Lagrangian which is invariant under SU(N) is then

$$\begin{aligned} \mathcal{L} &= i\bar{\psi}\gamma^\mu D_\mu\psi - \frac{1}{4}F_{a\mu\nu}F_a^{\mu\nu} \\ &= \mathcal{L}(\psi) + \mathcal{L}(G_a^\mu) \end{aligned} \quad (2.12)$$

The non-Abelian nature of the gauge group leads to the self interaction of the gauge fields as their kinetic term contains such terms as

$$gf_{abc}(\partial_\mu G_{a\nu})G_b^\mu G_c^\nu \quad (2.13)$$

and

$$\frac{g^2}{4} f_{abc} f_{aef} G_{b\mu} G_{c\nu} G_e^\mu G_f^\nu \quad (2.14)$$

which give rise to three- and four-point interactions of the gauge fields.

The case is much simpler if the gauge group is the Abelian group U(1), as there is only one generator and corresponding field. The above analysis is the same except that all the terms containing structure constants are dropped, as the single generator commutes with itself. Hence, $F_{\mu\nu}$ becomes

$$F_{\mu\nu} = \partial_\mu G_\nu - \partial_\nu G_\mu, \quad (2.15)$$

and the kinetic term only contains terms quadratic in the field G, describing the free propagation of the gauge particle, and not allowing any self-interaction. Note that in both Abelian and non-Abelian cases gauge invariance prohibits a mass term for the gauge fields.

If in the U(1) case the Dirac field is identified with the electron and the gauge field with the photon, then (2.13) is the Lagrangian of QED. Similarly, choosing the group to be SU(3) and associating the three Dirac fields with three quarks of different colours and the eight gauge fields with gluons, (2.13) is the QCD Lagrangian.

2.2 Quantization and Perturbation Theory

So far we have only been considering classical Lagrangians, and such Lagrangians can only yield classical theories. To quantize the theory we shall invoke the path integral formalism. This is an exceedingly complicated and lengthy procedure if done in full, and so only the main ideas will be sketched out here using a scalar field theory. The extension of this to the Standard Model will be discussed later. A more detailed review of the subject can be found in such books as Bailin and Love [1], Itzykson and Zuber [2], and Ryder [3].

Consider a Lagrangian which is no more than quadratic in the time derivatives of the field. If we suppose that the scalar field $\phi(x)$ has a source $J(x)$, then the transition amplitude from the vacuum at $t = -\infty$ to the vacuum at $t = +\infty$ in the presence of a source term $J(x)\phi(x)$, may be written as:

$$W[J] = N \int D\phi \exp(i \int d^4x (\mathcal{L}(\phi, \partial_\mu \phi) + J\phi), \quad (2.16)$$

where $D\phi$ denotes a path integral over all the functions ϕ , the normalization, N , is chosen so that $W[0] = 1$ and $\hbar = c = 1$. A more general Lagrangian can be created by defining a canonical momentum, π , and then $W[J]$ will be written in terms of a path integral over both ϕ and π and the action will be written in terms of the Hamiltonian. However, the integral over π will not be exact, and whilst $W[J]$ may be written in the form given above, the Lagrangian will be an effective Lagrangian. It will not be the exact one for the theory due to the approximations made when integrating over π .

The integrand of equation (2.16) is oscillatory and hence not obviously convergent. So conventionally a Wick rotation is made from Minkowski to Euclidean space, the integral evaluated there and then continued back, with the hope that this is a sensible procedure. In the following discussion it will be implicit that this has happened unless otherwise stated.

We shall now consider the case of the free field. The corresponding Lagrangian, which we shall denote by the subscript 0, is

$$\mathcal{L}_0 = \frac{1}{2} \partial_\mu \phi_0 \partial^\mu \phi_0 + \frac{1}{2} m^2 \phi_0^2, \quad (2.17)$$

where here m is the mass of the particle associated with the field. If we derive the Euler-Lagrange equation from this Lagrangian then we will obtain the classical field equation for a neutral free scalar field, known as the Klein-Gordon equation,

$$(\partial^\mu \partial_\mu + m^2) \phi_0(x) = 0. \quad (2.18)$$

In this case our equation for $W[J]$ becomes

$$W_0[J] = N_0 \int d\phi_0 \exp \left(i \int d^4y (\mathcal{L}_0 + J\phi_0) \right), \quad (2.19)$$

where N_0 has been chosen so that $W[0] = 1$. If we evaluate this exactly then we obtain

$$W_0[J] = \exp \left(-\frac{i}{2} \int d^4x' \int d^4x J(x') \Delta_F(x' - x) J(x) \right), \quad (2.20)$$

where Δ_F is the Feynman propagator

$$\Delta_F(x' - x) = \int \frac{d^4p}{(2\pi)^4} e^{-ip \cdot (x' - x)} \tilde{\Delta}_F(p), \quad (2.21)$$

and $\tilde{\Delta}_F(p)$ is its Fourier transform,

$$\tilde{\Delta}_F(p) = (p^2 - m^2 + i\epsilon)^{-1}. \quad (2.22)$$

In order to avoid the poles in p_0 when $p^2 = m^2$ we have introduced $i\epsilon$ in the Feynman propagator, with $\epsilon \rightarrow 0^+$. The above set of equations (2.20) to (2.22) define the generating functional for the free-field theory, so called because from it the Green's functions may now be generated.

If we now functionally differentiate (2.16) with respect to the source, J , then we will obtain

$$\frac{\delta^n W[J]}{\delta J(x_1) \dots \delta J(x_n)} = N i^n \int D\phi \phi(x_1) \dots \phi(x_n) \exp \left(i \int d^4x (\mathcal{L} + J\phi) \right), \quad (2.23)$$

since differentiating brings down a factor of $i\phi$. This latter expression is proportional to the vacuum to vacuum expectation value for a time ordered product of n field operators, also known as an n -particle Green's function

$$G^{(n)}(x_1 \dots x_n) = \langle 0 | T \left(\hat{\phi}(x_1) \dots \hat{\phi}(x_n) \right) | 0 \rangle$$

$$= (-i)^n \frac{\delta^n W[J]}{\delta J(x_1) \dots \delta J(x_n)} \Big|_{J(x)=0}, \quad (2.24)$$

where T is the time ordering operator, and $\hat{\phi}$ denotes a quantum field operator. So equation (2.24) relates an expression involving a classical field, ϕ to an expression containing a quantum operator, $\hat{\phi}$.

From this, and using the fact that the Green's function is symmetric in its variables, $W[J]$ can be written

$$W[J] = \sum_{n=0}^{\infty} \frac{i^n}{n!} \int d^4x_1 \dots \int d^4x_n G^{(n)}(x_1 \dots x_n) J(x_1) \dots J(x_n), \quad (2.25)$$

where the $n = 0$ term is 1.

The scattering amplitudes are closely related to Green's functions, and hence to the generating functional. Unfortunately, we can only evaluate $W[J]$ exactly in the free field case, and so we must derive a perturbative expansion for $W[J]$. If we write the Lagrangian as the free-field Lagrangian, \mathcal{L}_0 , and a piece involving the interaction terms, \mathcal{L}_1 , proportional to some expansion parameter, λ , then we can write the integrand of (2.16) as

$$\begin{aligned} \exp\left(i \int d^4x (\mathcal{L} + J\phi)\right) &= \sum_{n=0}^{\infty} \frac{i^n}{n!} \int d^4x_1 \dots d^4x_n \mathcal{L}_1(\phi(x_1)) \dots \mathcal{L}_1(\phi(x_n)) \\ &\quad \times \exp\left(i \int d^4x (\mathcal{L}_0 + J\phi)\right), \end{aligned} \quad (2.26)$$

where we have used the series expansion of the exponential of the interaction term, and defined the $n = 1$ term to be 1.

Since functionally differentiating $\exp(i \int d^4x (\mathcal{L}_0 + J\phi))$ with respect to J pulls down a factor of $i\phi$, it can be shown that

$$\begin{aligned} &\left(\int d^4x \mathcal{L}_1(\phi)\right) \exp\left(i \int d^4y (\mathcal{L}_0 + J\phi)\right) \\ &= \int d^4x \mathcal{L}_1\left(-i \frac{\delta}{\delta J(x)}\right) \exp\left(i \int d^4x (\mathcal{L}_0 + J\phi)\right). \end{aligned} \quad (2.27)$$

If we take the operator $\int d^4x \mathcal{L}_1 \left(-i \frac{\delta}{\delta J}\right)$ outside the functional integral (2.16), then, since it is independent of ϕ , we can deduce from equation (2.19) that

$$\begin{aligned} W[J] &= N \exp \left(i \int d^4x \mathcal{L}_1 \left(-i \frac{\delta}{\delta J}\right) \right) \int D\phi \exp \left(i \int d^4y (\mathcal{L}_0 + J\phi) \right) \\ &= \sum_{n=0}^{\infty} \frac{i^n}{n!} \int d^4x_1 \dots d^4x_n \mathcal{L}_1 \left(-i \frac{\delta}{\delta J(x_1)}\right) \dots \left(-i \frac{\delta}{\delta J(x_n)}\right) W_0[J] \end{aligned} \quad (2.28)$$

where we have chosen N so that $W[0] = 1$, and the $n = 0$ term is defined to be 1.

Since $W_0[J]$ is known, and \mathcal{L}_1 is proportional to the expansion parameter λ , we can see that equation (2.28) represents a perturbative expansion of $W[J]$ as a power series in λ . We can now derive the Green's functions for the perturbative series by using equation (2.24) and substituting equations (2.20)-(2.22) for $W_0[J]$. For instance, we could do this for $\lambda\phi^4$ theory, where \mathcal{L}_1 is $\lambda\phi^4$, and \mathcal{L}_0 and $W_0[J]$ are given by (2.17) and (2.20) respectively. However, it is an extremely lengthy process to calculate any term in the series and so it would be fairly uninformative to calculate such terms here. Hence, we shall just quote the result for the 2-particle Green's function

$$\begin{aligned} G^{(2)}(x_1, x_2) &= i\Delta_F(x_1 - x_2) \left(1 - \frac{i\lambda}{8} \int d^4x (i\Delta_F(x - x))^2 \right) \\ &\quad - \frac{i\lambda}{2} \int d^4x i\Delta_F(x_1 - x) i\Delta_F(x - x) i\Delta_F(x - x) i\Delta_F(x - x) i\Delta_F(x - x_2) + O(\lambda^2) \end{aligned} \quad (2.29)$$

In a free-field theory, $\lambda = 0$, the free-field Green's function $G_0^{(2)}(x_1, x_2)$, is just the first term, and represents the propagation of a scalar particle from x_1 to x_2 . This may be represented diagrammatically by a line from x_1 to x_2 . When $\lambda \neq 0$, the additional terms are generated by interactions. Propagators whose argument is zero are represented by a loop at x . Since x is an arbitrary point, and the Green's function does not depend on it, it is integrated over. However, these loop integrals, as they are called, may give rise to infinities which must be removed by a process known as renormalization before a finite answer can be obtained. Such representations are known as Feynman diagrams and the

associated factors as Feynman rules. The power of these diagrams and the rules that are associated with them is that it is possible to construct all the Green's functions for the theory from them.

By defining a new functional, $X[J]$, by

$$iX[J] \equiv \ln W[J], \quad (2.30)$$

a specialized class of Green's function's, called connected Green's functions, denoted $G_c^{(n)}$, can be defined

$$iX[J] = \sum_{n=1}^{\infty} \frac{i^n}{n!} \int d^4x_1 \dots \int d^4x_n G_c^{(n)}(x_1 \dots x_n) J(x_1) \dots J(x_n) \quad (2.31)$$

with

$$i^n G_c^{(n)}(x_1 \dots x_n) = i \left. \frac{\delta^n X[J]}{\delta J(x_1) \dots \delta J(x_n)} \right|_{J=0}. \quad (2.32)$$

When represented diagrammatically, each diagram that contributes to a Green's function has no subunits that are not connected to the rest of the diagram by at least one line.

A further refinement is to define one-particle-irreducible (OPI) Green's functions - all of whose graphs can not be split into smaller graphs by cutting only one line. To define these functions, what is known as the classical field, ϕ_c , is introduced,

$$\phi_c(x) = \frac{\delta X[J]}{\delta J(x)} \quad (2.33)$$

The effective action $\Gamma(\phi_c)$, defined by

$$\Gamma(\phi_c) = W[J] - \int d^4x J(x) \phi_c(x), \quad (2.34)$$

can not usually be evaluated exactly in an interacting theory, and a functional expansion

is made

$$\Gamma[\phi_c] = \sum_{n=1}^{\infty} \frac{i^n}{n!} \int d^4x_1 \dots \int d^4x_n \Gamma^{(n)}(x_1 \dots x_n) \phi_c(x_1) \dots \phi_c(x_n) \quad (2.35)$$

where $\Gamma^{(n)}$ is the OPI Green's function referred to above. A further difference between connected and OPI Green's functions is that while each external leg of a connected Green's function has a propagator factor associated with it, the OPI Green's function does not.

Often it is more convenient to work in momentum space, and by taking the Fourier transform of the Green's functions, the Feynman rules can be written in momentum space.

2.3 Calculating Observables

In a physical process the incoming and outgoing particles are taken to be asymptotically free and hence are 'on-mass-shell', i.e. $p_i^2 = m^2$ where m is the mass of the particle associated with the free scalar field, ϕ_0 , and p_i is the four momentum of the i^{th} particle. The boundary conditions on $W[J]$ are insufficient to ensure this, so $W[J]$ contains terms involving particles which are not on-mass-shell. Hence, Green's functions are not physical observables.

However, if we impose boundary conditions that ensure that incoming and outgoing particles are asymptotically free, it is possible to derive a functional, $S[\phi_0]$, which yields the physically observable scattering amplitudes of the theory. $S[\phi_0]$ is given in terms of $W[J]$ by the following expression

$$S[\phi_0] = \exp \left(\int d^4x \phi_0(x) (\partial^\nu \partial_\nu + m^2) \frac{\delta}{\delta J(x)} \right) W[J] \Big|_{J=0}. \quad (2.36)$$

2.4 Everything is Infinite!!

Unfortunately, when an attempt is made to evaluate the Feynman diagrams that contribute to a physical process, it is found that diagrams that contain one or more loops may result in infinities. As the momentum of the loop is unrestricted, these infinities arise from terms such as

$$\int d^4k \frac{1}{(k^2 - m^2)^l} \quad (2.37)$$

where k is the momentum around the loop. For large values of k , this integral goes as

$$\int d|k| \frac{|k|^3}{|k|^{2l}}. \quad (2.38)$$

For $l = 3$ this integral is convergent, but for $l = 2$ a logarithmic divergence arises, and if $l = 1$ the divergence is quadratic.

2.5 Dimensional Transmutation

In order to investigate a theory we often try to measure the unpredicted fundamental constants. For the moment suppose that there is only one of these, a dimensionless coupling, λ . Consider a dimensionless observable R . By dimensional analysis [4] we may anticipate that R will satisfy

$$Q \frac{dR}{dQ} = -b\rho(R) \quad (2.39)$$

where Q is some external energy, and ρ is a function given completely by the theory. If we integrate this latter equation then we can obtain

$$\ln Q + constant = - \int_{\infty}^R \frac{dx}{\rho(x)} = f(R(Q)) \quad (2.40)$$

where f , like ρ , is a function given to us by the theory. Here we would like the constant to be measured by experiment since it is our unknown unpredicted by the theory. We could measure this by letting $Q = \Lambda$ where Λ is such that

$$f(R(Q = \Lambda)) = 0. \quad (2.41)$$

Hence, we can deduce that

$$R(Q) = f^{-1}(\ln(Q/\Lambda)). \quad (2.42)$$

and so we can now make predictions about R at other values of Q . Ideally, we would try to measure Λ using a closed form calculation of f . Λ is the only unknown parameter of the theory and so has replaced the coupling λ as the fundamental constant of the theory.

Suppose that instead we had introduced an energy $Q = \mu$, called the renormalization scale, at which we had measured R . Then we would have

$$R(\mu) = f^{-1}(\ln(\mu/\Lambda)). \quad (2.43)$$

However, we also can write that

$$R(Q) = f^{-1}(f(R(\mu)) + \ln(Q/\mu)) \quad (2.44)$$

and this cannot be dependent on μ since $R(Q)$ is an observable and the introduction of an arbitrary parameter μ cannot alter our value of $R(Q)$.

Because all of the equations above are dimensionless overall and the underlying theory could have been defined entirely in terms of massless quantities, it is perhaps surprising that the dimensionless parameter λ has been replaced by Λ with the dimensions of energy (or mass). In the process by which this happens, known as dimensional transmutation, the arbitrary scale μ plays a key role.

Limiting ourselves to one observable is a little unrealistic. So we must now generalize to any observable $\sigma(Q)$. We can deduce directly that

$$\sigma(Q) = \sigma(Q/\mu, R(\mu)). \quad (2.45)$$

This latter equation must be independent of μ and so we can deduce that

$$\mu \frac{d\sigma}{d\mu} = 0. \quad (2.46)$$

Hence, we obtain that

$$\left(\mu \frac{\partial}{\partial \mu} - \rho(R(\mu)) \frac{\partial}{\partial x} \right) \sigma(Q/\mu, x) \Big|_{x=R(\mu)} = 0 \quad (2.47)$$

and this demonstrates the importance of $\rho(x)$.

Naturally physics is also independent of whichever observable R we choose to use as a reference and it is particularly easy to convert to another, say σ , for which instead of (2.39) we now have

$$Q \frac{d\sigma}{dQ} = -\rho_\sigma(\sigma(Q)). \quad (2.48)$$

Trivially

$$\rho_\sigma(\sigma) = b \frac{d\sigma}{dR} \rho(R). \quad (2.49)$$

However, to satisfy the equivalent of (2.41) for σ will usually involve a different value of Λ , but numerically this can be compensated for by a change of units altering the particular value of μ we have in mind. Conversely, changes in μ , keeping Λ constant, correspond to a change of reference quantity. Crucially, as is clear from dimensional analysis, changes in μ can also be compensated for by changes in Q . Thus

$$\sigma(zQ, R(\mu), \mu) = \sigma(Q, R(\mu), \mu z^{-1}). \quad (2.50)$$

Using invariance under a change from μ to $\mu' = \mu z^{-1}$, the right hand side becomes

such that

$$\sigma(zQ, R(\mu), \mu) = \sigma(Q, R(\mu z), \mu). \quad (2.51)$$

Setting $Q = \mu$ on the right hand side and renaming $Qz = W$, we can conclude that

$$\sigma(W, R(\mu), \mu) = \sigma(\mu, R(W), \mu). \quad (2.52)$$

Hence, the energy dependence of σ can be transferred from the function into one of its arguments.

Therefore, it turns out that individual functions are expressible in a variety of different, yet fundamentally equivalent, forms. However, in reality when we calculate such a function we invariably have to make an approximation and it is unclear that these different prescriptions will be treated in the same way.

As is quite obvious from the above arguments we do in fact have a great deal of choice for which parameter we choose to expand our perturbative series in. We could either perform our expansion of $\sigma(Q/\mu, R(\mu))$ in terms of $R(\mu)$, which is analogous to $\alpha_s(\mu)$ in QCD, or we could equally expand $\sigma(1, R(Q))$ in terms of $R(Q)$. Obviously our best choice of expansion parameter is dependent on the properties of the relevant perturbative series.

2.6 Renormalization

As has been stated earlier the problem in calculating with the bare lagrangian, \mathcal{L}_0 is that the answer tends to be infinite and so is of little use to physicists. In order to overcome this difficulty it is first necessary to regularize and then to renormalize the theory.

Regularization is a method of isolating the divergences in the Feynman integrals. It makes the task of renormalization much more explicit and easy to follow. There are several techniques of regularization. Perhaps the most intuitive one is to introduce

a cut-off κ in the momentum integrals. In electrodynamics a particular example is to modify the free (photon) propagator

$$\frac{1}{k^2} \rightarrow \frac{1}{k^2} - \frac{1}{k^2 - \kappa^2} = -\frac{\kappa^2}{k^2(k^2 - \kappa^2)}. \quad (2.53)$$

Similar to this is the Pauli-Villars regularization in which a fictitious field of mass M is introduced. In both these cases the limit $\kappa \rightarrow \infty$ ($M \rightarrow \infty$) is taken, and the renormalization quantities are independent of κ (M). However, these methods become problematic particularly when non-Abelian gauge theories are considered. A trouble free and elegant method is that of dimensional regularization, which has, therefore, become popular. The idea is to treat the loop-integrals (which cause the divergences) as integrals over d -dimensional momenta, and then take the limit $d \rightarrow 4$. It turns out that the singularities of 1-loop graphs are simple poles in $d - 4$. It should be noted that when we regularize a theory it is necessary to introduce a parameter, μ , with the dimensions of mass.

Once we have regularized our theory we can then invoke renormalization. In terms of bare quantities the example Lagrangian that we shall consider will be

$$\mathcal{L}_B = \frac{1}{2}(\partial_\mu \phi_B)(\partial^\mu \phi_B) - \frac{1}{4!}g_B \phi_B^4 \quad (2.54)$$

i.e. the Lagrangian of massless ϕ^4 theory. Here g_B is the bare coupling and ϕ_B is the bare wavefunction. These bare quantities are related to their physical counterparts via

$$\phi_B = Z_\phi^{\frac{1}{2}} \phi, \quad g_B = g Z_1 Z_\phi^{-4}. \quad (2.55)$$

Now we can write our Lagrangian in the following way

$$\mathcal{L} = \frac{1}{2}(\partial_\mu \phi)(\partial^\mu \phi) - \frac{1}{4!}g \phi^4 + \frac{1}{2}(Z_\phi^2 - 1)(\partial_\mu \phi)(\partial^\mu \phi) - (1 - Z_1) \frac{g}{4!} \phi^4. \quad (2.56)$$

The terms to the right are referred to as counterterms and contain all the divergences.

Their real usefulness only becomes apparent in order-by-order renormalization using Feynman diagrams when diagrams arising from them will explicitly cancel the divergences in the diagrams of the bare theory. For present purposes we need only assume that both the bare parameters and the renormalization constants can be made infinitesimal leaving finite physical parameters and an algorithm for calculating observables which gives finite answers.

A renormalizable theory is defined to be a theory where a finite number of renormalization constants are required to renormalize it. Hence, the theory just discussed is renormalizable because only two renormalization constants are required.

As we saw earlier it is necessary to introduce a new parameter μ , when we regularize. Hence, the renormalized OPI function $\Gamma^{(n)}$ will depend on μ

$$\Gamma^{(n)}(p_i, g, \mu) = Z_\phi^{n/2} (g\mu^\epsilon) \Gamma_B^{(n)}(p_i, g_B) \quad (2.57)$$

through the dependence of Z_ϕ on μ . The unrenormalized function $\Gamma_B^{(n)}$ is independent of μ , and so is invariant under the group of transformations

$$\mu \rightarrow e^S \mu \quad (2.58)$$

These transformations form the renormalization group. Introducing the dimensionless differential operator $\mu(\partial/\partial\mu)$ we have

$$\mu \frac{\partial}{\partial\mu} \Gamma_B^{(n)} = 0 \quad (2.59)$$

and so

$$\mu \frac{d}{d\mu} \left[Z_\phi^{-n/2} (g\mu^\epsilon) \Gamma^{(n)}(p_i, g, \mu) \right] = 0 \quad (2.60)$$

where g is independent of μ . Performing the differentiation leads to

$$\left[\mu \frac{\partial}{\partial\mu} + \beta(g) \frac{\partial}{\partial g} - n\gamma(g) \right] \Gamma^{(n)}(q_i, g, \mu) = 0 \quad (2.61)$$

where

$$\begin{aligned}\beta(g) &= \mu \frac{\partial g}{\partial \mu} \\ \gamma(g) &= \mu \frac{\partial}{\partial \mu} \ln Z_\phi.\end{aligned}\tag{2.62}$$

This latter equation is known as the renormalization group equation (RG equation). It expresses the invariance of the renormalized $\Gamma^{(n)}$ under a change of regularization parameter, μ .

Let us now write down a similar equation expressing the invariance of $\Gamma^{(n)}$ under a change of scale. $\Gamma^{(n)}$ has mass dimension D

$$D = d + n\left(1 - \frac{d}{2}\right)\tag{2.63}$$

where d is the number of dimensions and n is the number of vertices. If we now let $p_i \rightarrow p_i e^t$ then the renormalization group equation yields the inhomogenous Callan-Symanzik equation

$$\left[-\frac{\partial}{\partial t} + \beta(g)\frac{\partial}{\partial g} + D - n\gamma(g)\right] \Gamma^{(n)}(p_i e^t, g, \mu) = 0.\tag{2.64}$$

The solution to this equation is

$$\Gamma^{(n)}(p_i e^t, g(\mu), \mu) = \Gamma^{(n)}(p_i, g(\mu e^t), \mu) \exp\left[tD - n \int_0^t dt' \gamma(g(\mu e^{t'}))\right].\tag{2.65}$$

The term

$$\exp\left[-n \int_0^t dt' \gamma(g(\mu e^{t'}))\right]\tag{2.66}$$

is known as the anomalous dimension and $\exp(tD)$ is known as the canonical dimension. In the case of an observable $\sigma(Q^2/\mu^2, R(\mu))$ and because the theory is massless, changes in μ and units could compensate transformations like $Q \rightarrow e^t Q$ in the external energies.

2.7 Extension to the Standard Model

So far we have only been talking about ϕ^4 theory. Unfortunately, such a theory only has similarities with the theories that appear to work in reality. However, a structure that is far more realistic is

$$\begin{aligned}
\mathcal{L} = & \bar{L}i\gamma^\mu\partial_\mu L + \bar{R}i\gamma^\mu\partial_\mu R - g(\bar{q}\gamma^\mu T_a q)G_\mu^a - \frac{1}{4}G_{\mu\nu}^a G_a^{\mu\nu} \\
& - \frac{1}{4}W_\mu^a \nu W_a^{\mu\nu} - \frac{1}{4}B_\mu^a \nu B_a^{\mu\nu} \\
& - \bar{L}\gamma^\mu(g'\frac{1}{2}\tau_a W_\mu^a + g''\frac{Y}{2}B_\mu)L - \bar{R}\gamma^\mu g''\frac{Y}{2}B_\mu R \\
& + |(i\partial_\mu - g'\frac{1}{2}\tau_a W_\mu^a - g''\frac{Y}{2}B_\mu)\phi|^2 - V(\phi) \\
& - (G_1\bar{L}\phi R + G_2\bar{L}\phi_c R + \text{hermitean conjugate})
\end{aligned} \tag{2.67}$$

where

$$G_{\mu\nu}^a = \partial_\mu G_\nu^a - \partial_\nu G_\mu^a - gf_{abc}G_\mu^b G_\nu^c \tag{2.68}$$

$$W_{\mu\nu}^a = \partial_\mu W_\nu^a - \partial_\nu W_\mu^a - g'f'_{abc}W_\mu^b W_\nu^c \tag{2.69}$$

$$B_{\mu\nu} = \partial_\mu B_\nu - \partial_\nu B_\mu \tag{2.70}$$

The elementary fields correspond to three massive leptons (electron, muon, and tau) and their neutrino companions, six quarks (up, down, strange, charm, bottom, and top), the photon, the intermediate vector bosons (W^\pm and Z^0), eight gluons and a Higgs boson. This is the so called Standard Model. It is no more than the $SU(3)\times SU(2)\times U(1)$ non-Abelian gauge theory with its latter two symmetries spontaneously broken by a minimal Higgs mechanism.

Quantizing this theory is far from trivial and is beyond the scope of this thesis. so again the reader is directed to the textbooks for a full account of how all this is done.

For the remainder of this thesis our concern will be with circumstances where most of (2.67) will be irrelevant, and a good description of experiment is provided by

Quantum Chromodynamics (QCD) defined by

$$\mathcal{L} = \bar{\psi}(i\gamma^\mu\partial_\mu - m)\psi - \frac{1}{2}(\bar{\psi}\gamma^\mu\lambda_i\psi)G_\mu^i - \frac{1}{4}G_{\mu\nu}G_i^{\mu\nu} \quad (2.71)$$

with the gauge group taken to be SU(3). Of the particles listed above only the quarks and the gluons possess the colour quantum number and so the other particles can be ignored. The gluons are assigned to the vector gauge particles G_μ^i ($i = 1, 8$) and the quarks to the fermionic ψ .

Perturbative calculations of QCD β -functions reveal one of the theories crucial properties, asymptotic freedom. Asymptotic freedom means that the coupling constant α_s decreases as the energy increases and perturbative theory becomes far more applicable.

Conversely, at low energies QCD behaves in a more strongly interacting fashion and the perturbative approximation must break down. To one loop in perturbation theory it can be shown that

$$\alpha_s(Q) \sim \frac{1}{\ln Q^2/\Lambda^2}. \quad (2.72)$$

This indicates that $Q \simeq \Lambda$ is the transition between the perturbative regime and the non-perturbative regime.

2.8 The MS and \overline{MS} Subtraction Procedures

Throughout this thesis we will frequently refer to two commonly used renormalization schemes, namely MS and \overline{MS} . Therefore, at this point it is wise to digress and introduce the two schemes. In order to do this, we shall consider the loop diagram

$$\Sigma_{\mu\nu} = \text{---}\mu \text{---} \bigcirc \text{---}\nu \text{---}$$

If we apply our Feynman rules to this and apply dimensional regularization with the number of dimensions $d = 4 - 2\epsilon$, then we will obtain the expression

$$\Sigma_{\mu\nu} = T_F N_F \frac{g^2}{16\pi^2} \frac{4}{3} \left[\frac{1}{\epsilon} + \frac{\ln 4\pi \mu^2}{q^2} - \gamma_E + \frac{7}{6} + O(\epsilon) \right] T_{\mu\nu} \quad (2.73)$$

where g^2 is the coupling at each vertex. In the minimal subtraction (MS) scheme we subtract the $1/\epsilon$ term from the latter equation. Therefore, in the MS scheme we obtain

$$\Sigma_{\mu\nu} = T_F N_f \frac{g^2}{16\pi^2} \frac{4}{3} \left[\ln 4\pi \frac{\mu^2}{q^2} - \gamma_E + \frac{7}{6} \right] T_{\mu\nu}. \quad (2.74)$$

In the modified minimal subtraction scheme we remove a factor $(\ln 4\pi - \gamma_E)$ along with $\frac{1}{\epsilon}$ to obtain

$$\Sigma_{\mu\nu} = T_F N_f \frac{g^2}{16\pi^2} \frac{4}{3} \left[\ln \frac{\mu^2}{q^2} + \frac{7}{6} \right] T_{\mu\nu}. \quad (2.75)$$

These two procedures are just two of an infinity of possible subtractions. The parametrization of renormalization schemes will be discussed in detail in chapter 3.

Chapter 3

Measuring $\Lambda_{\overline{MS}}$ at LEP

3.1 Introduction

The CERN LEP collaborations now all have high-statistics data samples which enable them to make accurate measurements of a wide range of e^+e^- QCD observables [5-13], such as jet fractions, thrust distributions, the hadronic width of the Z^0 , energy-energy correlations, etc. For most of these quantities non-perturbative effects such as hadronization corrections are expected to be reasonably small and next-to-leading order (NLO) calculations are available in renormalization group (RG) improved QCD perturbation theory [14, 15]. For the hadronic width of the Z^0 alone we have a next-NLO (NNLO) calculation available [16, 17].

By comparing such calculations with the data one hopes to be able to extract Λ_{QCD} , the fundamental SU(3) standard model parameter, or equivalently α_s , the \overline{MS} scheme coupling constant. (See section 2.8 for a review of the \overline{MS} and MS subtraction procedures.) This is done by comparing the relevant truncated perturbative expansion for the LEP observable, R , which is either

$$R = a\alpha_s + b\alpha_s^2 \tag{3.1}$$

or

$$R = a\alpha_s + b\alpha_s^2 + c\alpha_s^3, \quad (3.2)$$

with the experimental data points, and then solving for α_s .

Unfortunately, this intention is hampered by our rather limited current knowledge of what QCD actually predicts for any of these quantities due to the dependence of perturbative calculations at NLO on the unphysical renormalization scale, μ , and more generally on the renormalization scheme (RS) in higher-orders. In a complete all-orders calculation of any quantity the μ -dependence would cancel and so, as was explained in the last chapter, it is an arbitrary parameter. Hence, when we rely on a truncated expansion in α_s such cancellations no longer quite occur and so any prediction is rendered ambiguous.

Since it was first clearly formulated in ref [18] this ‘scheme dependence problem’ has been the subject of much discussion but as yet has produced little consensus. The response of theorists to the dependence of NLO predictions on μ has generally been to choose a particular scale which is considered to be the ‘best’ or the ‘correct’ choice. This is very much contrary to the fundamental principle that μ is an arbitrary and unphysical quantity. Due to this ambiguity one particular choice has not been able to command universal support. Specific reservations about the way that this has been done at LEP will be expressed in section 3.3 of this chapter, but it is obvious that all is not well when the approach to the problem involves increasing the consistency amongst observables by expanding the error bars to include a ‘theoretical uncertainty’ (essentially obtained by averaging across camps of theorists). Such a procedure clouds the information which is obtained from the observable which is being measured, and, therefore, limits the extent to which QCD can be investigated in detail.

In some sense all the previously proposed approaches have been an attempt to estimate the uncalculated higher-order terms in the perturbation series. This has been done by stating that some favoured choice of scale along with a NLO calculation will give a reliable prediction as if we knew the full series. On the other hand, the position

expressed in this thesis is essentially that the higher order terms are simply unknown and that we therefore should restrict our attention to the more modest aim of deciding what it is actually possible to learn about the uncalculated terms from the information at our disposal.

A widespread belief already exists that the severity of the scale dependence for any particular observable is related to the size of its higher-order corrections. This overlooks the problem that the size of the unknown terms is itself a scheme dependent problem, since there is always a scheme in which there are no corrections whatsoever. Again such beliefs overlook the fact that the total uncalculated corrections to a μ -dependent NLO prediction must also depend on the scale so that their sum does not. However, this μ -dependence would only be a fundamental problem if it were unknown, unpredictable, and uncontrollable, when in fact the higher-orders can be split into a predictable contribution incorporating all the awkward μ -dependence and a remaining piece containing the genuinely unknown aspects. This will all be demonstrated in section 3.4.

All this is really just a consequence of the fact that the μ -dependence in a NLO calculation has a universal form, and so in the proceeding sections we shall see that a convenient means of comparing theory and data, in which the scale dependence is trivial, can be written down. The formalism to be proposed has the advantages of being derived non-perturbatively and as far as possible entirely in terms of RS-invariant quantities. In particular, α_s is avoided in favour of $\tilde{\Lambda}_{\overline{MS}}$, the dimensional transmutation parameter of QCD, as the free parameter of the theory. This approach is taken because α_s is just a consequence of theory and has no direct experimental significance. Indeed its definition changes from order to order in perturbation theory. It remains true that $\tilde{\Lambda}$ is RS-dependent, but with the difference that the values in different schemes are exactly related given NLO calculations of any observable in the two schemes. This $\tilde{\Lambda}$ is to be as directly related as possible to $R(Q)$, any generic LEP observable dependent on a single dimensionful scale Q such as \sqrt{s} , the e^+e^- centre of mass energy. Since this $R(Q)$ will play a role analogous to α_s , we shall refer to this approach as the

‘Effective Charge formalism’. This formalism was originally introduced by Grunberg [19] and has also been discussed by Dhar and Gupta [20]. Unfortunately, there has been a widespread view that Grunberg’s approach constitutes no more than a particular choice of RS. Indeed the insistence on using the RS-invariant $R(Q)$ rather than the RS-dependent α_s in the role of coupling means that this formalism has similarities with the fastest apparent convergence (FAC) criterion for choosing the scheme, by which the RS is chosen such that the higher corrections vanish. This perturbative property often simplifies calculations but in the proceeding discussion its main benefit is that by non-perturbatively identifying each observable as a coupling we have clarified our problem. It cannot be overemphasized that the effective charge (EC) formalism is both derived non-perturbatively and is more general than the adoption of a particular scheme, even if certain aspects of the formalism can be interpreted in terms of the FAC scheme.

The formalism not only provides a clear framework for displaying data, but also provides a method for extracting $\tilde{\Lambda}$ without any scale ambiguity whatsoever. This is a result of the way in which $R(Q)$ runs as a renormalization group improved coupling with Q . This evolution is described by a function $\rho(R)$ which is the main ingredient for a convenient RS-invariant measure of the importance of the higher-order corrections, and also forms the β -function which corresponds to the FAC scheme. Thus, the effective charge β -function $\rho(R)$ can, at least in principle, be experimentally measured, so that by detailed investigations of the running of $R(Q)$ with Q one can determine $\tilde{\Lambda}_{\overline{MS}}$ even in the absence of NNLO perturbative calculations. Applied in this way the formalism gives a non-perturbative determination of $\tilde{\Lambda}_{\overline{MS}}$ which does not depend on the particular scheme that we have applied, and is only limited by the experimental uncertainty. Unfortunately, at present we do not have sufficiently precise information about the running with energy of these observables at LEP, and obtaining data at various energies requires combining results from different detectors and machines. In an ideal world LEP would take data at energies below $\sqrt{s} = M_z$ and study the running of the observables in detail. As shall be discussed, this would enable reasonably precise determinations of $\tilde{\Lambda}_{\overline{MS}}$, and more importantly would also indicate whether NNLO perturbative corrections

by themselves are sufficient to describe the data. This latter point would enable a theorist to make a decision on whether or not a calculation, which is likely to be extremely arduous, is worth doing [21].

Even without information on NNLO corrections and the detailed running of the observables with energy, there is still much to be learned from the effective charge formalism. It is possible to exhibit the relative size of the uncalculated higher-order corrections for different quantities. In the effective charge language these are related to how the energy dependence of the quantity at the experimental energy differs from its asymptotic dependence as $Q \rightarrow \infty$. If this difference cannot be neglected, then NNLO calculations or measurements of the running are necessary before $\tilde{\Lambda}$ can be determined. This can be decided in the effective charge formalism given only a NLO calculation and data at one energy.

The proposal outlined in this chapter is not a solution to the scheme dependence problem in the usual sense. However, the ideas that are proposed are such that the scheme dependence problem is avoided. This demonstrates that the whole scheme dependence problem is just an artifact of the way people conventionally approach a problem in perturbative QCD. A preliminary discussion of this latter point has appeared in references [22] and [26].

The plan of this chapter is as follows. In section 3.2 we shall firstly introduce some of the observables that will be used during the course of the rest of the thesis. Then in section 3.3 we shall review the RS dependence problem and outline the traditional approach to α_S extraction. In section 3.4 we shall introduce in detail the effective charge formalism sketched above and stress its advantages over the conventional approach. We shall attempt to determine $\tilde{\Lambda}_{\overline{MS}}$ using the rather limited information on NNLO corrections and energy dependence of observables currently available.

3.2 Definitions: The Observables

In this thesis I shall have occasion to mention some of the QCD observables that are measured at LEP. The observables that will be mentioned here are all related to e^+e^- annihilation. For the processes $e^+e^- \rightarrow q\bar{q}$ and $e^+e^- \rightarrow q\bar{q}g$ the QCD matrix elements are fully known to $O(\alpha_s^2)$ [14], and the necessary integrations over the relevant parts of phase space can be performed using the Monte Carlo package EVENT developed by Kunszt and Nason¹ [15], to yield next-to-leading perturbative coefficients in the \overline{MS} scheme.

3.2.1 Jet Fractions.

When an electron beam is collided with a positron beam jets are observed. These jets result from the following processes which are depicted in Figures 3.1(a) and (b).

$$e^+e^- \rightarrow q\bar{q} \quad (2 \text{ jets})$$

$$e^+e^- \rightarrow q\bar{q}g \quad (3 \text{ jets})$$

As depicted in the figures it is not the quarks or the gluons that are observed but the hadron showers which are a result of the ‘fragmentation’ of the gluons and the quarks.

For the jet fractions a range of definitions have been discussed, each of broadly the same experimental practicability, but with differing higher order and hadronisation corrections. Some of these are simple in conception, such as that hadrons must fall inside a cone of a specified size in order to constitute a jet, and others are more complicated and are often represented in the form of an algorithm with the energy-momenta of the particles in an event as input parameters.

By far the most significant subset is that of the JADE-type algorithms [23] in which the experimentalists assign a number y_{ab} to each pair (a, b) of particles. Then the two

¹Paulo Nason is thanked for supplying the computer code for generating NLO corrections to the e^+e^- matrix elements.

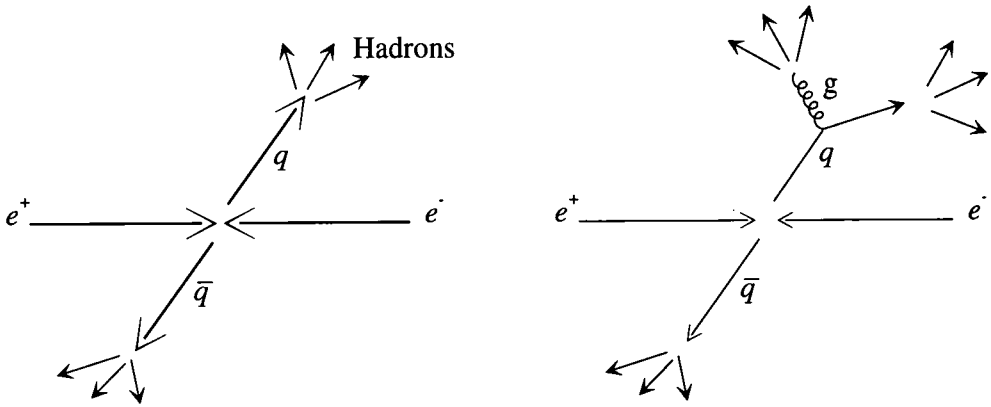


Figure 3.1: (a) The 2-jet Case

(b) The 3-jet Case

particles with the smallest value of y_{ab} , denoted as y_{ij} , have their energy and momentum combined to form a ‘pseudoparticle’ provided that y_{ij} satisfies the condition

$$y_{ij} \leq y_c s \quad (3.3)$$

where y_c is an arbitrary parameter. These two particles are eliminated from further consideration, and instead the pseudoparticle is included on an equal footing with the other particles. This procedure is repeated until all the particle pairs fail (3.3), and then the total number of remaining particles and pseudoparticles is the number of jets in the event. Both y_{ij} and the rule for forming a pseudoparticle from its parent remain to be defined and different choices give rise to the variety of JADE-type algorithms used as seen in Table 3.1.

Name	y_{ij}	Recombination
E	$(\mathbf{p}_i + \mathbf{p}_j)^2$	$\mathbf{p}_k = \mathbf{p}_i + \mathbf{p}_j$
E ₀	$(\mathbf{p}_i + \mathbf{p}_j)^2$	$E_k = E_i + E_j$ $\mathbf{p}_k = \frac{E_k}{ \mathbf{p}_i + \mathbf{p}_j } (\mathbf{p}_i + \mathbf{p}_j)$
JADE	$2E_i E_j (1 - \cos\theta_{ij})$	$\mathbf{p}_k = \mathbf{p}_i + \mathbf{p}_j$
DURHAM	$2\min(E_i^2, E_j^2)(1 - \cos\theta_{ij})$	$\mathbf{p}_k = \mathbf{p}_i + \mathbf{p}_j$

Table 3.1

At first sight it may appear that the E algorithm is the most natural, but adding the 4-vectors of massless particles does not produce a massless pseudoparticle, while most theoretical work concerns massless partons, so it is usually felt to be advantageous to ensure that all particles are massless throughout, a requirement responsible for much of the variation in Table 3.1 [24]. All the algorithms are infra-red safe but subject to hadronization corrections varying from small to fairly large. Most of the current interest, therefore, revolves around the two algorithms, E₀ and Durham (or k_T), which both appear to have small (< 5%) corrections [25].

In the next chapter we will be concentrating on the Durham algorithm because this is the only algorithm for which the phase space can be factorized, and, consequently, exponentiation (see section 4.2) is possible [35]

Having divided the observed events into two, three etc. jet events, the ratios

$$R_n(y_c) \equiv \frac{\sigma(n - jet)}{\sigma_{tot}} \quad (3.4)$$

known as jet fractions are actual observables. These observables must obey the condition:

$$\sum_{n=2}^{\infty} R_n(y_c) = 1. \quad (3.5)$$

These have perturbative expansions in the coupling $a = \alpha_s/\pi$ of the form

$$R_2 = 1 - K_{21}a - K_{22}a^2 - K_{23}a^3 + \dots$$

$$\begin{aligned}
R_3 &= K_{31}a + K_{32}a^2 + K_{23}a^3 + \dots \\
R_4 &= K_{42}a^2 + K_{43}a^3 + \dots \\
&\vdots \quad \vdots
\end{aligned}
\tag{3.6}$$

Of the coefficients only the one-loop K_{21} , the tree level K_{31} , K_{42} and K_{53} , [27], the two-loop K_{22} and the one-loop K_{32} are known fully for the common algorithms [28], [15], although approximations of predicted accuracy ($\sim 10\%$) are known for the higher tree-level ones [29]. Relatively simple examination of the formulae in Table 3.1 can reveal relationships between coefficients for different algorithms using kinematics only. Thus K_{31} , is identical for both E0 and JADE, while it is larger for E.

3.2.2 Thrust

An alternative to dividing an event up into jets is to classify its shape. For any event one can define the thrust

$$T = \max \left(\frac{\sum_a |\mathbf{p}_a \cdot \hat{\mathbf{n}}|}{\sum_a |\mathbf{p}_a|} \right)
\tag{3.7}$$

with the sums taken over all the particle 3-momenta in the centre of mass frame and the maximum is found by varying the unit vector $\hat{\mathbf{n}}$. For a large event sample, a distribution in T can be established.

The weighted cross section (setting $\mu^2 = s$) is given by

$$\frac{1}{\sigma_0} (1 - T) \frac{d\sigma}{dT} = \frac{\alpha_s(\sqrt{s})}{2\pi} A_t(T) + \left(\frac{\alpha_s(\sqrt{s})}{2\pi} \right)^2 B_t(T)
\tag{3.8}$$

where σ_0 is the leading order cross section of the reaction

$$e^+e^- \rightarrow \text{hadrons},
\tag{3.9}$$

A_t and B_t are universal functions, which only depend upon the perturbative structure of the theory, and the thrust definition. The leading order contribution, A_t , is known in

analytic form [30], and B_i in the \overline{MS} renormalization scheme can be computed with the NLO e^+e^- package of [15].

3.2.3 Energy-Energy Correlation

The energy-energy correlation was proposed in Ref. [32], and several experimental groups have studied it. It can be defined in terms of the two particle inclusive cross section

$$\frac{d\sigma}{dx_A dx_B d\Omega_1 d\Omega_2}, \quad (3.10)$$

which is the differential inclusive cross section for producing two hadrons A and B with a fraction x_A and x_B of the total initial energy, in the reaction $e^+e^- \rightarrow A + B + X$. We define

$$\frac{1}{\sigma} \frac{d\Sigma}{d\Omega_1 d\Omega_2} = \frac{1}{4} \sum_{AB} \int_0^1 dx_A dx_B \frac{d\sigma}{dx_A dx_B d\Omega_1 d\Omega_2}. \quad (3.11)$$

An equivalent definition in terms of a calorimetric measurement is given by

$$\frac{1}{\sigma} \frac{d\Sigma}{d\Omega_1 d\Omega_2} = \frac{1}{N} \sum_{j=1}^N \left(\frac{1}{s} \frac{dE^j}{d\Omega_1} \right) \left(\frac{1}{s} \frac{dE^j}{d\Omega_2} \right) \quad (3.12)$$

where j refers to the specific event out of N events, and $dE/d\Omega_1$ and $dE/d\Omega_2$ is the energy flow per unit solid angle in the directions Ω_1 and Ω_2 . In practice, it is simpler to consider an average EEC, where one averages over all the orientations of the event, keeping fixed only the angle χ between the directions Ω_1 and Ω_2

$$\frac{1}{\sigma} \frac{d\Sigma}{d\cos\chi} = \int d\Omega_1 d\Omega_2 \frac{1}{\sigma} \frac{d\Sigma}{d\Omega_1 d\Omega_2} \delta(\Omega_1 \cdot \Omega_2 - \cos\chi). \quad (3.13)$$

As usual, we express the cross-section as

$$\frac{\sin^2\chi}{\sigma_0} \frac{d\Sigma}{d\cos\chi} = \frac{\alpha_s(\sqrt{s})}{2\pi} A_{EEC}(\chi) + \left(\frac{\alpha_s(\sqrt{s})}{2\pi} \right)^2 B_{EEC}(\chi) \quad (3.14)$$

where again $\mu^2 = s$. Again the lowest order term A_{EEC} is known explicitly [32], and B_{EEC} in the \overline{MS} renormalization scheme can be computed with the NLO e^+e^- package of [15].

3.2.4 Asymmetry In The Energy-Energy Correlation Function

The asymmetry in the energy-energy correlation function (AEEC) is usually defined as

$$\frac{d\Sigma_{AEEC}}{d\cos\chi}(\chi) = \frac{d\Sigma_{EEC}}{d\cos\chi}(180^\circ - \chi) - \frac{d\Sigma_{EEC}}{d\cos\chi}(\chi) \quad (3.15)$$

It should be noted that this observable has smaller radiative corrections than the EEC itself. The original motivation for this observable [31] was the expectation of smaller non-perturbative $1/Q^2$ effects than were associated with EEC.

3.2.5 The Total Hadronic Cross-Section, R_Z

A fully inclusive and theoretically better understood, measure of purely hadronic events is the total hadronic cross-section, known as the R-ratio when normalised as

$$R \equiv \frac{\sigma(e^+e^- \rightarrow \text{hadrons})}{\sigma(e^+e^- \rightarrow \mu^+\mu^-)}. \quad (3.16)$$

In the \overline{MS} scheme this has the very well-known expansion [17, 16] ($\mu^2 = q^2$, $N_f = 5$)

$$\begin{aligned} R &= \frac{11}{3}(1 + a + 1.409a^2 - 12.8a^3 + O(a^4)) \\ &= \frac{11}{3}(1 + \delta_{QCD}). \end{aligned} \quad (3.17)$$

Close to the Z^0 peak there are substantial electroweak corrections to this QCD result, so the data to be used is that taken at $Q = 34$ GeV where these can be neglected. On

the peak, δ_{QCD} can be checked using the ratio of hadronic and leptonic decay widths

$$\begin{aligned} R_Z &\equiv \frac{\Gamma_{had}}{\Gamma_{LEP}} \\ &= (19.97 \pm 0.03)(1 + \delta_{QCD}) \end{aligned} \quad (3.18)$$

where the numerical factor is electroweak [33]. These massless QCD results can be modified to include heavy quark masses [34], but the changes are small ($K_1 = 1.05$, $K_2^{\overline{MS}} = 0.9$) and insignificant in the present context. Unfortunately, because both R and R_Z are $O(1)$ in α_s , δ_{QCD} is small and its accurate measurement difficult, but they have the advantage that hadronization can be ignored. For the previous observables, while probably being fairly small at the kinematical values that will be used later, the size of the hadronization corrections varies across the distribution [15].

3.3 Review of the Scheme Dependence Problem

3.3.1 Parametrizing RS Dependence

Consider a generic dimensionless LEP observable $R(Q)$, where Q denotes the single dimensionful scale on which it depends, typically the e^+e^- centre of mass energy \sqrt{s} . In RG improved perturbation theory we can write without loss of generality,

$$R(Q) = a + r_1 a^2 + r_2 a^3 + \dots \quad (3.19)$$

where a denotes the RG improved coupling $a \equiv \alpha_s/\pi$. Notice that by dividing any observable depending only on a single dimensionful scale by its possibly dimensionful tree-level perturbative coefficient (which will be RS invariant), and raising to a suitable power, we can always obtain a series of the form (3.19) representing a dimensionless $R(Q)$.

The coupling a and series coefficients r_i depend on the RS employed. Using the

compact notation and conventions introduced by Stevenson [18] a is specified by a β -function equation

$$\frac{da}{d\tau} = -a^2(1 + ca + c_2a^2 + \dots) \equiv -\beta(a), \quad (3.20)$$

where $\tau \equiv b \ln \frac{\mu}{\tilde{\Lambda}}$, with μ the renormalisation scale and $\tilde{\Lambda}$ the dimensional transmutation mass parameter of QCD, here differing from the traditional definition by a factor $(2c/b)^{-c/b}$. b and c are RS invariants dependent only on the number of quark flavours N_f and the number of colours N_c ; for $N_c = 3$ we have $b = (33 - 2N_f)/6$ and $c = (153 - 19N_f)/2(33 - 2N_f)$. In all our LEP determinations we take $N_f = 5$ and assume massless quarks. For massive quarks the scheme dependence discussion will also go through in any mass-independent RS, i.e. one in which the coefficients $c_2, c_3 \dots$ do not depend on the fermion masses [38].

The higher coefficients c_2, c_3, \dots are RS-dependent. Indeed Stevenson [18], extending the work of Stueckelberg and Petermann [39], has shown that one may consistently use the parameters τ, c_2, c_3, \dots to label the renormalization scheme. In the conventional approach when retaining terms up to and including $r_n a^{n+1}$ in equation (3.19) one truncates the β -function of equation (3.20) retaining terms up to and including $c_n a^{n+2}$. On integrating up the truncated equation (3.20) one can define $a^{(n)}(\tau, c_2, \dots, c_n)$ and correspondingly one finds for consistency $r_1(\tau), r_2(\tau, c_2), r_3(\tau, c_2, c_3), \dots, r_n(\tau, c_2, c_3, \dots, c_n)$. In this way the n^{th} -order truncated approximant is also labelled by the scheme variables, $R^{(n)}(\tau, c_2, \dots, c_n)$. Of course when summed to all orders this dependence must cancel and a formally RS-independent sum be obtained.

The formal consistency of perturbation theory further ensures that

$$R^{(n)}(\tau', c'_2, \dots, c'_n) - R^{(n)}(\tau, c_2, \dots, c_n) = k a^{n+2} + O(a^{n+3}), \quad (3.21)$$

so that differences between results in two different RS's are formally effects one order higher in perturbation theory. Of course k depends on $\{\tau, c_2, \dots, c_n\}$ and

$\{\tau', c'_2, \dots, c'_n\}$ and may well not be a small coefficient.

3.3.2 The RS dependence of $R^{(1)}(\tau)$.

Before discussing the general situation further let us consider the simplest $n = 1$, NLO case. This is the accuracy to which all but one of the LEP observables have been calculated.

To NLO we have

$$R^{(1)}(\tau) = a^{(1)}(\tau) + r_1(\tau)(a^{(1)}(\tau))^2 \quad (3.22)$$

where $a^{(1)}(\tau)$ is obtained by integrating up the NLO truncation of equation (3.20)

$$\frac{da}{d\tau} = -a^2(1 + ca). \quad (3.23)$$

With the boundary condition $a^{(1)}(0) = \infty$ one obtains

$$\tau = \frac{1}{a^{(1)}(\tau)} + c \ln \left(\frac{ca^{(1)}(\tau)}{1 + ca^{(1)}(\tau)} \right) \equiv F(a^{(1)}(\tau)) \quad (3.24)$$

where we define the function F for later use, so that $a^{(1)}(\tau) = F^{-1}(\tau)$.

How does $r_1(\tau)$ depend on τ explicitly? To see this, consider two different RS's, RS and RS' . The connection between the corresponding renormalised couplings a and a' will then be such that

$$\beta(a) = \frac{da}{da'} \beta'(a') \quad (3.25)$$

and we can define

$$a' = a(1 + \nu_1 a + \nu_2 a^2 + \dots). \quad (3.26)$$

Inserting (3.26) into the series for $R(a')$ and $R(a)$ in the two RS's and equating coefficients one finds

$$r_1 = \nu_1 + r'_1. \quad (3.27)$$

By integrating up $\beta(a)$ and $\beta'(a')$ as in (3.24) and taking the difference we find

$$\begin{aligned}\tau - \tau' &= \frac{1}{a} + c \ln \left(\frac{ca}{1+ca} \right) + O(a) \\ &\quad - \frac{1}{a'} - c \ln \left(\frac{ca'}{1+ca'} \right) + O(a')\end{aligned}\tag{3.28}$$

where the $O(a)$ and $O(a')$ terms reflect contributions beyond NLO in the β -functions. Using equation (3.26) and equating coefficients of corresponding powers of a gives

$$\tau - \tau' = \nu_1.\tag{3.29}$$

Eliminating ν_1 between equations (3.27) and (3.29) we finally arrive at

$$r_1' - r_1 = \tau' - \tau.\tag{3.30}$$

This implies that

$$r_1(\tau) = \tau + r_1(0).\tag{3.31}$$

It is useful to identify the RS-invariant combination [18]

$$\rho_0 = \tau - r_1(\tau).\tag{3.32}$$

Since $R(Q)$ is a function of a single dimensionful scale Q it follows that

$$\rho_0(Q) = \tau - r_1(\tau) \equiv b \ln \frac{Q}{\bar{\Lambda}},\tag{3.33}$$

with $\rho_0(Q)$ and $\bar{\Lambda}$ RS-invariants. $\bar{\Lambda}$ is dependent only on the particular QCD observable R . This strongly suggests that these quantities should have a *physical* significance as opposed to RS-dependent quantities such as $r_1(\tau)$ and $a(\tau)$ which depend on unphysical parameters. As we shall show in section 3.4 this is indeed the case, $\rho_0(Q)$ and $\bar{\Lambda}$ are

connected with the asymptotic ($Q \rightarrow \infty$) dependence of $R(Q)$ on Q with

$$R(Q)^{Q \rightarrow \infty} \sim \frac{1}{\rho_0(Q)} = \frac{1}{b \ln \frac{Q}{\bar{\Lambda}}}, \quad (3.34)$$

and so $\rho_0(Q)$, or equivalently $\bar{\Lambda}$ could in principle be directly measured given unlimited experimental energies.

This observable-dependent ‘physical’ quantity $\bar{\Lambda}$ is directly connected to $\tilde{\Lambda}_{RS}$ the universal dimensional transmutation parameter of QCD which we are attempting to determine. To see this, recall that

$$\tau = b \ln \frac{\mu}{\tilde{\Lambda}_{RS}} \quad (3.35)$$

is the variable which specifies the RS in NLO. Notice it is *not* sufficient to specify that one has chosen a given renormalisation scale μ in order to specify the RS even at NLO. The renormalisation scheme is specified by τ which involves $\tilde{\Lambda}_{RS}$ as well.

Since $\rho_0(Q)$ is an invariant we see that for two different RS’s, RS and RS'

$$b \ln \frac{\mu}{\tilde{\Lambda}_{RS}} - r_1^{RS}(\mu) = b \ln \frac{\mu}{\tilde{\Lambda}_{RS'}} - r_1^{RS'}(\mu), \quad (3.36)$$

where $r_1^{RS}(\mu)$ denotes the NLO correction evaluated in the renormalisation scheme RS and $r_1^{RS}(\mu) \equiv r_1(\tau)$ with $\tau = b \ln \mu / \tilde{\Lambda}_{RS}$. From equation (3.33) with $\mu = Q$ we find directly that

$$\bar{\Lambda} = \tilde{\Lambda}_{RS} \exp(r_1^{RS}(\mu = Q)/b) \quad (3.37)$$

and so given a NLO calculation in some RS the invariant $\bar{\Lambda}$ is exactly related to the dimensional transmutation parameter $\tilde{\Lambda}_{RS}$. Notice that $r_1^{RS}(\mu = Q)$ is a *Q-independent* quantity.

Rearranging equation (3.36) yields

$$\tilde{\Lambda}_{RS'} = \tilde{\Lambda}_{RS} \exp[(r_1^{RS}(\mu) - r_1^{RS'}(\mu))/b] \quad (3.38)$$

The exponent is a universal μ -independent constant which exactly relates the $\tilde{\Lambda}$'s in the two schemes, given NLO calculations in these two RS's. The implication of this important result [18, 40] is that it does not matter which $\tilde{\Lambda}_{RS}$ we choose to try to extract from the data. If the RS is mass-independent then $\tilde{\Lambda}_{RS}$ will be universal and can be exactly related to $\tilde{\Lambda}_{RS'}$ in any other scheme by a universal factor given exactly if we have a NLO calculation for any observable in both RS's. Thus there is no non-trivial residual scheme dependence implied in our convenient choice of $\tilde{\Lambda}_{\overline{MS}}$ as the fundamental parameter we wish to extract.

As an illustration consider the minimal subtraction (MS) renormalisation procedure and the \overline{MS} or modified minimal subtraction procedure where the $\ln(4\pi) - \gamma_E$ terms present in dimensional regularization are subtracted off ($\gamma_E = 0.5772\dots$ is Euler's constant). For any observable, and independent of μ [41],

$$r_1^{MS}(\mu) - r_1^{\overline{MS}}(\mu) = \frac{b}{2}(\ln(4\pi) - \gamma_E). \quad (3.39)$$

So using equation (3.37) we have

$$\tilde{\Lambda}_{\overline{MS}} = \tilde{\Lambda}_{MS} \exp\left(\frac{\ln(4\pi) - \gamma_E}{2}\right) = 2.66\tilde{\Lambda}_{MS}. \quad (3.40)$$

This relation is independent of N_f or N_c . For the MS and \overline{MS} procedures the higher order RS-dependent β -function coefficients are identical, $c_k^{MS} = c_k^{\overline{MS}}$ ($k \geq 2$). The only difference is in the subtraction procedure and hence in the definition of the renormalisation scale μ . A choice of scale μ using the MS procedure corresponds, therefore, to the *same* renormalization scheme as use of the \overline{MS} procedure with scale 2.66μ .

We are finally in a position to exhibit the explicit dependence of $R^{(1)}(\tau)$ on τ . In fact it is easier to equivalently consider the dependence on $a^{(1)}(\tau)$. Using equation (3.33) to write $r_1(\tau)$ in terms of ρ_0 and τ , and using (3.24) for $a^{(1)}(\tau)$ in terms of τ we find

$$R^{(1)}(\tau) = a^{(1)}(\tau) + (a^{(1)}(\tau))^2 F(a^{(1)}(\tau)) - \rho_0(Q)(a^{(1)}(\tau))^2. \quad (3.41)$$

When plotted versus $a(\tau)$, $R^{(1)}$ has the generic approximately inverted-parabolic shape shown in Figure 3.1, provided that $\rho_0 > 0$. From (3.33) this condition will automatically hold provided that $Q > \bar{\Lambda}$.

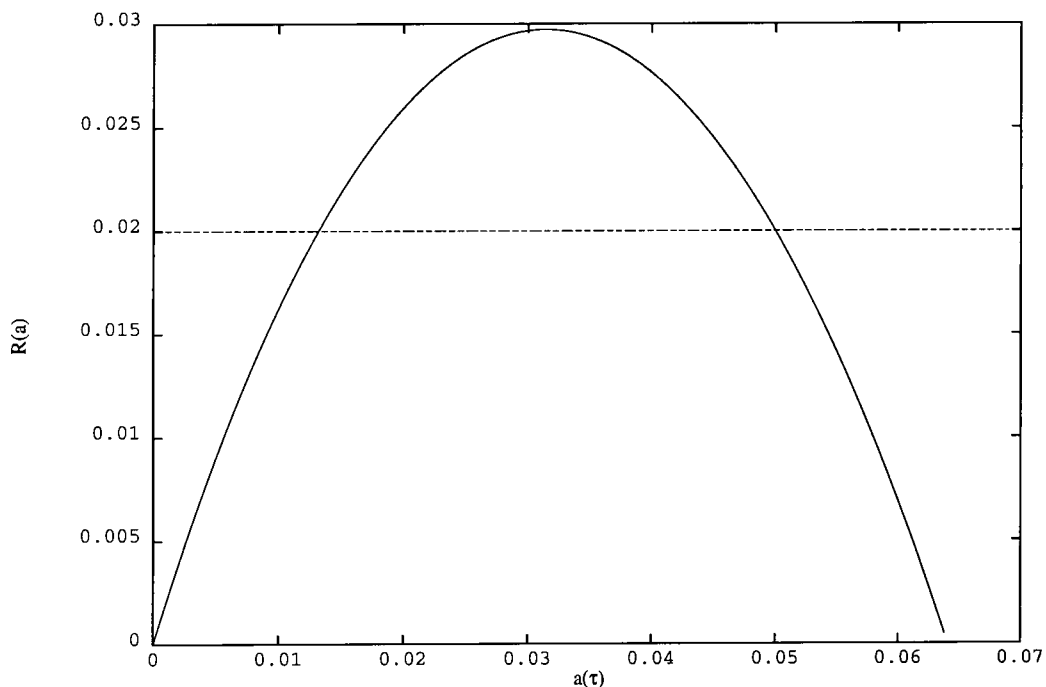


Figure 3.2: The generic approximately inverted-parabolic behaviour of the NLO approximant $R^{(1)}(\tau)$ versus $a(\tau)$. The figure is plotted for $\rho_0 = 25$ and $N_f = 5$. The dashed line represents measured data (see text).

3.3.3 RS dependence of $r_n(\tau, c_2, \dots, c_n)$

Before we discuss this NLO scheme dependence in more detail let us complete the picture by discussing the explicit scheme dependence of the higher coefficients $r_2(\tau, c_2)$, $r_3(\tau, c_2, c_3)$, ... as well. Integrating up the β -function truncated at n^{th} order with an infinite constant of integration (related to the definition of $\tilde{\Lambda}$, see 3.4) we obtain,

analogous to equation (3.24) ,

$$\begin{aligned} \tau &= \frac{1}{a^{(n)}} + c \ln \left(\frac{ca^{(n)}}{1 + ca^{(n)}} \right) + \int_0^{a^{(n)}} dx \left[-\frac{1}{x^2 B^{(n)}(x)} + \frac{1}{x^2(1 + cx)} \right], \\ B^{(n)}(x) &\equiv (1 + cx + c_2x^2 + c_3x^3 + \dots + c_nx^n). \end{aligned} \quad (3.42)$$

This transcendental equation can then be solved explicitly for $a^{(n)}(\tau, c_2, \dots, c_n)$.

To obtain the explicit RS dependence of the r_i it is convenient to identify a special RS, the effective charge (EC) scheme [19, 20], in which $r_1 = r_2 = r_3 = \dots = r_n = 0$. Then $R^{(n)} = a^{(n)}$ in this scheme, and the coupling constant is the physical observable. This choice of RS will correspond to particular values of the scheme parameters, $\tau_{EC} = \rho_0, c_2^{EC} \equiv \rho_2, c_3^{EC} \equiv \rho_3 \dots$

The fact that $\tau_{EC} = \rho_0$ follows directly from equation (3.33) , $r_1(\tau) = \tau - \rho_0$ then $r_1(\tau_{EC}) = \tau_{EC} - \rho_0 = 0 \Rightarrow \tau_{EC} = \rho_0$. From equation (3.25) we have that for two RS's, barred and unbarred,

$$\bar{\beta}(\bar{a}) = \frac{d\bar{a}}{da} \beta(a(\bar{a})). \quad (3.43)$$

If the barred RS is chosen to be the EC scheme then

$$\bar{\beta}(\bar{a}) \equiv \rho(\bar{a}) = \bar{a}^2(1 + c\bar{a} + \rho_2\bar{a}^2 + \dots + \rho_k\bar{a}^k + \dots), \quad (3.44)$$

with $\bar{a} = R$. Then (3.43) gives

$$\rho(R) = \beta(a(R)) \frac{dR}{da}, \quad (3.45)$$

where $a(R)$ is the inverted perturbation series. By expanding out the right-hand side as a power series in R and equating coefficients we obtain [42]

$$\begin{aligned} \rho_2 &= c_2 + r_2 - r_1c - r_1^2 \\ \rho_3 &= c_3 + 2r_3 - 4r_1r_2 - 2r_1\rho_2 - r_1^2c + 2r_1^3 \\ \vdots & \quad \vdots \end{aligned} \quad (3.46)$$

These objects are Q -independent RS invariants constructed from the r_i and c_i in any RS. For instance given NLO and NNLO calculations of $r_1^{\overline{MS}}(Q), r_2^{\overline{MS}}(Q)$ and since $c_2^{\overline{MS}}$ is known [43, 44], one can construct

$$\rho_2 = c_2^{\overline{MS}} + r_2^{\overline{MS}} - r_1^{\overline{MS}} c - (r_1^{\overline{MS}})^2. \quad (3.47)$$

As we shall see in the next section just like the NLO invariant ρ_0 , the NNLO and higher ρ_2, ρ_3, \dots invariants have a physical significance, whereas quantities such as $r_1^{\overline{MS}}(Q), c_2^{\overline{MS}}$ are intermediate RS-dependent quantities which should be eventually eliminated in favour of RS invariants.

Having obtained ρ_2, ρ_3 from NNLO, and higher order calculations in any convenient RS, we can exhibit the explicit τ, c_2, c_3, \dots dependence of the perturbative coefficients by rearranging equation (3.46). We have that

$$\begin{aligned} r_1(\tau) &= (\tau - \rho_0), \\ r_2(\tau, c_2) &= (\tau - \rho_0)^2 + c(\tau - \rho_0) + (\rho_2 - c_2), \\ r_3(\tau, c_2, c_3) &= (\tau - \rho_0)^3 + \frac{5}{2}c(\tau - \rho_0)^2 + (3\rho_2 - 2c_2)(\tau - \rho_0) + \frac{1}{2}(\rho_3 - c_3) \\ &\vdots \quad \quad \quad \vdots \end{aligned} \quad (3.48)$$

The result for $r_n(\tau, c_2, \dots, c_n)$ is a polynomial in $(\tau - \rho_0)$ of degree n with coefficients involving $\rho_n, \rho_{n-1}, \dots, c$ and c_2, c_3, \dots, c_n , such that $r_n(\rho_0, \rho_2, \dots, \rho_n) = 0$.

3.3.4 NLO extraction of $\alpha_s(M_Z)$.

Let us now return to Figure 3.2 and discuss how one might attempt to use it to extract $\tilde{\Lambda}_{\overline{MS}}$ or $\alpha_s(M_Z)$ in the \overline{MS} scheme.

Notice first that the curve $R^{(1)}(\tau)$ of equation (3.41) is a *universal* function of τ and ρ_0 (for given fixed N_f), where the value of the invariant ρ_0 depends on the particular observable R . ρ_0 is of course directly related to $\tilde{\Lambda}_{\overline{MS}}$ given a NLO calculation of

$r_1^{\overline{MS}}(Q)$, with

$$\rho_0 = b \ln \frac{Q}{\tilde{\Lambda}_{\overline{MS}}} - r_1^{\overline{MS}}(Q). \quad (3.49)$$

$R^{(1)}(\tau)$ has a maximum at $a(\tau) \simeq 1/\rho_0$ ($\tau \simeq \rho_0$) where $R^{(1)}(\rho_0) \simeq 1/\rho_0$. The full-width at half-maximum in $a(\tau)$ is approximately $\sqrt{2}/\rho_0$. $R^{(1)}$ vanishes at $a = 0$ ($\tau = \infty$) and at $a(\tau) \simeq 2/\rho_0$ ($\tau \simeq \rho_0/2$). For comparison Figure 3.2 is drawn with $\rho_0 = 25$ and $N_f = 5$.

Let us suppose that the horizontal dashed line in Figure 3.2 represents the measured experimental data. If ρ_0 is sufficiently small that the maximum $R^{(1)} \simeq 1/\rho_0$ lies above the data then the curve will cut the data at two scales τ_1, τ_2 (as illustrated). Conversely, if ρ_0 is made larger the curve will be below the data line. Thus an infinite set of τ, ρ_0 pairs fit the data perfectly. If we wish to *measure* ρ_0 (and hence $\tilde{\Lambda}_{\overline{MS}}$) we must *specify* τ . This is the NLO scheme dependence problem. At NNLO one would have a surface $R^{(2)}(\tau, c_2)$ and to extract ρ_0 one would need to specify τ and c_2 , and so on with one extra unphysical parameter for each order in perturbation theory. At least in NLO for a given value of ρ_0 ($\tilde{\Lambda}_{\overline{MS}}$) there is a *maximum* possible $R^{(1)}$.

In NNLO and higher one can show [45] that for a given value of ρ_0 ($\tilde{\Lambda}_{\overline{MS}}$) there exists a choice of τ, c_2, \dots, c_n such that $R^{(n)}$ has *any* desired positive value. Thus, for *any* $\tilde{\Lambda}_{\overline{MS}}$ we can choose a sequence of schemes such that $R^{(2)} = R^{(3)} = \dots = R^{(n)} = R_{exp}$, the experimentally measured value.

Various ‘‘solutions’’ of the scheme dependence problem, i.e. motivations for particular choices of τ, c_2, \dots, c_n have been proposed.

(1) *Principle of Minimal Sensitivity (PMS)* [18]

The idea here is that since the exact (all-orders) result is independent of $\tau, c_2, c_3, \dots, c_n$ one should choose the n^{th} -order approximation $R^{(n)}(\tau, c_2, \dots, c_n)$ to mimic this property and be as insensitive as possible to the chosen value of the unphysical parameters. That

is one arranges that

$$\left. \frac{\partial R^{(n)}}{\partial \tau} \right|_{\tau=\bar{\tau}} = \left. \frac{\partial R^{(n)}}{\partial c_2} \right|_{c_2=\bar{c}_2} = \dots = \left. \frac{\partial R^{(n)}}{\partial c_n} \right|_{c_n=\bar{c}_n} = 0 \quad (3.50)$$

and the PMS scheme is specified by $\bar{\tau}, \bar{c}_2, \dots, \bar{c}_n$. At NLO one has to solve

$$\left. \frac{\partial R^{(1)}}{\partial \tau} \right|_{\tau=\bar{\tau}} = 0, \quad (3.51)$$

and this corresponds to solving the transcendental equation

$$\frac{1}{a} + c \ln \left[\frac{ca}{1+ca} \right] + \frac{1}{2} \frac{c}{1+ca} = \rho_0. \quad (3.52)$$

The solution $a(\bar{\tau}) = \bar{a}$ then gives

$$R_{PMS}^{(1)} = \frac{\bar{a}(1 + \frac{1}{2}c\bar{a})}{(1 + c\bar{a})}. \quad (3.53)$$

The stationary PMS point of $R^{(1)}(\tau)$ is the maximum at $\tau = \bar{\tau} \simeq \rho_0 - c/2$ (this is a somewhat better approximation than the cruder $\tau \simeq \rho_0$ given previously for the position of the maximum). ρ_0 is adjusted so that $R_{PMS}^{(1)} = R_{exp}$.

(2) Effective Charge (EC) Scheme [19, 20]

This corresponds to a choice of scheme such that $r_1 = r_2 = \dots = r_n = 0$, hence $a^{(n)} = R^{(n)}$ is an effective charge. As we have seen the scheme parameters are then $\{\rho_0, \rho_2, \rho_3, \dots, \rho_n\}$, where the ρ_i are the RS-invariants in equation (3.46). Once these have been computed up to ρ_n from higher-order calculations in any technically-convenient RS (e.g. \overline{MS}) they can be inserted in the integrated β -function equation (3.42) which can then be solved with $a^{(n)} = R$ for given ρ_0 . ρ_0 can then be obtained by requiring $R = R_{exp}$.

This particular approach is sometimes also referred to as the fastest apparent convergence criterion. In this language it appears rather artificial, but as we shall emphasise in section 3.4 its advantage is that the all-orders coupling constant *and* β -function are experimentally observable physical quantities, allowing a *non-perturbative* approach to supplement $\tilde{\Lambda}_{\overline{MS}}$ measurement, and a physical definition of the uncertainty.

It should be emphasised that EC and PMS predictions in NLO are very similar since, as we have seen, $\tau_{EC} = \rho_0$, $\tau_{PMS} \simeq \rho_0 - c/2$. It is also true that in NNLO EC and PMS remain close to each other [46, 47]. For the PMS approach, however, the coupling constant and β -function are unphysical quantities, and it is not clear even that their all-orders versions are defined, given the complex nature of the coupled equations which must be solved.

(3) *Physical Scale* [48]

According to this viewpoint the renormalization scale should be chosen to be close to the physical scale in the problem, $\mu = Q$. If predictions in the vicinity of $\mu = Q$ are strongly μ -dependent then this is supposedly an indication that the perturbation series is intrinsically badly behaved. This viewpoint is usually justified by noting that perturbative coefficients in higher orders will be polynomials in $\ln \mu/Q$,

$$r_n = \sum_{l=0}^n K_{nl} (b \ln \frac{\mu}{Q})^l. \quad (3.54)$$

To avoid unnecessarily large logarithms one should therefore set $\mu \simeq Q$. Whilst this is true as far as it goes, it tacitly assumes that the NLO RS dependence is completely given by the dependence on the renormalisation scale. In fact as we have seen $r_n(\tau, c_2, \dots, c_n)$ where $\tau = b \ln \mu / \tilde{\Lambda}_{RS}$ so the coefficients K_{nl} in (3.54) will depend on $\tilde{\Lambda}_{RS}$. The meaning of μ of course depends for instance on whether it is $\mu(\overline{MS})$ or $\mu(MS)$. In

contrast we have from (3.48) that

$$r_n(\tau, c_2, \dots, c_n) = \sum_{l=0}^n \tilde{K}_{nl} (\tau - \rho_0)^l. \quad (3.55)$$

So to avoid unnecessarily large terms we should clearly choose $\tau \simeq \rho_0$, the effective charge scheme! To make contact with (3.54) notice that

$$(\tau - \rho_0) = \left[b \ln \frac{\mu}{Q} + r_1^{RS}(Q) \right] = b \ln \left[\frac{\mu}{Q} e^{r_1^{RS}(Q)/b} \right]. \quad (3.56)$$

So we can write (3.55) as

$$r_n(\tau, c_2, \dots, c_n) = \sum_{l=0}^n \tilde{K}_{nl} \left[b \ln \left(\frac{\mu e^{r_1^{RS}(Q)/b}}{Q} \right) \right]^l \quad (3.57)$$

In (3.55) and (3.57) the coefficients \tilde{K}_{nl} do not depend on the NLO RS choice, only on c_2, c_3, \dots and the RS invariants ρ_2, ρ_3, \dots , whereas in (3.54) the K_{nl} will depend on $r_1^{RS}(Q)$ and so have a hidden dependence on the NLO RS choice which is customarily ignored in the usual ‘physical scale’ argument. Applying the argument to (3.57) instead one would infer that one should set $\mu \simeq Q e^{-r_1^{RS}(Q)/b} = Q \tilde{\Lambda}_{RS} / \bar{\Lambda}$, which of course corresponds to the effective charge scheme, $\tau = \rho_0$. For particular cases the extra factor may be large.

Recall that $\bar{\Lambda}$ is an RS-invariant characterising how the observable runs with Q asymptotically. Different observables will have different $\bar{\Lambda}$'s. If it happens that $\tilde{\Lambda}_{RS} \simeq \bar{\Lambda}$ ($r_1^{RS}(Q) \simeq 0$) then predictions will be stable and large logarithms avoided for $\mu \simeq Q$, but no special physical significance should be accorded to this fact. It is always possible to modify the subtraction procedure so that $\tilde{\Lambda}_{RS} = \bar{\Lambda}$, since $\tilde{\Lambda}$'s in different RS's are related according to (3.38).

We conclude that a modified ‘avoidance of unnecessarily large logarithms’ physical scale argument which correctly labels the NLO RS dependence actually leads to the effective charge scheme, $\tau = \rho_0$.

(4) Fitting μ and $\tilde{\Lambda}$ to the data

For most of the LEP observables we have a differential distribution in a kinematical variable rather than a single experimental data value as in Figure 3.2. For instance a thrust distribution in the thrust variable T , or a multijet rate in the jet resolution cut y_c . Denoting such a generic kinematical variable by λ , we should really add an extra perpendicular axis to Figure 3.2 and consider the λ dependence as well, $R^{(1)}(\tau, \lambda)$. The NLO coefficient will also depend on λ and so for a given choice of $\tilde{\Lambda}_{\overline{MS}}$ we will have $\rho_0(\lambda)$ from (3.49). If $\tilde{\Lambda}_{\overline{MS}}$ is sufficiently large then the experimental data $R_{exp}(\lambda)$ will intersect $R^{(1)}(\tau, \lambda)$ for at least one τ value for any λ and so the data can be fitted perfectly with a suitable λ -dependent RS parameter choice $\tau(\lambda)$. In general there will be two intersection points as in Figure 3.2 and so two functions $\tau_1(\lambda), \tau_2(\lambda)$ will fit the data perfectly. Since this can be done for any suitably large $\tilde{\Lambda}_{\overline{MS}}$ there is no unique best fit.

The OPAL analysis [5, 6] uses a mixture of approaches (3) and (4). The data for each observable over a range of the corresponding kinematical variable is compared with the NLO prediction with the \overline{MS} scale chosen as $\mu = M_Z$, and a best fit for $\tilde{\Lambda}_{\overline{MS}}$ performed. The resulting $\alpha_S(M_Z)$ values are shown in Figure 3.3(a), reproduced from reference [12]. There is evidently a considerable scatter in the α_S values obtained.

One then performs a simultaneous best fit for μ and $\tilde{\Lambda}_{\overline{MS}}$ for each observable over a range of the kinematical variables. This provides a second $\alpha_S(M_Z)$ value. The quoted central value of $\alpha_S(M_Z)$ is then taken to lie mid-way between these extremes (perhaps modified by hadronization) and the difference between them is taken as indicative of the size of the uncalculated higher-order corrections. By enlarging the ‘scheme dependence error’ in this way one obtains greater apparent consistency between different observables as shown in Figure 3.3(b).

In our view one learns nothing useful from an analysis of this kind. Consider Figure 3.3(a) and the considerable scatter of α_S values obtained from different observables

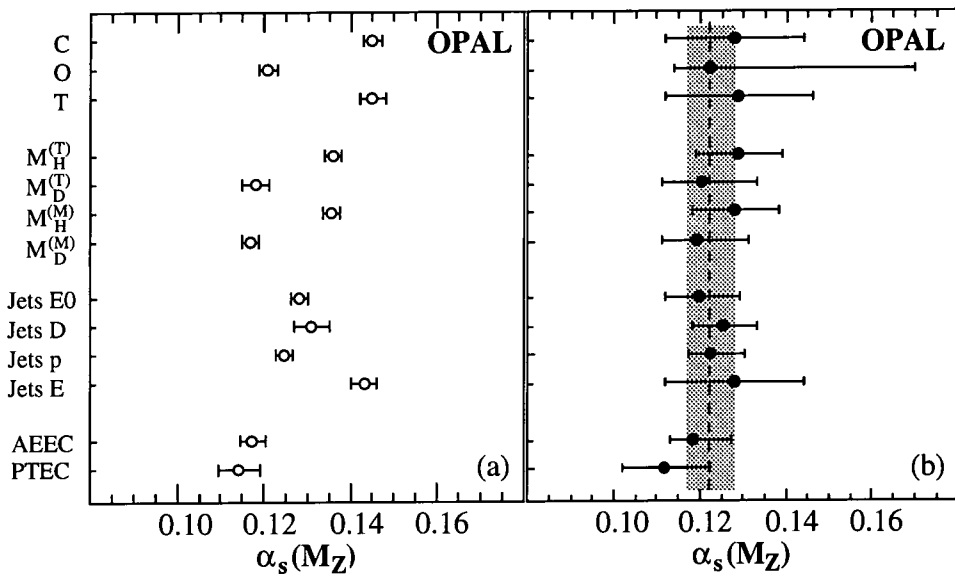


Figure 3.3: (a) $\alpha_s(M_Z)$ obtained by fitting NLO perturbative calculations with $\mu = M_Z$ to OPAL data. (b) As (a) but with enlarged ‘theoretical errors’ using $\mu = M_Z$ and fits to data, as described in the text. Reproduced from reference [11].

fitted with $\mu = M_Z$. Choosing $\mu = M_Z$ means that from (3.57) the higher-order coefficients are given by

$$r_n(\mu = M_Z) = \sum_{l=0}^n \tilde{K}_{nl} (r_1^{\overline{MS}}(M_Z))^l \quad (3.58)$$

where the \tilde{K}_{nl} depend on the invariants $\rho_2, \rho_3, \dots, \rho_n$ and on the NNLO and higher RS parameters c_2, c_3, \dots, c_n . We have tabulated in Table 3.2 the $r_1^{\overline{MS}}(M_Z)$ values for some of the observables introduced in section 3.2 at particular values of the kinematical parameters using the NLO package of reference [15], and in the case of R_Z the NLO calculations of [41]. One sees that they are large and rather scattered, e.g for the jet rates $r_1^{\overline{MS}}(M_Z) \sim 10$ which results in rather small EC (or PMS) scales, $\mu_{EC} \sim 0.07 M_Z$. As emphasized earlier no physical significance attaches to these small scales, since the scale itself is just an artifact of the unphysical subtraction procedure employed. Thus from (3.58) one may expect large and rather scattered higher order corrections for the different observables with $\mu = M_Z$, which translates itself into the expectation of scattered values of $\alpha_S(M_Z)$, which indeed are observed.

Observable		$r_1^{\overline{MS}}(M_Z)$
T	T=0.9	13.41
$R_2(E_0)$	$y_{cut} = 0.08$	10.22
$R_3(E_0)$	$y_{cut} = 0.08$	10.09
$R_2(D)$	$y_{cut} = 0.08$	7.23
$R_3(D)$	$y_{cut} = 0.08$	7.15
EEC	$\chi = 60^\circ$	11.30
AEEC	$\chi = 60^\circ$	5.13
R_Z		1.41

Table 3.2: NLO coefficients $r_1^{\overline{MS}}(M_Z)$ from [15] for various LEP observables at the particular values of the kinematical variables noted.

If we instead choose $\mu = M_Z e^{-r_1^{\overline{MS}}(M_Z)/b} \equiv \mu_{EC}$ (the effective charge scale) for each observable then the higher order coefficients are given by

$$r_n(\mu = \mu_{EC}) = \tilde{K}_{n0} \quad (3.59)$$

where \tilde{K}_{n0} does not depend on the NLO RS choice (τ), only on the NNLO and higher RS parameters and the RS-invariants ρ_2, ρ_3, \dots . Any scatter now observed in the extracted $\tilde{\Lambda}_{\overline{MS}}$ or $\alpha_S(M_Z)$ for different observables will be attributable to these NNLO and higher RS invariants being large, and not to the scatter due to the NLO scheme dependence logarithms involving $r_1^{\overline{MS}}(M_Z)$, which are avoided by the choice $\mu = \mu_{EC}$. As we shall discuss in section 3.4 there is still scatter when this is done but it is somewhat reduced.

With the choice $\mu = M_Z$ predictable scatter due to *avoidable* already known NLO scheme dependence logarithms is superimposed on top of the interesting scatter due to the size of the NNLO and higher invariants which is telling us about NNLO and higher order uncalculated corrections. The choice $\mu = \mu_{EC}$ removes the predictable scatter and provides genuine information on the interesting NNLO and higher-order uncalculated corrections.

The \overline{MS} scales obtained by fitting to the data for an observable over some range of the associated kinematical parameters tend to be considerably smaller than M_Z , as for the EC or PMS scale. Typically for values of the kinematical variable λ well away from the 2-jet region where large logarithms will be important, $\rho_0(\lambda)$ and $r_1(\lambda)$ do not vary strongly with λ . This means that one cannot obtain best fits over such a range of λ . It is only by including the 2-jet region that one can obtain stable best fits, but then fitting for a λ -independent scale over a range where $\rho_0(\lambda)$ and $r_1(\lambda)$ (and presumably uncalculated higher order corrections) are strongly λ -dependent represents a rather severe compromise, and it is not obvious what one learns.

In conclusion, we believe that the standard NLO analyses used to extract α_S from LEP data do not serve to disentangle the genuinely new and interesting NNLO and

higher order uncalculated corrections from predictable higher order corrections connected with the choice of RS at NLO. The resulting quoted values of $\alpha_S(M_Z)$ (or $\tilde{\Lambda}_{\overline{MS}}$) with attendant scheme dependence uncertainties therefore reflect the ad hoc way in which they were extracted, rather than the actual values of these parameters. In contrast, by choosing the effective charge scale for each observable one exposes the relative importance of uncalculated NNLO and higher corrections. An effective charge formalism which can be supplemented with non-perturbative information is described in the next section.

3.4 The Effective Charge Formalism

3.4.1 The Q dependence of $R(Q)$

For the dimensionless QCD observable $R(Q)$ we can define

$$\frac{dR}{d \ln Q} \equiv \xi(R). \quad (3.60)$$

$dR/d \ln Q$ and hence $\xi(R(Q))$ are, at least in principle, experimentally observable quantities, although collider experiments are usually designed to make high-statistics observations at a fixed energy Q rather than examining the detailed running of observables with energy. To make contact with the standard perturbative approach we note that (3.60) is the β -function equation in the effective charge scheme where the coupling $a = R(Q)$ and the β -function is $\rho(R)$ as defined in equation (3.44). So we have

$$\frac{dR}{d \ln Q} = \xi(R(Q)) = -b\rho(R) \approx -bR^2(1+cR+\rho_2R^2+\dots)+e^{-S/R}R^\delta(K_0+K_1R+\dots). \quad (3.61)$$

The effective charge β -function $\rho(R)$ may be regarded as a physical observable. As measured from data it will include a resummed version of the (perhaps asymptotic)

formal perturbative series exhibited in (3.61) together with the non-perturbative terms involving $e^{-1/R}$ which are invisible in perturbation theory. (Here $S, \delta, K_0, K_1, \dots$ are observable-dependent constants which we shall not specify further [51].) Hence by comparing with data one can test how well the first few terms of the perturbative series serve to represent the observed running of $R(Q)$. That is, from measurements of $R_{exp}(Q)$ and $dR_{exp}(Q)/d \ln Q$, one can test the extent to which

$$\frac{dR_{exp}}{d \ln Q} \approx -bR_{exp}^2(1 + cR_{exp}) \quad (3.62)$$

describes the data. A marked discrepancy would either indicate the importance of the NNLO invariant ρ_2 and higher terms, or the relative importance of the non-perturbative contributions, or both.

Given a collider program dedicated to the investigation of the Q -dependence of observables the above tests would indeed be powerful and useful. The focus of present studies, however, is the accurate measurement of R at fixed Q , i.e. $Q = M_Z$, and the comparison of these results with NLO matrix element calculations in order to extract $\tilde{\Lambda}_{\overline{MS}}$. To obtain $R(Q)$ we clearly need to integrate equation (3.60). The boundary condition will be the assumption of asymptotic freedom, that is $R(Q) \rightarrow 0$ as $Q \rightarrow \infty$, which corresponds to the requirement that $\xi(R(Q)) < 0$ for $Q > Q_0$, with Q_0 some suitably low energy. (Equivalently, $\rho(R(Q)) > 0$ for $Q > Q_0$, assuming $b > 0$ or $N_f < 33/2$ for $N_C = 3$ QCD.) Any zero of $\xi(R(Q))$, $\xi(R^*) = 0$, say, would correspond to $R(Q) \rightarrow R^*$ as $Q \rightarrow \infty$ and ultraviolet fixed point behaviour.

Integrating equation (3.60) we obtain

$$\ln \frac{Q}{\bar{\Lambda}} = \int_0^{R(Q)} \frac{1}{\xi(x)} dx + (infinite\ constant) \quad (3.63)$$

where $\bar{\Lambda}$ is a finite constant which depends on the way the infinite constant is chosen.

The infinite constant can be chosen to be

$$(\text{Infinite constant}) = - \int_0^\infty \frac{dx}{\eta(x)}, \quad (3.64)$$

where $\eta(x)$ is any function which has the same $x \rightarrow 0$ behaviour as $\xi(x)$. We know from equation (3.61) that $\xi(x)$ has the universal $x \rightarrow 0$ behaviour $\xi(x) = -b\rho(x) \approx -bx^2(1+cx)$ so we choose $\eta(x) = -bx^2(1+cx)$. Inserting this choice for $\eta(x)$ and rearranging equation (3.63) we find

$$b \ln \frac{Q}{\bar{\Lambda}} = \int_{R(Q)}^\infty \frac{dx}{x^2(1+cx)} + \int_0^{R(Q)} dx \left[-\frac{1}{\rho(x)} + \frac{1}{x^2(1+cx)} \right]. \quad (3.65)$$

The first integral on the right-hand side is just $F(R)$ where F is the function defined in equation (3.24),

$$F(x) \equiv \frac{1}{x} + c \ln \left[\frac{cx}{1+cx} \right]. \quad (3.66)$$

We define for later convenience

$$\Delta\rho_0(Q) \equiv \int_0^{R(Q)} dx \left[-\frac{1}{\rho(x)} + \frac{1}{x^2(1+cx)} \right]. \quad (3.67)$$

Notice that despite appearances the integrand of $\Delta\rho_0$ is regular at $x = 0$. Then we have

$$F(R(Q)) = b \ln \frac{Q}{\bar{\Lambda}} - \Delta\rho_0(Q). \quad (3.68)$$

As $Q \rightarrow \infty$, $R(Q) \rightarrow 0$ so that $\Delta\rho_0 \rightarrow 0$ and thus asymptotically

$$F(R(Q)) \approx b \ln \frac{Q}{\bar{\Lambda}} \quad (3.69)$$

with the constant of integration given by

$$\bar{\Lambda} = \lim_{Q \rightarrow \infty} Q \exp(-F(R(Q))/b). \quad (3.70)$$

Notice that in arriving at (3.68) we did not need to refer to perturbation theory, except to assume the asymptotic $x \rightarrow 0$ ($Q \rightarrow \infty$) behaviour $\xi(R(Q)) \approx -bR^2(1 + cR)$. Despite this, the constant $\bar{\Lambda}$ obtained with the particular choice $\eta(x) = -bx^2(1 + cx)$ is precisely the $\bar{\Lambda}$ introduced in equation (3.33). That is

$$\bar{\Lambda} = \tilde{\Lambda}_{\overline{MS}} \exp(r_1^{\overline{MS}}(\mu = Q)/b). \quad (3.71)$$

We can see this immediately since if a denotes the coupling in the RS with $\mu = Q$ using the \overline{MS} subtraction procedure in NLO, and with higher order β -function coefficients zero [52] we have

$$b \ln \frac{Q}{\tilde{\Lambda}_{\overline{MS}}} = F(a) \quad (3.72)$$

giving a well-defined all-orders coupling. Further

$$R = a + r_1^{\overline{MS}}(Q)a^2 + \dots \quad (3.73)$$

$a \rightarrow 0$ as $Q \rightarrow \infty$, so asymptotically as $Q \rightarrow \infty$ we have

$$F(R) \approx F(a) - r_1^{\overline{MS}}(Q) + \dots \quad (3.74)$$

where the ellipsis denotes terms which vanish as $Q \rightarrow \infty$. Inserting (3.74) into (3.70) and using (3.72) we find (3.71) as $Q \rightarrow \infty$.

So finally we have

$$\begin{aligned} F(R(Q)) &= b \ln \frac{Q}{\bar{\Lambda}} - \Delta\rho_0(Q) \\ &= b \ln \frac{Q}{\tilde{\Lambda}_{\overline{MS}}} - r_1^{\overline{MS}}(Q) - \Delta\rho_0(Q) \\ &= \rho_0(Q) - \Delta\rho_0(Q). \end{aligned} \quad (3.75)$$

We could, of course, have written down the result of equation (3.75) perturbatively in the EC scheme at once by simply using the integrated beta-function equation of

equation (3.42) with $\tau = \rho_0$, $B^{(n)} = \rho^{(n)} = 1 + cx + \rho_2 x^2 + \dots + \rho_n x^n$, and $a^{(n)} = R^{(n)}$. However, our purpose here has been to stress that equation (3.75) holds *beyond perturbation theory* for the measured observable $R(Q)$ and $\Delta\rho_0(Q)$ constructed from the measured running of $R(Q)$, $dR(Q)/d\ln Q = -b\rho(R(Q))$. That is, we can write a *non-perturbative* closed expression *exactly* relating the universal constant $\tilde{\Lambda}_{\overline{MS}}$ to observable quantities.

Since $\Delta\rho_0(Q_0)$ involves an integral in $R(Q)$ between $R(Q_0)$ and 0, to actually measure it would require knowledge of $R(Q)$ (equivalently $dR/d\ln Q$) on the full range $[Q_0, \infty]$. We of course only know $R(Q)$ on some finite energy range, so if we want to obtain $\tilde{\Lambda}_{\overline{MS}}$ from equation (3.75) and measurements of $R(Q)$ there will always be an uncertainty related to our lack of knowledge about the behaviour of $R(Q)$ beyond the highest energy reached, or correspondingly related to our lack of knowledge about $\rho(R)$ for $R < R(Q_0)$, with Q_0 the highest energy reached. As we shall discuss in sub-section 3.4.3 we can use measurements of the running of $R(Q)$ to determine $\rho(R)$ in the vicinity of $R = R(Q_0)$, and perturbative QCD calculations to determine $\rho(R)$ in the vicinity of $R = 0$. Putting these two pieces of information together we can make unambiguous statements about the validity of perturbation theory and the nature of the function $\rho(R)$, which can assist our attempts to determine $\tilde{\Lambda}_{\overline{MS}}$.

Notice the fundamental significance of the NLO perturbative coefficient $r_1^{\overline{MS}}(Q)$ in all of this. Knowledge of the full behaviour of $R(Q)$ at large Q would allow one to extract $\overline{\Lambda}$ from equation (3.70), but this by itself is *observable-dependent* and so one would not test QCD. A test is only possible if one also knows $r_1^{\overline{MS}}(Q)$ (from Feynman diagram calculations) and can then obtain the *universal* $\tilde{\Lambda}_{\overline{MS}}$ from equation (3.71).

The universal $\tilde{\Lambda}_{\overline{MS}}$ of course depends on the number of active quark flavours, $\tilde{\Lambda}_{\overline{MS}}^{(N_f)}$; the RS invariants b and c occurring in equation (3.75) also involve N_f . Since $\tilde{\Lambda}_{\overline{MS}}$ in equation (3.75) involves the $Q \rightarrow \infty$ behaviour of $R(Q)$, one might wonder what value for N_f should be taken. With three generations of quarks, $N_f = 6$ presumably represents the asymptotic number of active flavours and so, introducing the notation

$b(N_f)$, $c(N_f)$, the function $\eta(x)$ in equation (3.64) should be chosen as $\eta(x) = -b(6)x^2(1 + c(6)x)$.

So finally (3.75) with the explicit N_f dependence exhibited becomes

$$\left\{ \frac{1}{R(Q)} + c(6) \ln \left[\frac{c(6)R(Q)}{1 + c(6)R(Q)} \right] \right\} \quad (3.76)$$

$$= b(6) \ln \frac{Q}{\tilde{\Lambda}_{\overline{MS}}^{(6)}} - r_1^{\overline{MS}}(Q, N_f = 6) - \int_0^{R(Q)} dx \left[\frac{b(6)}{\xi(x)} + \frac{1}{x^2(1 + c(6)x)} \right].$$

Obviously the strict asymptotic $Q \rightarrow \infty$ behaviour of $R(Q)$ and $dR/d \ln Q = \xi(R(Q))$ is an idealized concept since we could never actually measure it. For instance, it presumably makes no sense to consider QCD in isolation beyond the GUT energy scale. Rather than using (3.76) for LEP observables where we have $N_f = 5$ active flavours, it makes more sense to consider the equation for $R(Q)$ in a world with $N_f = 5$ active flavours, replacing $b(6)$, $c(6)$, and $\tilde{\Lambda}_{\overline{MS}}^{(6)}$ in (3.76) by $b(5)$, $c(5)$, and $\tilde{\Lambda}_{\overline{MS}}^{(5)}$. The decoupling theorem [53] means that we can consider an $N_f = 5$ version of QCD for energies below top threshold. As we shall discuss we shall be interested in how the observed Q -evolution of $R(Q)$ at LEP energies compares with its asymptotic $Q \rightarrow \infty$ evolution in a *hypothetical* world with $N_f = 5$ flavours. This will decide how accurately we can determine the universal constant $\tilde{\Lambda}_{\overline{MS}}^{(5)}$. To have any chance of determining $\tilde{\Lambda}_{\overline{MS}}^{(6)}$ we would require measurements around the top threshold and at higher energies, which we do not currently possess.

A further subtlety connected with the effective charge formalism concerns the fact that one can always define effective charges other than $a = R$. More generally one could define $f(a) = R$ where $f(a) = a + f_2 a^2 + f_3 a^3 + \dots$ is any analytic function of a . Chyla has suggested that this arbitrariness is just the scheme dependence problem in disguise [49]. In our view this is incorrect (see also Grunberg's response [50]). In fact the arbitrariness in defining the effective charge is completely equivalent to redefining the observable to be $\tilde{R} = f^{-1}(R)$, maintaining the standard definition of effective charge $a = \tilde{R}$. One can of course always consider \tilde{R} as the measured observable rather

than R , and then NLO truncation of the perturbation series for \tilde{R} using some RS will give different results from those obtained with R . Such a redefinition of the observable would only be useful if some information on the uncalculated higher order corrections, i.e. knowledge of the function $\rho(R)$, were available to inform the choice.

3.4.2 EC formalism in NLO - the $\Delta\rho_0$ plot.

Let us suppose that we have measurements for a number of LEP observables at a fixed energy ($Q = M_Z$), and knowledge of their NLO QCD perturbative corrections $r_1^{\overline{MS}}(Q)$. What can we learn?

Recall from equation (3.75) that

$$\begin{aligned} F(R(Q)) &= b \ln \frac{Q}{\tilde{\Lambda}_{\overline{MS}}^{(5)}} - r_1^{\overline{MS}}(Q) - \Delta\rho_0(Q) \\ &= \rho_0(Q) - \Delta\rho_0(Q), \end{aligned} \quad (3.77)$$

where b , c and $r_1^{\overline{MS}}(Q)$ are evaluated with $N_f = 5$. As $Q \rightarrow \infty$, $\Delta\rho_0(Q) \rightarrow 0$ and

$$F(R(Q)) \approx \rho_0(Q). \quad (3.78)$$

At sufficiently large Q , $\Delta\rho_0 \ll \rho_0$ and (3.78) may be used to obtain $\tilde{\Lambda}_{\overline{MS}}^{(5)}$. We have that

$$\tilde{\Lambda}_{\overline{MS}}^{(5)} = Q \exp[-(F(R(Q)) + r_1^{\overline{MS}}(Q) + \Delta\rho_0(Q))/b]. \quad (3.79)$$

Given only a NLO perturbative calculation we have no information on $\Delta\rho_0(Q)$. From the measured observable R_{exp} and the NLO perturbative coefficient we can then extract

$$\exp(\Delta\rho_0(Q)/b) \tilde{\Lambda}_{\overline{MS}}^{(5)} = Q \exp[-(F(R_{exp}(Q)) + r_1^{\overline{MS}}(Q))/b]. \quad (3.80)$$

To relate this to the discussions of section 3.3, the quantity on the left of equation (3.80) is just the value of $\tilde{\Lambda}_{\overline{MS}}^{(5)}$ which would be extracted from the data at NLO choosing $\mu = M_Z \exp(-r_1^{\overline{MS}}/b) = \mu_{EC}$, the effective charge scale. If $\Delta\rho_0(Q) \ll 1$,

then this NLO estimate will be accurate. Indeed the fractional error in $\tilde{\Lambda}_{\overline{MS}}$ will be

$$\left| \frac{\delta\Lambda}{\Lambda} \right| = \left| 1 - \exp\left(\frac{\Delta\rho_0(Q)}{b}\right) \right| \approx \frac{\Delta\rho_0(Q)}{b}. \quad (3.81)$$

The size of $\Delta\rho_0(M_Z)$ will depend on the QCD observable. If the $\tilde{\Lambda}_{\overline{MS}}^{(5)}$ values obtained from equation (3.80) exhibit significant scatter, then this indicates that $\Delta\rho_0(Q)$ is not negligible for at least some of the observables. Recall that $\Delta\rho_0(Q)$ is defined non-perturbatively in terms of the running of $R(Q)$ by equation (3.67) where $dR/d\ln Q = \xi(R(Q)) = -b\rho(R(Q))$. If Q is sufficiently large that $dR/d\ln Q$ has its asymptotic ($Q \rightarrow \infty$) Q -dependence, that is if $\rho(R) \approx R^2(1 + cR)$, then $\Delta\rho_0(Q) \approx 0$. Thus significant scatter in the $\tilde{\Lambda}_{\overline{MS}}^{(5)}$ extracted at NLO with the effective charge scale unambiguously indicates that the current experimental Q is not yet large enough for all observables to be evolving with Q asymptotically. If we want to reliably determine $\tilde{\Lambda}_{\overline{MS}}^{(5)}$ additional information on the ‘sub-asymptotic’ effects is required.

The presence of these effects is a physical fact which can be directly observed from the Q -dependence of data, and cannot be remedied by changing the unphysical renormalization scheme. We stress once again how different this is from the scatter obtained with $\mu = M_Z$ which will be partly due to different values of $r_1^{\overline{MS}}(M_Z)$ and hence which can be modified by changing the unphysical subtraction procedure.

To make this distinction more precise, let us define $\tilde{\Lambda}(NLO, r_1)$ to be the $\tilde{\Lambda}_{\overline{MS}}^{(5)}$ value extracted at NLO using an RS with $r_1^{\overline{MS}}(\mu) = r_1$. The NLO coefficient r_1 may be taken to label the RS at NLO. Using a to denote the coupling constant in this RS we have

$$R = a + r_1 a^2, \quad (3.82)$$

and

$$b \ln \frac{\mu}{\tilde{\Lambda}(NLO, r_1)} = F(a). \quad (3.83)$$

Then using equations (3.79),(3.82), and (3.83) it is straightforward to show that

$$\begin{aligned}\tilde{\Lambda}(NLO, r_1) &= \exp[(\Delta F(r_1, R) + \Delta\rho_0)/b]\tilde{\Lambda}_{\overline{MS}}^{(5)} \\ &= \exp(\Delta F(r_1, R)/b)\tilde{\Lambda}(NLO, 0),\end{aligned}\quad (3.84)$$

where

$$\begin{aligned}\Delta F(r_1, R) &\equiv F(R) - F\left(\frac{-1 + \sqrt{1 + 4r_1 R}}{2r_1}\right) + r_1, \\ \Delta F(0, R) &= 0.\end{aligned}\quad (3.85)$$

$\tilde{\Lambda}(NLO, 0)$ is just the $\tilde{\Lambda}_{\overline{MS}}^{(5)}$ extracted choosing $\mu = \mu_{EC}$ ($r_1 = 0$), given by equation (3.80).

From equation (3.84) we see that the NLO scatter in $\tilde{\Lambda}_{\overline{MS}}^{(5)}$ is factorized into two components. The first is an *already known* r_1 -dependent contribution involving $\Delta F(r_1, R)$ which may be obtained exactly from (3.85) with $R = R_{exp}$, and does *not* involve the unknown NNLO and higher RS invariants. The second component, $\Delta\rho_0 \approx \rho_2 R$, does not depend on r_1 but does involve the unknown higher invariants, and represents the irreducible uncertainty in determining $\tilde{\Lambda}_{\overline{MS}}$ at NLO. The uninformative r_1 -dependent part of the scatter can therefore be completely removed by choosing $\mu = \mu_{EC}$, which sets $\Delta F = 0$. The scatter is then completely given by $\Delta\rho_0$.

Rather than focusing on the scatter in $\tilde{\Lambda}_{\overline{MS}}$, we prefer for presentational reasons to concentrate on the relative size of $\Delta\rho_0$. We can define for each observable

$$\Delta\rho_0^{exp}(Q) \equiv b \ln \frac{Q}{\tilde{\Lambda}_{\overline{MS}}^{(5)}} - r_1^{\overline{MS}}(Q) - F(R_{exp}(Q)).\quad (3.86)$$

Given a NLO perturbative calculation of $r_1^{\overline{MS}}(Q)$ and experimental measurements of R_{exp} we can then measure $\Delta\rho_0$ from the data up to $b \ln \tilde{\Lambda}_{\overline{MS}}^{(5)}$ which should be a universal constant. Changing $\tilde{\Lambda}_{\overline{MS}}$ merely translates the $\Delta\rho_0$ obtained up or down by the *same amount* for each observable, so we can choose an arbitrary reference value for $\tilde{\Lambda}_{\overline{MS}}^{(5)}$. For two different observables A and B , the difference $\Delta\rho_0^{exp}_A - \Delta\rho_0^{exp}_B$ can then be

measured absolutely and so the *relative* size of $\Delta\rho_0$ may be investigated. If $\Delta\rho_0 \approx 0$ for each observable, corresponding to small sub-asymptotic effects, then the $\Delta\rho_0^{exp}$ points should lie on a horizontal straight line with some small scatter. Substantial deviations from a horizontal straight line therefore unambiguously indicate the presence of sizeable sub-asymptotic effects. The scatter in $\Delta\rho_0^{exp}$ is of course entirely equivalent to the scatter in the $\tilde{\Lambda}_{\overline{MS}}^{(5)}$ extracted at NLO with $\mu = \mu_{EC}$, these correspond to the reference $\tilde{\Lambda}_{\overline{MS}}^{(5)}$ values for which $\Delta\rho_0^{exp} = 0$. We shall return to these $\tilde{\Lambda}_{\overline{MS}}^{(5)}$ values later.

If one has a NNLO perturbative calculation or measurement of R_{exp} at more than one energy then, as we shall discuss in the next subsection, one can attempt to estimate $\Delta\rho_0$ directly. One can then see if for all observables a single value of $\tilde{\Lambda}_{\overline{MS}}^{(5)}$ brings $\Delta\rho_0^{exp}$ into agreement with the directly estimated $\Delta\rho_0$.

We now turn to extracting $\Delta\rho_0^{exp}$ from LEP data. The observables we shall use are the ones appearing in Table 3.2 and in section 3.2. The E0 and D labels denote different recombination algorithms used to cluster hadrons together. Details of these algorithms and results for the NLO perturbative coefficients $r_1^{\overline{MS}}(Q)$ can be found in reference [15] for the E0 algorithm, and for the D (Durham or k_T) algorithm in reference [25].

T denotes the thrust variable, and χ the energy-energy correlation (EEC) angle. We used recent OPAL data on the differential distributions in these quantities [6, 54]. The asymmetry in the energy-energy correlation (AEEC) obtained by subtracting the EEC measured at χ and $(180^\circ - \chi)$ was also considered. Details of the definitions of these quantities and their NLO perturbative coefficients are contained in section 3.2.

From the measured hadronic width of the Z^0 (Γ_{had}) and the Z^0 leptonic decay width (Γ_{lep}) one can obtain $R_Z \equiv \Gamma_{had}/\Gamma_{lep} = (19.97 \pm 0.03)(1 + \delta_{QCD})$, where δ_{QCD} has a perturbation series of the form (2.1) with $r_1^{\overline{MS}}(M_Z) = 1.41$. The electroweak contribution (19.97 ± 0.03) is from reference [33]. This coefficient is for massless quarks, if one includes heavy quark masses [34], one finds $\delta_{QCD} = (1.05a + 0.9a^2)$ instead in the \overline{MS} scheme with $\mu = M_Z$. Within the errors the values of $\Delta\rho_0^{exp}$ obtained are consistent, so we shall use massless QCD. For the experimental value we take the 1993 LEP average $R_Z = 20.763 \pm 0.049$ [13].

As noted earlier the reference value of $\tilde{\Lambda}_{\overline{MS}}^{(5)}$ assumed for $\Delta\rho_0^{exp}$ is irrelevant since we are concentrating here on the scatter of $\Delta\rho_0^{exp}$ values. We shall choose $\tilde{\Lambda}_{\overline{MS}}^{(5)} = 110$ MeV which corresponds to the central value obtained from a non-perturbative lattice analysis of the 1P-1S splitting in the charmonium system [55]. Whilst at present limited by the use of a quenched approximation, such calculations could in future provide reliable estimates of $\tilde{\Lambda}$. In Figure 3.4 we show the $\Delta\rho_0^{exp}$ values obtained for the LEP observables discussed above. We have taken for each observable the particular values of the kinematical variables given in Table 3.2. Of course for each observable we actually have a $\Delta\rho_0^{exp}$ distribution in the associated kinematical variable. In Figures 3.5-3.8 we give the $\Delta\rho_0^{exp}$ distributions for the jet rates $R_2(E_0)$, $R_3(E_0)$, $R_2(D)$, $R_3(D)$ as functions of the jet resolution cut y_c . We see that for $y_c \gtrsim 0.04$, $\Delta\rho_0$ is constant within the errors. For smaller y_c there is a much stronger dependence. In this small y_c region we may expect sizeable corrections involving $\ln y_{cut}$. An attempt to resum leading and next-to-leading logarithms to all-orders for $\Delta\rho_0$ for $R_2(D)$ will be discussed in Chapter 4. In Figures 3.5-3.8 we used published OPAL data [6] without correcting for hadronization effects. These are expected to be totally negligible for $y_c \gtrsim 0.04$, but will be important in the small y_c region. For thrust and EEC the $\Delta\rho_0^{exp}$ distributions are flat away from $T \approx 1$ and $\chi \approx 180^\circ$ where large corrections involving $\ln(1 - T)$ and $\ln(\cos^2 \frac{\chi}{2})$ respectively will be important. The plots of $\Delta\rho_0^{exp}$ against T and χ are shown in Figures 3.9 and 3.10 respectively.

Returning to Figure 3.4 we see that there is significant scatter, in particular between the jet rates with E0 and D recombination algorithms. To proceed further then we need either NNLO calculations or information on the Q -dependence of these observables. The only NNLO calculation completed so far is that for R_Z [16]. For $R_3(E_0)$ and EEC there are published data from the JADE collaboration at the PETRA e^+e^- machine with \sqrt{s} in the range 22-44 GeV [23, 56], using a comparable analysis. In the next subsection we shall attempt to use this data together with the LEP data for these quantities to obtain absolute estimates of $\Delta\rho_0$ from the Q -dependence.

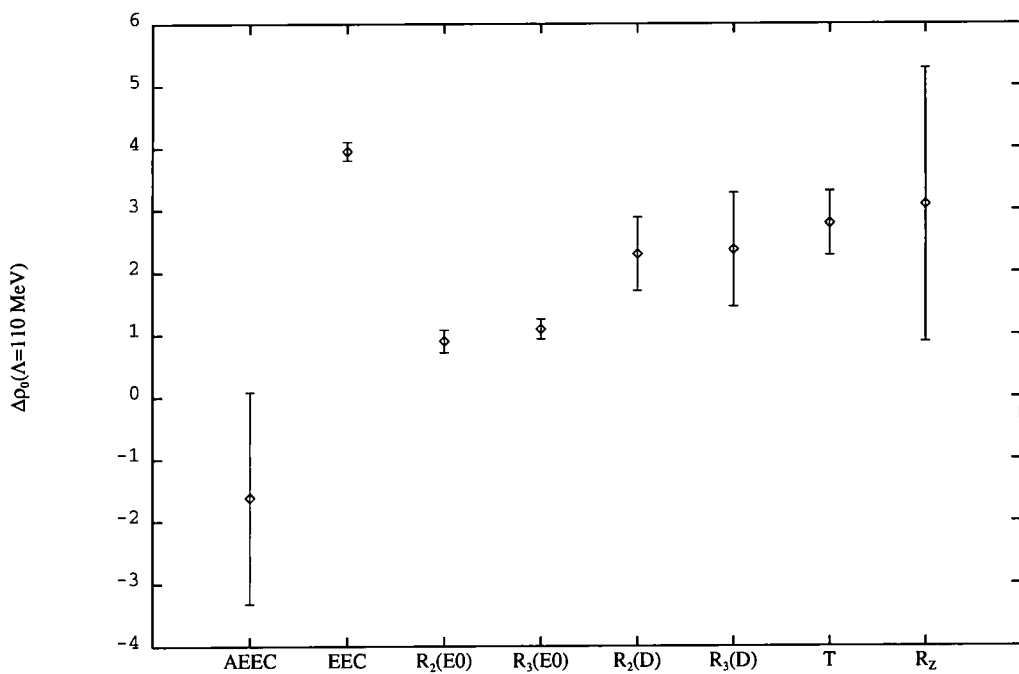


Figure 3.4: $\Delta\rho_0^{exp}$ of equation (3.86) for various LEP observables (see text for details). A reference value of $\tilde{\Lambda}_{\overline{MS}}^{(5)} = 110 \text{ MeV}$ is chosen.

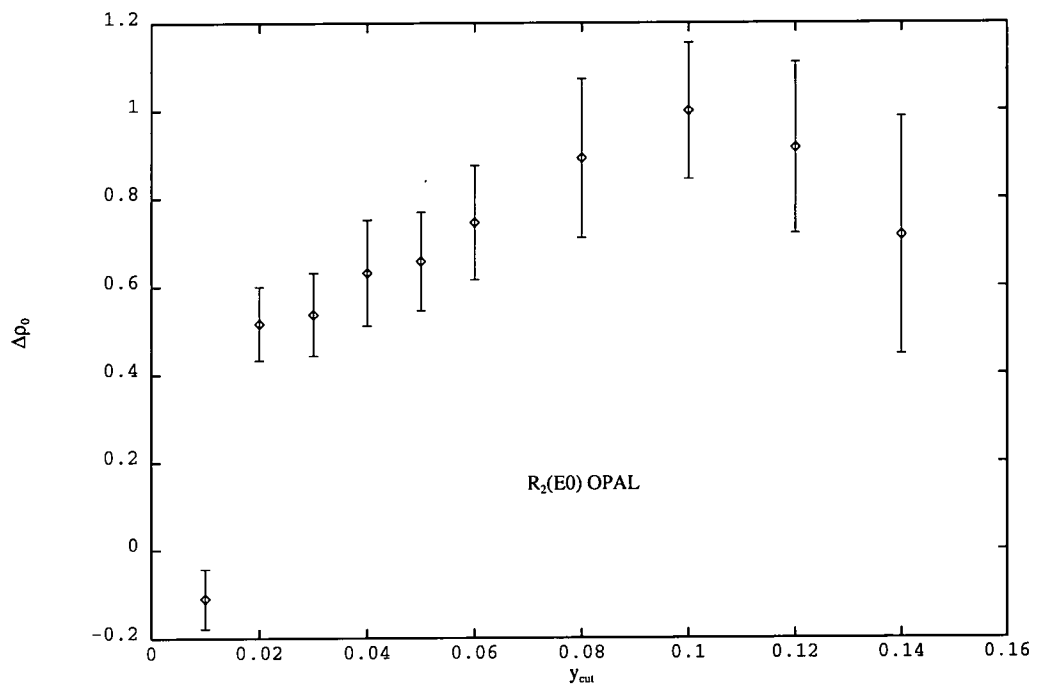


Figure 3.5: The y_{cut} dependence of $\Delta\rho_0^{exp}$ for $R_2(E0)$. OPAL data of reference [6] is used uncorrected for hadronization. A reference value of $\tilde{\Lambda}_{\overline{MS}}^{(5)} = 110$ MeV is chosen.

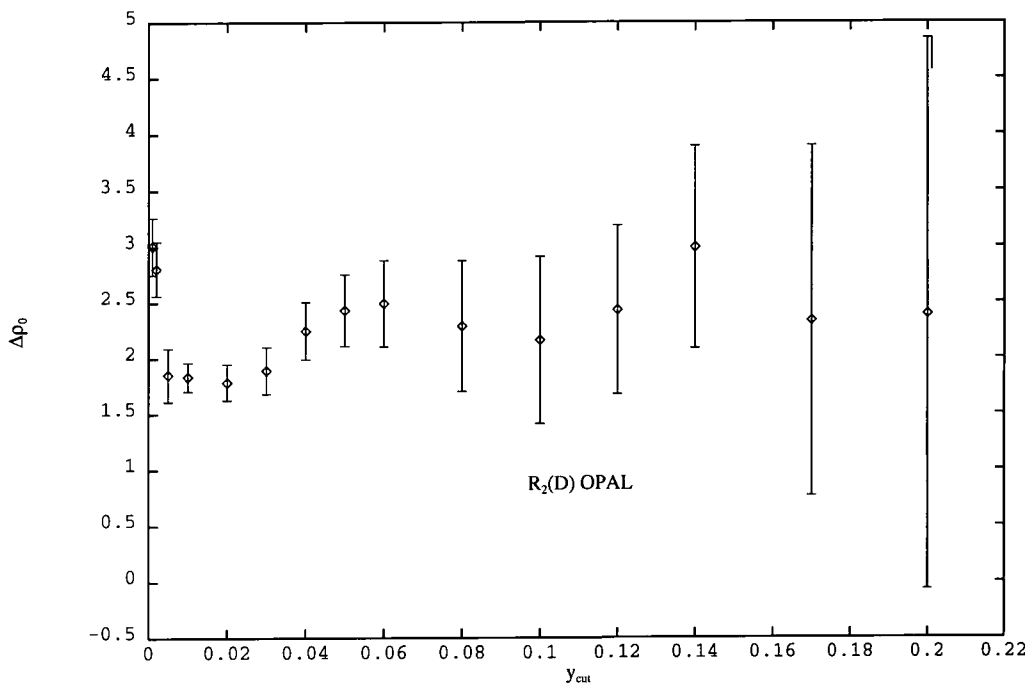


Figure 3.6: The y_{cut} dependence of $\Delta\rho_0^{exp}$ for $R_2(D)$. OPAL data of reference [6] is used uncorrected for hadronization. A reference value of $\tilde{\Lambda}_{\overline{MS}}^{(5)} = 110$ MeV is chosen.

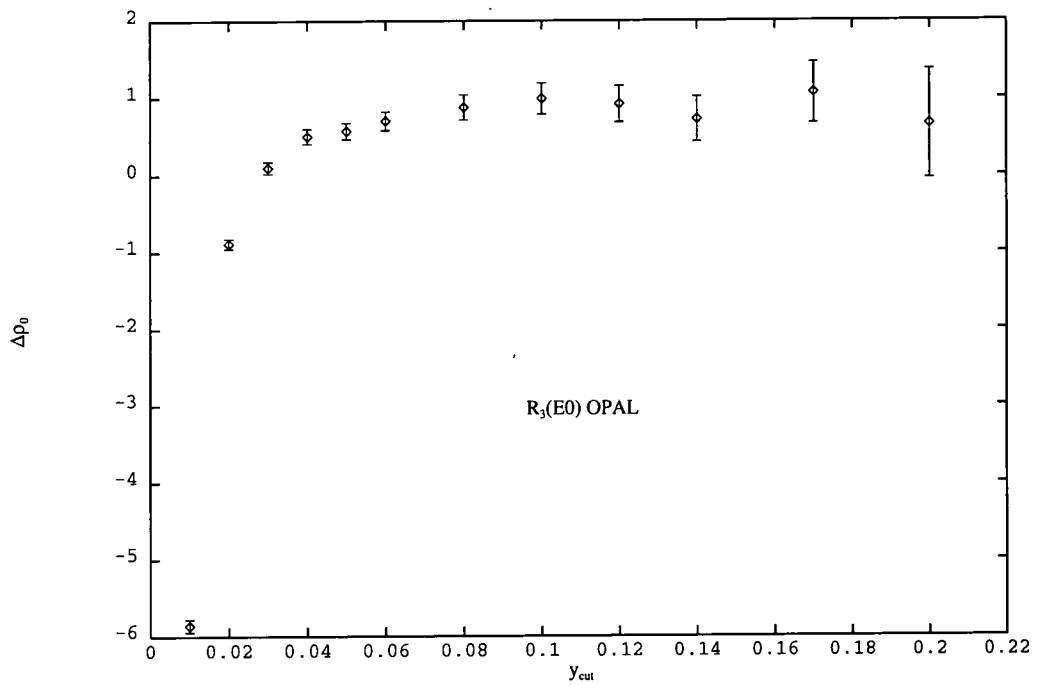


Figure 3.7: The y_{cut} dependence of $\Delta\rho_0^{exp}$ for $R_3(E0)$. OPAL data of reference [6] is used uncorrected for hadronization. A reference value of $\tilde{\Lambda}_{\overline{MS}}^{(5)} = 110$ MeV is chosen.

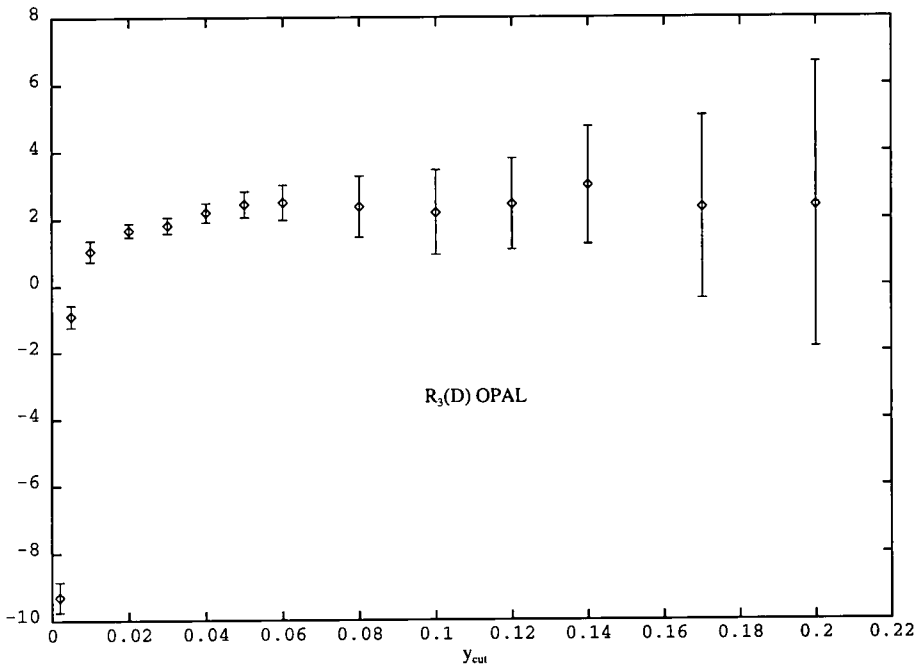


Figure 3.8: The y_{cut} dependence of $\Delta\rho_0^{exp}$ for $R_3(D)$. OPAL data of reference [6] is used uncorrected for hadronization. A reference value of $\tilde{\Lambda}_{\overline{MS}}^{(5)} = 110$ MeV is chosen.

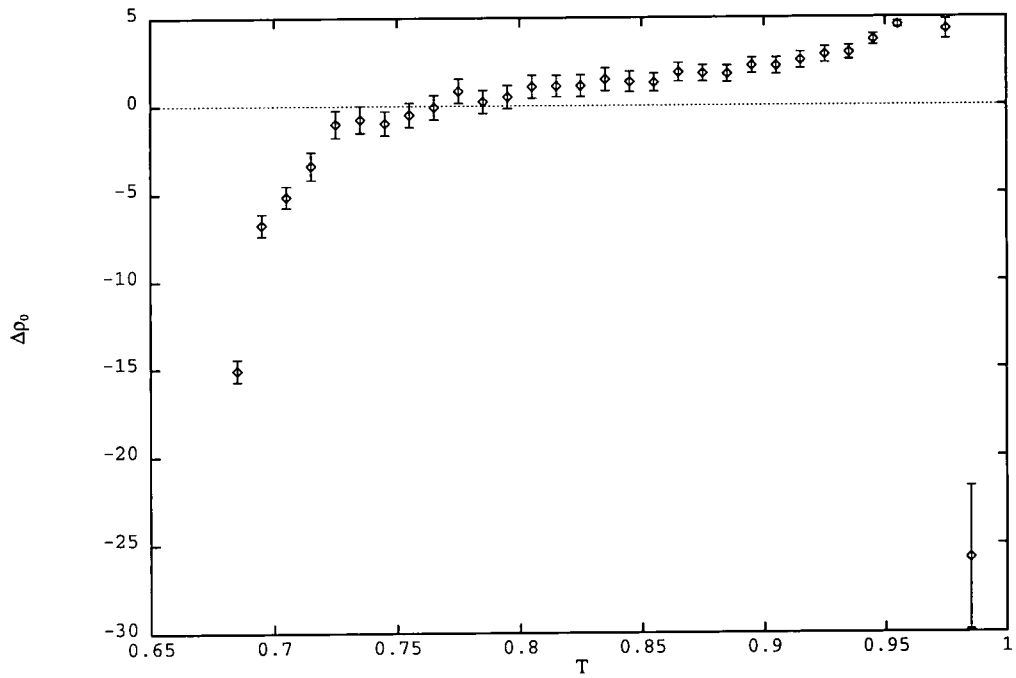


Figure 3.9: The dependence of $\Delta\rho_0^{exp}$ on the observable Thrust, T . OPAL data of reference [6] is used uncorrected for hadronization. A reference value of $\tilde{\Lambda}_{\overline{MS}}^{(5)} = 110$ MeV is chosen.

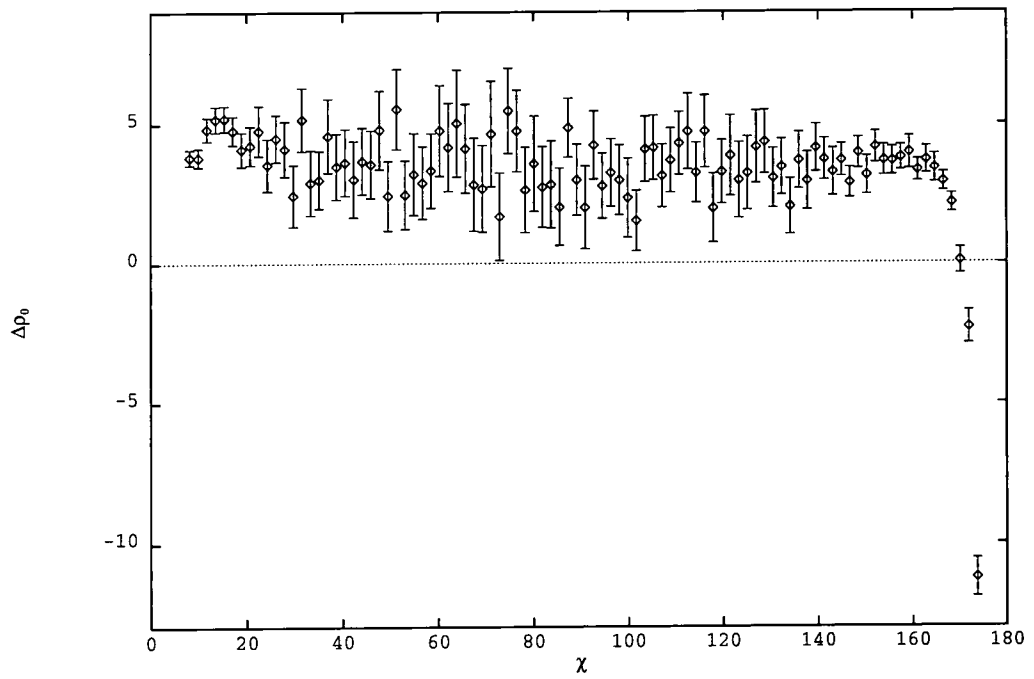


Figure 3.10: The χ dependence of $\Delta\rho_0^{exp}$ for the energy-energy correlation function. OPAL data of reference [6] is used uncorrected for hadronization. A reference value of $\hat{\Lambda}_{\overline{MS}}^{(5)} = 110$ MeV is chosen.

Observable	LEP	LEP	$\Delta\rho_0 \approx 0$	$\Delta\rho_0 \approx 0$
	$\Lambda_{\overline{MS}}^{(5)}$ $\mu = M_Z$	$\Lambda_{\overline{MS}}^{(5)}$ $\mu = \mu_{EC}$	$\Lambda_{\overline{MS}}^{(5)} = 200 \text{ MeV}$ $\mu = M_Z$	$\Lambda_{\overline{MS}}^{(5)} = 200 \text{ MeV}$ $\mu = \mu_{EC}$
T	883.0	197.9	894.4	200
$R_2(E_0)$	335.7	140.4	498.5	200
$R_3(E_0)$	326.8	139.5	488.3	200
$R_2(D)$	420.3	252.1	328.3	200
$R_3(D)$	425.6	257.4	325.2	200
EEC	839.1	268.2	597.4	200
AEEC	89.23	63.79	294.2	200
R_Z	254.4	245.7	206.9	200

Table 3.3: The first two columns show the central values of $\tilde{\Lambda}_{\overline{MS}}^{(5)}$ (in MeV) extracted by comparing NLO perturbative QCD predictions for the observables of Table 3.2, taking $\mu = M_Z$ and $\mu = \mu_{EC}$, with OPAL data [6]. The third and fourth columns give the NLO $\tilde{\Lambda}_{\overline{MS}}^{(5)}$ values extracted with $\mu = M_Z$ and $\mu = \mu_{EC}$, assuming $\Delta\rho_0 = 0$ for each observable, and an actual value of $\Lambda_{\overline{MS}}^{(5)} = 200 \text{ MeV}$.

We conclude by tabulating in Table 3.3 the $\tilde{\Lambda}_{\overline{MS}}^{(5)}$ values obtained by fitting to LEP data at NLO for these same observables at the same values of the kinematical parameters as in Table 3.2 using $\mu = M_Z$ and $\mu = \mu_{EC}$. The $\mu = \mu_{EC}$ values correspond to the $\tilde{\Lambda}_{\overline{MS}}^{(5)}$ values for which $\Delta\rho_0 = 0$, and so the scatter is directly related to points in the $\Delta\rho_0$ plot of Figure 3.4. The $\mu = M_Z$ values show much greater scatter, since as discussed in section 3.3 the scatter in $r_1^{\overline{MS}}(M_Z)$ is superimposed on top of the physically-relevant scatter in $\Delta\rho_0$.

To further emphasise this, suppose that we lived in an ‘asymptotic world’ where $Q =$

M_Z was sufficiently large that $\Delta\rho_0 \approx 0$ for all observables. Thus for all observables

$$F(R_{exp}(M_Z)) = b \ln \frac{M_Z}{\tilde{\Lambda}_{\overline{MS}}^{(5)}} - r_1 \overline{MS}. \quad (3.87)$$

Supposing that $\tilde{\Lambda}_{\overline{MS}}^{(5)} = 200$ MeV, then (3.87) may be used to generate data ‘ $R_{exp}(M_Z)$ ’ in such an ‘asymptotic world’. By construction the $\tilde{\Lambda}_{\overline{MS}}^{(5)}$ obtained by fitting at NLO with $\mu = \mu_{EC}$ will be 200 MeV for all observables, but that obtained with $\mu = M_Z$ will still exhibit significant, but completely predictable, scatter. These ‘asymptotic world’ results are also tabulated in Table 3.3.

3.4.3 $\Delta\rho_0$ from NNLO calculations and Q-dependence.

If we have available a NNLO perturbative calculation then the RS invariant ρ_2 defined in equation (3.46) can be obtained. For R_Z , $\rho_2 = -15.1$ ($N_f = 5$) using the NNLO calculation of reference [16]. For all the other observables NNLO corrections have yet to be calculated and so ρ_2 is unknown. If we insert the perturbative expansion of $\rho(x)$ (equation (3.44)) into (3.67) we obtain

$$\begin{aligned} \Delta\rho_0 &= \int_0^R dx \frac{(\rho_2 + \rho_3 x + \dots)}{(1 + cx)(1 + cx + \rho_2 x^2 + \dots)} \\ &\approx \rho_2 R + \left(\frac{\rho_3}{2} - c\rho_2\right)R^2 + O(R^3) \equiv \Delta\rho_0^{NNLO} + O(R^2). \end{aligned} \quad (3.88)$$

Using the 1993 LEP average data we have $R_Z = (19.97 \pm 0.03)(1 + \delta_{QCD})$ with $\delta_{QCD} = 0.040 \pm 0.004$ [13]. Thus with $\rho_2 = -15.1$ we have $\Delta\rho_0^{NNLO} \simeq \rho_2 \delta_{QCD} \simeq -0.60 \pm 0.06$. Adjusting the reference value of $\tilde{\Lambda}_{\overline{MS}}^{(5)}$ so that $\Delta\rho_0^{exp}$ for R_Z corresponds with this $\Delta\rho_0^{NNLO}$ results in $\tilde{\Lambda}_{\overline{MS}}^{(5)} = 288 \pm 200$ MeV. This is of course just the $\tilde{\Lambda}_{\overline{MS}}$ obtained at NNLO using the EC scheme with $\tau = \rho_0$ and $c_2 = \rho_2$.

To obtain estimates of $\Delta\rho_0$ for the other observables one can try to use their Q-dependence. Suppose that we have measurements of R at two energies $Q = Q_1$ and $Q = Q_2$ ($Q_1 > Q_2$), then we can construct $\Delta\rho_0^{exp}(Q_1)$ and $\Delta\rho_0^{exp}(Q_2)$ of equation

(3.86) from the data (with the same reference value of $\tilde{\Lambda}_{\overline{MS}}^{(5)}$). Then

$$\begin{aligned}\Delta\rho_0^{exp}(Q_1) - \Delta\rho_0^{exp}(Q_2) &= b \ln \frac{Q_1}{Q_2} - F(R(Q_1)) + F(R(Q_2)) \\ &= \int_{R(Q_2)}^{R(Q_1)} I(x) dx = (R(Q_1) - R(Q_2))I(\bar{R}),\end{aligned}\quad (3.89)$$

where

$$I(x) \equiv \left[-\frac{1}{\rho(x)} + \frac{1}{x^2(1+cx)} \right] \quad (3.90)$$

is the integrand of $\Delta\rho_0$ and $R(Q_1) < \bar{R} < R(Q_2)$. Thus the integrand of $\Delta\rho_0$ may be measured from the Q -dependence of the data,

$$I(\bar{R}) = \frac{\Delta\rho_0^{exp}(Q_1) - \Delta\rho_0^{exp}(Q_2)}{(R(Q_1) - R(Q_2))}. \quad (3.91)$$

Obviously by measuring $dR/d\ln Q$ at $Q = Q_0$ with sufficient accuracy one can in principle determine $I(R(Q_0))$ and so by suitably detailed measurement over the energy range $[Q_1, Q_2]$ one can determine $I(x)$ on the interval $[R(Q_1), R(Q_2)]$.

The situation for measurements at Q_1 and Q_2 is shown in Figure 3.11 for $I(x)$ versus x . The uncertainty in \bar{R} is represented by the horizontal error bar between $R(Q_1)$ and $R(Q_2)$ and the measurement errors in $R(Q_1)$ and $R(Q_2)$ themselves contribute a vertical error bar.

We have from equation (3.88) that

$$I(x) = \rho_2 + (\rho_3 - 2c\rho_2)x + O(x^2). \quad (3.92)$$

So $I(0) = \rho_2$. Thus from a NNLO perturbative calculation we can obtain the integrand at the origin. Notice that, like $\bar{\Lambda}$, the RS invariant ρ_2 is connected with the asymptotic Q -dependence of $R(Q)$. A next-NNLO calculation would provide ρ_3 and tell us the slope of $I(x)$ at the origin, $\rho_3 - 2c\rho_2$.

If NNLO perturbation theory is adequate to determine $\Delta\rho_0$, then $\Delta\rho_0 \approx \Delta\rho_0^{NNLO} =$

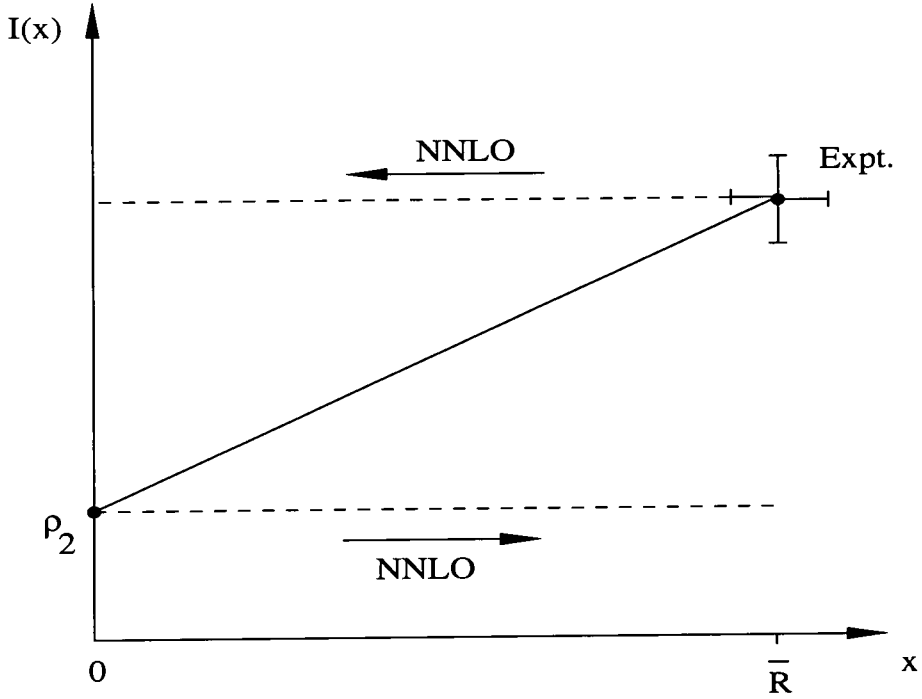


Figure 3.11: Learning about the integrand of $\Delta\rho_0$, $I(x)$ of equation (3.90). NNLO perturbative calculations can provide $I(0) = \rho_2$, and measurements at energies Q_1 and Q_2 can provide a point away from the origin.

$\rho_2 R(Q)$, corresponding to $I(x) \approx \rho_2 = \text{constant}$, on the range $[0, R(Q)]$. Thus, if NNLO perturbation theory is adequate, then we expect $I(\bar{R}) \approx \rho_2$ and so from the measurements of $R(Q_1)$ and $R(Q_2)$ we can estimate $\Delta\rho_0^{est}(Q_1) = I(\bar{R})R(Q_1)$ from (3.91),

$$\Delta\rho_0^{est}(Q_1) = \frac{(\Delta\rho_0^{exp}(Q_1) - \Delta\rho_0^{exp}(Q_2))}{(R(Q_1) - R(Q_2))} R(Q_1). \quad (3.93)$$

If NNLO calculations eventually become available for the observables one can then check explicitly whether $\Delta\rho_0^{NNLO} \approx \Delta\rho_0^{est}$. A marked discrepancy would indicate the importance of next-NNLO and higher perturbative effects and/or large ‘non-perturbative’ $e^{-1/R}$ effects. Given ρ_2 one can then estimate ρ_3 from the slope of the straight line joining $I(0)$ and $I(\bar{R})$ and obtain an improved estimate of $\Delta\rho_0^{est}(Q_1)$ from

the area under the trapezium (see Figure 3.11).

In this way perturbative calculations and experimental Q -dependence measurements serve as complementary pieces of information. The NNLO and higher perturbative calculations effectively provide details of the $Q \rightarrow \infty$ running of $R(Q)$ which could never be obtained experimentally. Together they can help to constrain the behaviour of the function $\xi(R) = -b\rho(R)$, and hence to refine the estimates of $\tilde{\Lambda}_{\overline{MS}}^{(5)}$.

The running of the observables with energy has been used before as a test of QCD. For instance $R_3(E0, y_c = 0.08)$ has been studied as a function of Q over the PETRA-LEP energy range [11]. The apparent running has been compared with the NLO QCD expectations for various choices of renormalization scale μ , and $\tilde{\Lambda}$. It has even been suggested [57] that the LEP measurements may indicate slightly less running than is expected from QCD, and that light gluinos, which would modify the QCD β -function, cannot be excluded. Such a claim seems ludicrously premature given our lack of knowledge of NNLO and higher QCD effects.

If we take data for $R_3(E0, y_c = 0.08)$ at $Q_2 = 34$ GeV from JADE [23], and at $Q_1 = 91$ GeV from OPAL [6], then we obtain from (3.93), $\Delta\rho_0^{est}(91) = -5.5 \pm 3$, which corresponds to $I(\overline{R}) = -110 \pm 60$. So if NNLO perturbation theory is adequate for this observable we estimate $\rho_2 = -110 \pm 60$, for the as yet uncalculated NNLO RS invariant. For the EEC with $\chi = 60^\circ$ measured by JADE at $Q_2 = 34$ GeV [56], and by OPAL at $Q_1 = 91$ GeV [54] we similarly find $\Delta\rho_0^{est}(91) = -1.5 \pm 1.5$, which corresponds to $I(\overline{R}) = -21 \pm 21$, and an estimate of $\rho_2 = -21 \pm 21$. Since $\Delta\rho_0^{exp}$ is very insensitive to y_c and χ , comparable results are obtained for other choices of these variables.

In Figure 3.12 we plot $\Delta\rho_0$ for R_Z , $R_3(E0, y_c = 0.08)$ and $R_{EEC}(\chi = 60^\circ)$ with $Q = M_Z$. The diamonds correspond to absolute predictions. For R_Z we take $\Delta\rho_0^{NNLO} = -0.60 \pm 0.06$, and $R_3(E0, y_c = 0.08)$ and for $R_{EEC}(\chi = 60^\circ)$ the $\Delta\rho_0^{est}(91)$ values noted above obtained from Q -dependence. The crosses correspond to the $\Delta\rho_0^{exp}$ for these observables with the reference $\tilde{\Lambda}_{\overline{MS}}^{(5)}$ chosen as 288 MeV so that $\Delta\rho_0^{exp}$ for R_Z agrees with $\Delta\rho_0^{NNLO}$. There is then agreement, within the considerable errors, between

$\Delta\rho_0^{exp}$ and $\Delta\rho_0^{est}$ for R_3 and R_{EEC} . Demanding consistency between $\Delta\rho_0^{exp}$ and $\Delta\rho_0^{est}$, $\Delta\rho_0^{NNLO}$ then requires $\tilde{\Lambda}_{\overline{MS}}^{(5)} = 288 \pm 100$ MeV.

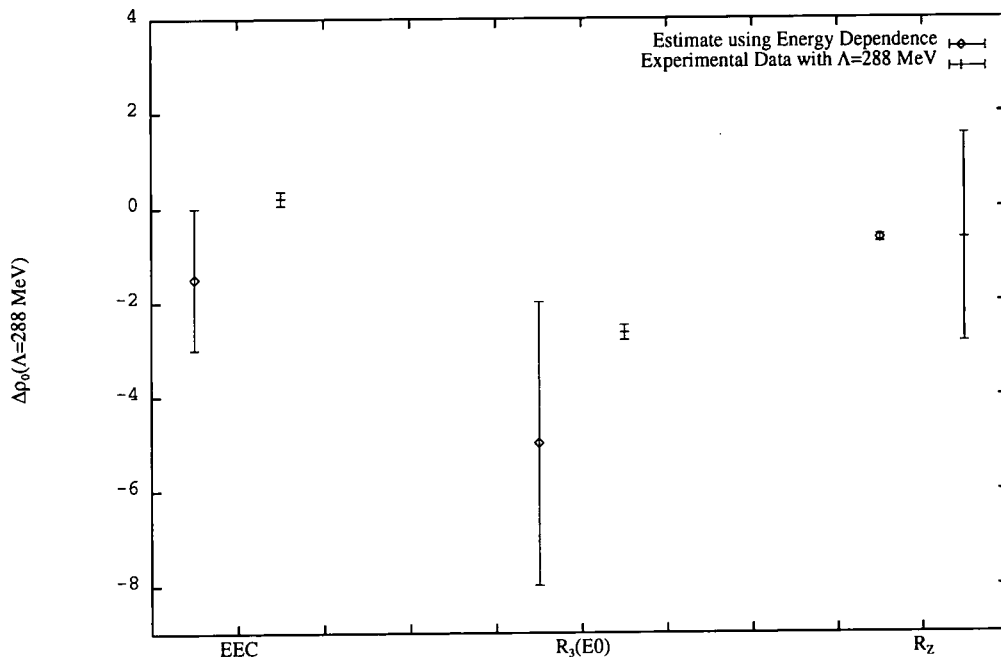


Figure 3.12: Absolute estimates of $\Delta\rho_0$ for LEP observables at $Q = 91$ GeV are compared with the observed $\Delta\rho_0^{exp}$ with $\tilde{\Lambda}_{\overline{MS}}^{(5)} = 288$ MeV. For $EEC(\chi = 60^\circ)$ and $R_3(E0, y_c = 0.08)$ the absolute estimates are $\Delta\rho_0^{est}$ of equation (3.34) obtained from Q -dependence using JADE data. For R_Z $\Delta\rho_0^{NNLO}$ from the NNLO calculation of reference [16] is used.

Although only performed for a limited number of observables, we regard this consistency between $\Delta\rho_0^{exp}$ and the absolute $\Delta\rho_0$ obtained from NNLO calculations and Q -dependence measurements as very encouraging. Ideally one would like to see additional LEP measurements for all observables off the Z peak at a lower value of Q to avoid the uncertainties due to combining measurements from different machines and detectors. One could then perform an exhaustive analysis of the kind described here and obtain a reliable determination of $\tilde{\Lambda}_{\overline{MS}}^{(5)}$. Scatter in the $\tilde{\Lambda}_{\overline{MS}}^{(5)}$ values obtained by adjust-

ing $\Delta\rho_0^{exp}$ to agree with $\Delta\rho_0^{est}$ (obtained from Q -dependence using (3.93)) would then unambiguously indicate the importance of next-NNLO corrections or non-perturbative $e^{-1/R}$ effects for some of the observables.

It is interesting that the above Q -dependence estimates of ρ_2 , and the exact NNLO calculation of ρ_2 for R_Z , suggest ρ_2 large ($O(10)$) and *negative*. This has implications for the infra-red behaviour of $R(Q)$ since it is consistent with fixed-point behaviour, that is $\rho(R^*) = 0$ implying $R \rightarrow R^*$ as $Q \rightarrow 0$ [47, 58].

Chapter 4

Resumming Leading and Next-to-Leading Logarithms

4.1 Introduction

When trying to make predictions using perturbative QCD we are up against a very major problem, namely that at present the full perturbative calculation of observables is only complete up to the second order in a ($= \alpha_s/\pi$). For some hard jet observables one can identify predictable large logarithms of the kinematical parameters, and in favourable cases these contributions can be resummed to all-orders of perturbation theory.

As will be seen later the observables that we shall be considering exhibit the property of *exponentiation*. In fact this property is crucial to the arguments that will be followed in this chapter. Hence, a short review of exponentiation is appropriate at this point.

4.2 Exponentiation

The appearance of large double logarithms is a common feature of any hard process in the 2-jet limit (i.e. the semi-inclusive or Sudakov region), where the emission of the radiation is inhibited by the kinematics. For instance, in the case of jet cross-sections at

$y_c \ll 1$, the jet invariant mass is constrained to be so small as to allow only emission of gluons that are soft and collinear with respect to the parton generating the jet. The double logarithmic terms $a \ln^2(1/y_c)$ are due to such soft and collinear gluons.

It is possible to resum the leading and the next-to-leading logarithms in the perturbative coefficients

$$r_k = A_k L^{2k} + B_k L^{2k-1} + \dots \quad (4.1)$$

where $L \equiv \ln 1/\lambda$. Hence, in the region where $\lambda \rightarrow 0$ the resummed coefficients will become large, and the uncalculable part of the expression will become relatively small. That is, in the limit $\lambda \rightarrow 0$ we have that the perturbative series for our observable $R(\lambda)$ will become

$$R(\lambda) = \sum_{k=1}^{\infty} (A_k L^{2k} + B_k L^{2k-1}) a^{k+1}. \quad (4.2)$$

It is important to realise that when we do such a resummation the A_k are completely RS-independent, whereas the B_k (i.e. the next-to-leading logarithm contribution) are dependent upon the NLO RS choice $\tau = \mu/\tilde{\Lambda}_{RS}$. This resummation is only possible if the large logarithmic corrections to the relevant quantity exponentiate.

Consider the normalized event cross-section, $R(y)$, defined by

$$R(y) = \int_0^y dy \frac{1}{\sigma} \frac{d\sigma}{dy}, \quad (4.3)$$

where $R(y)$ is the 2-jet cross-section $R_2(D)(y_c)$, or the integral of the thrust cross-section

$$R(1-T) = \int_0^{1-T} \frac{1}{\sigma} \frac{d\sigma}{dT} dT \quad (4.4)$$

or for the energy-energy correlation function it is

$$R(\cos^2 \chi/2) = \int_0^{\cos^2 \chi/2} \frac{1}{\sigma} \frac{d\sigma}{d \cos^2 \chi/2} d(\cos^2 \chi/2). \quad (4.5)$$

By exponentiation we mean that at small λ the logarithm of the shape cross-section

takes the form

$$\ln R(y) \sim Lg_1(aL) \quad (4.6)$$

where the function g_1 has a power series expansion in aL . More precisely, the factorization of QCD matrix elements in the 2-jet region implies that, provided the phase space by which $R(y)$ is defined also has factorization properties that are specified, then

$$R(y) = C(a)\Sigma(y, a) + D(y, a), \quad (4.7)$$

where

$$C(a) = 1 + \sum_{n=1}^{\infty} C_n a^n \quad (4.8)$$

$$\begin{aligned} \ln \Sigma(y, a) &= \sum_{n=1}^{\infty} \sum_{m=1}^{n+1} G_{nm} a^n L^m \\ &= Lg_1(aL) + g_2(aL) + ag_3(aL) + \dots, \end{aligned} \quad (4.9)$$

and $D(y, a)$ vanishes as $y \rightarrow 0$ order-by-order in perturbation theory. The word exponentiation refers to the fact that the terms $a^n L^m$ with $m > n + 1$ are absent from $\ln R(y)$, whereas they do appear in $R(y)$ itself. The function g_1 resums all the leading contributions $a^n L^{n+1}$, while g_2 contains the next-to-leading logarithmic terms $a^n L^n$, and g_3 etc. represent the remaining *subdominant* logarithmic corrections $a^n L^m$ with $0 < m < n$. All the functions g_i vanish at $L = 0$ since they resum terms with $m > 0$.

Consider the simpler case of Quantum Electrodynamics (QED). In QED photons are not charged and this implies that multiple soft photon emission is an independent process. Thus, the probability $d\omega(1, \dots, n)$ for n -soft photon emission factorizes in the product of single photon factors $d\omega(i)$

$$d\omega(1, \dots, n) = \frac{1}{n!} \prod_{i=1}^n d\omega(i). \quad (4.10)$$

Starting from this factorized result we can obtain the corresponding cross-sections

contribution by integration over the relevant phase-space $\Theta(1, \dots, n; \lambda)$. Therefore, if the phase space factorizes in the soft limit

$$\Theta(1, \dots, n; \lambda) \simeq \prod_{i=1}^n \Theta(i, \lambda), \quad (4.11)$$

then the factorization of multiphoton amplitudes leads to an exponentiation of the cross-section

$$\begin{aligned} & 1 + \sum_{n=1}^{\infty} \int d\omega(1, \dots, n) \Theta(1, \dots, n; \lambda) \\ & \simeq 1 + \sum_{n=1}^{\infty} \frac{1}{n!} \prod_{i=1}^n \int d\omega(i) \Theta(i; \lambda) \\ & = \exp \left[\int d\omega(i) \Theta(i; \lambda) \right]. \end{aligned} \quad (4.12)$$

The property (4.10) comes from QED dynamics whilst (4.12) depends on the kinematic definition of the cross-section. The cross-section exponentiates in the Sudakov region if and only if its definition does not induce kinematic correlations among soft photons.

The main difference between the case of QCD and that of QED is due to the fact that the gluons have colour charge. Therefore, they can radiate in cascade and soft gluon emission is no longer an independent process. Strong gluon correlations are enforced by the dynamics, multiple gluon emission is not factorized into single emission contributions and we can only expect some kind of generalized exponentiation.

Nevertheless, a simple exponentiation structure is still valid for highly inclusive cross-sections like a large class of 2-jet dominated quantities.

It can be shown that thrust, energy-energy correlation, and the jet-fractions defined in the Durham algorithm exponentiate. It should be noted that the jet-fractions in the E and E0 scheme do not exponentiate and so such an analysis is impossible with these algorithms. For thrust $\lambda = 1 - T$, for energy-energy correlation $\lambda = \cos^2 \chi/2$, and for the jet-fractions $\lambda = y_c$.

4.3 What Has Been Done To Date?

There has been much recent interest, both theoretical and experimental in the possibility of resumming leading and next-to-leading logarithms (NLL) in the kinematical variables, described above, to all-orders for LEP observables.

The procedure that seems to be favoured by experimentalists is that of Catani et. al.. In order to compare the predictions of such an analysis with data the result of the resummation and the $O(\alpha_s^2)$ calculation have to be combined by employing one of four types of matching procedure, namely ‘ln(R)-matching’, ‘R-matching’, ‘modified R-matching’ and ‘modified ln(R) matching’. The various matching schemes all embody the full $O(\alpha_s^2)$ result, together with the resummation and next-to-leading logarithms, but they differ in higher orders.

Once this has been done and all the relevant boundary conditions have been applied there still remains the problem of scheme dependence.

4.4 The Effective Charge Scheme

The advantage of the EC formalism here is that from the leading and next-to-leading logarithms in r_k one can obtain the leading and next-to-leading logarithms in the RS invariants $\rho_k = \tilde{A}_k L^{2k} + \tilde{B}_k L^{2k-1} + O(L^{2k-2})$. One can then *unambiguously* construct

$$\begin{aligned}\rho^{DLL}(x) &= x^2(1 + cx + \rho_2^{DLL}x^2 + \dots + \rho_k^{DLL} + \dots), \\ \rho_k^{DLL} &\equiv \tilde{A}_k L^{2k} + \tilde{B}_k L^{2k-1}.\end{aligned}\tag{4.13}$$

$\rho^{DLL}(x)$ is constructed from RS-invariants and so does not involve the renormalization scale, or the NLO perturbative coefficient. There is, therefore, no analogue of the matching prescription ambiguity and one can obtain an expression for $\Delta\rho_0^{DLL}$. This will be done in the next couple of sections.

This may be directly compared with $\Delta\rho_0^{exp}$. If the observed λ -dependence of $\Delta\rho_0^{exp}$

in the small- λ region disagrees with that predicted from $\Delta\rho_0^{DLL}$ then one has unambiguous evidence that the DLL approximation is inadequate, that is that the neglected sub-leading logarithms and constants are important.

4.5 An Expression For ρ^{DLL}

As demonstrated earlier in this chapter we have expressions of the form

$$R^{DLL}(a) = f(a) + g(a) \quad (4.14)$$

where $R^{DLL}(a)$ is the sum of the leading logarithm contribution and the next-to-leading logarithm contribution to the perturbative expansion of the observable. For convenience the leading logarithm contribution will be denoted by $f(a)$ and the next-to-leading logarithm contribution by $g(a)$. Notice that we strictly resum only leading and next-to-leading logarithms in each order, since only these contributions are actually known to all-orders. We therefore have an improvable approximation to which could be added next-to-next-to-leading logarithms if these become available. For many of the LEP observables we know R^{DLL} explicitly and so in order to obtain the ultimate goal of knowing the double leading logarithm approximation for $\Delta\rho_0$ we need to find the leading logarithm and next-to-leading logarithm contributions for our RS invariants ρ_i .

In order to obtain $\rho(R)$ we require $a(R)$, which will be obtained from equation (4.14). Therefore, we can deduce that the double leading logarithm approximation will be of the form

$$a^{DLL}(R) = F(R) + G(R) \quad (4.15)$$

where $F(R)$ is the leading logarithm and $G(R)$ is the next-to leading logarithm contribution to $a(R)$.

It is useful to keep track separately of the next-to-leading logarithm contribution by

attaching a parameter λ to it, which will eventually be set equal to 1. So we write

$$\tilde{R}^{DLL}(a; \lambda) = f(a) + \lambda g(a) \quad (4.16)$$

$$R^{DLL}(a) = \tilde{R}^{DLL}(a; 1). \quad (4.17)$$

If we now reverse $\tilde{R}^{DLL}(a; \lambda)$, then we will find that

$$\tilde{a}(R; \lambda) = F(R) + \lambda G(R) + O(\lambda^2). \quad (4.18)$$

The λ -independent term will come from reversing $f(a)$ so

$$F(R) = f^{-1}(R). \quad (4.19)$$

To obtain $G(R)$ we can write using a Taylor expansion for \tilde{R}^{DLL} ,

$$\begin{aligned} R = \tilde{R}^{DLL}(a; \lambda) &= f(F(R) + \lambda G(R)) + \lambda g(F(R) + \lambda G(R)) \\ &= f(F(R)) + \lambda G(R) f'(F(R)) + \lambda g(F(R)) + O(\lambda^2) \\ &= R + \lambda [G(R) f'(F(R)) + g(F(R))] + O(\lambda^2). \end{aligned} \quad (4.20)$$

Clearly, the coefficient of λ must vanish for consistency so that we find

$$G(R) = -\frac{g(F(R))}{f'(F(R))}. \quad (4.21)$$

As we have seen before in equation (3.45) we have the following expression for $\rho(R)$

$$\rho(R) = (a(R))^2 (1 + ca(R)) \frac{dR}{da} \quad (4.22)$$

Since the contribution due to the constant c is always subleading (i.e neither leads to a NLL or a LL contribution) we can simply set $c = 0$. Hence, using our expression for

$a(R)$ we can deduce that

$$\begin{aligned}
\rho(R) &= \frac{F^2 + 2\lambda FG + \lambda^2 G^2}{\frac{da}{dR}} + O(\lambda^2) \\
&= (F^2 + 2\lambda FG)(F' + \lambda G')^{-1} + O(\lambda^2) \\
&= \frac{(F^2 + 2\lambda FG)}{F'} \left(1 - \lambda \frac{G'}{F'}\right) + O(\lambda^2) \\
&= \frac{F^2}{F'} + \lambda \left(\frac{2FG}{F'} - \frac{F^2 G'}{(F')^2} \right) + O(\lambda^2)
\end{aligned} \tag{4.23}$$

Since the coefficient λ labels the next-to-leading logarithm term we can deduce that

$$\begin{aligned}
\rho^{LL}(R) &= \frac{F^2}{F'} \\
\rho^{NLL}(R) &= \frac{2FG}{F'} - \frac{F^2 G'}{F'^2}
\end{aligned} \tag{4.24}$$

4.6 The Double Leading Logarithm Approximation For

$$\Delta\rho_0$$

To double leading logarithm accuracy we require the following

$$\Delta\rho_0^{DLL} = \Delta\rho_0^{LL} + \Delta\rho_0^{NLL} \tag{4.25}$$

where $\Delta\rho_0^{LL}$ contains only the leading logarithm contributions and $\Delta\rho_0^{NLL}$ contains only the next-to-leading logarithm contributions.

As demonstrated above we can derive ρ^{DLL} where

$$\rho^{DLL} = \rho^{LL} + \rho^{NLL} \tag{4.26}$$

for the observables being considered. As stated earlier the contribution due to the constant c is always subleading and so we can simply set $c = 0$. Hence we now write

simply

$$\Delta\rho_0 = \int_0^{R_{exp}} \left[-\frac{1}{\rho(x)} + \frac{1}{x^2} dx \right]. \quad (4.27)$$

Now, as before, we can write that

$$\tilde{\Delta}\rho_0 = \Delta\rho_0^{LL} + \lambda\Delta\rho_0^{NLL} \quad (4.28)$$

and that

$$\tilde{\rho} = \rho^{LL} + \lambda\rho^{NLL} \quad (4.29)$$

Now, we can easily deduce that the following is true

$$\Delta\rho_0^{DLL} = \tilde{\Delta}\rho_0 \Big|_{\lambda=0} + \frac{d}{d\lambda} \tilde{\Delta}\rho_0 \Big|_{\lambda=0} \quad (4.30)$$

Therefore, if we now substitute in the latter two equations for $\tilde{\Delta}\rho_0$ and $\tilde{\rho}$, then we obtain that

$$\begin{aligned} \Delta\rho_0^{DLL} &= \int_0^{R_{exp}} \left(-\frac{1}{\rho^{LL} + \lambda\rho^{NLL}} \right) \Big|_{\lambda=0} + \frac{1}{x^2} dx \\ &+ \frac{d}{d\lambda} \left[\int_0^{R_{exp}} -\frac{1}{\rho^{LL} + \lambda\rho^{NLL}} + \frac{1}{x^2} \right] \Big|_{\lambda=0} \\ &= \int_0^{R_{exp}} \left(-\frac{1}{\rho^{LL}} + \frac{1}{x^2} \right) dx + \int_0^{R_{exp}} \frac{\rho^{NLL}}{(\rho^{LL})^2} dx \end{aligned} \quad (4.31)$$

Thus, we have now derived a means of calculating the double leading logarithm approximation for $\Delta\rho_0$ given the observable in terms of its leading and next-to-leading logarithm components of its perturbative expansion.

So we now need to apply this method to obtain $\Delta\rho_0^{DLL}$ expressions for the three observables for which we have resummed leading and next-to-leading logarithm expressions, namely the 2-jet and 3-jet cross-section (in the Durham algorithm), thrust, and the energy-energy correlation function.

4.7 The 2-jet Fraction In The Durham Algorithm, $R_2(D)$

For the 2-jet fraction $R_2(D)$ we have that

$$R_2(D) = 1 + r_0 R(a) \quad (4.32)$$

where R has a perturbative expansion series of the form (3.19). In order to proceed the leading logarithm and the next-to-leading logarithm resummation for $R_2(D)$.

Catani et. al. [35] has demonstrated that the leading logarithm and the next-to-leading logarithm resummation for $R_2(D)$ is given by

$$R_2^{DLL} = \exp \left(-\frac{4C_F}{\pi} \int_{Q_0}^Q dq \frac{\alpha_s(q)}{q} \left(\ln \left(\frac{Q}{q} \right) - \frac{3}{4} \right) \right) \quad (4.33)$$

where $Q_0 = Q\sqrt{y_c}$. However, we have the following identity

$$\int_{Q_0}^Q \frac{dq}{\pi} \frac{\alpha_s}{q} = -\frac{1}{b} \ln \left(1 - \frac{abL}{2} \right) \quad (4.34)$$

where $a = \alpha_s/\pi$, $b = (33 - 2N_f)/6$, and $L \equiv \ln 1/y_c$. Also we know that

$$\frac{d\alpha_s}{dq} = -b \frac{\alpha_s^2}{\pi q} \quad (4.35)$$

and

$$\alpha_s(Q\sqrt{y_c}) = \frac{\alpha_s(Q)}{1 + \frac{\alpha_s(Q)}{2\pi} b \ln y_c} \quad (4.36)$$

If we integrate the expression for R_2^{DLL} and then employ the latter three identities, then we can deduce that

$$R_2^{DLL}(D) = \exp \left[-4C_F \left[-\frac{L}{2b} + \frac{1}{ba} \left(\frac{3}{4}a - \frac{1}{b} \right) \ln \left(1 - \frac{baL}{2} \right) \right] \right] \quad (4.37)$$

where a is now equal to $\alpha_s(Q)/\pi$. However, upon expansion this latter expression produces more than the desired leading and next-to-leading logarithm contributions

in each order of a . The reason for this apparent discrepancy is that Catani [36] are resumming the terms in the exponent and not the contributions for R_2 . It can easily be seen that the leading and next-to-leading logarithm contributions to $R_2(D)$ in each order of a are given by the expression

$$R_2^{DLL}(D) = \exp \left[\frac{3C_F L}{2} \left(1 - \frac{L}{3}\right) a - \frac{bC_F L^3}{6} a^2 \right] \quad (4.38)$$

where again $a = a(\mu = Q)$ and $L = \ln 1/y_c$. The b dependent term in the exponent may be absorbed into a by a change of scale $Q \rightarrow y_c^{1/3} Q$. Since the RS invariants ρ_k are independent of the renormalization scale to construct them we can equally use

$$R_2^{DLL}(D) = \exp \left[\frac{3C_F L}{2} \left(1 - \frac{L}{3}\right) a \right] \quad (4.39)$$

Hence, in the above notation we can now write that leading and next-to-leading logarithms summed to all-orders are given by the expression

$$R^{DLL}(a) = \frac{1 - R_2^{DLL}(D)}{r_0}. \quad (4.40)$$

We now need to isolate the leading logarithm contribution $f(a)$ and the next-to-leading logarithm contribution $g(a)$ to proceed. So if we expand this latter equation and then resum the leading and the next-to-leading logarithms separately, then we obtain

$$f(a) = -\frac{2}{L^2 C_F} (e^{-C_F L^2 a/2} - 1) \quad (4.41)$$

and

$$g(a) = -\frac{3a}{L} e^{-C_F L^2 a/2} - \frac{6}{C_F L^3} (e^{-C_F L^2 a/2} - 1). \quad (4.42)$$

From this we can deduce that the resummed leading logarithm contribution to $a(R)$ is

$$F(R) = -\frac{2}{C_F L^2} \ln \left(1 - \frac{L^2 C_F R}{2} \right) \quad (4.43)$$

since $F(R) \equiv f^{-1}(R)$. We can use this expression to determine the resummed next-to-leading logarithm contribution to $a(R)$

$$\begin{aligned} G(R) &= -\frac{g(F(R))}{f'(F(R))} \\ &= -\frac{6}{C_F L^3} \ln\left(1 - \frac{L^2 C_F R}{2}\right) - \frac{3}{L} \frac{R}{\left(1 - \frac{L^2 C_F R}{2}\right)}. \end{aligned} \quad (4.44)$$

Using equations (4.24), (4.43) and (4.44) we can see that the resummed leading and next-to-leading logarithm contribution for our RS invariants ρ are given by

$$\begin{aligned} \rho^{LL}(R) &= \frac{F^2}{F'} \\ &= \frac{4}{C_F^2 L^4} \left(\ln^2\left(1 - \frac{L^2 C_F R}{2}\right) \right) \left(1 - \frac{L^2 C_F R}{2}\right) \end{aligned} \quad (4.45)$$

and

$$\begin{aligned} \rho^{NLL}(R) &= \frac{2FG}{F'} - \frac{F^2 G'}{(F')^2} \\ &= -\frac{4}{C_F L^2} \ln\left(1 - \frac{L^2 C_F R}{2}\right) \left(1 - \frac{L^2 C_F R}{2}\right) \\ &\quad \times \left(-\frac{6}{C_F L^3} \ln\left(1 - \frac{L^2 C_F R}{2}\right) - \frac{3}{L} \frac{R}{1 - \frac{L^2 C_F R}{2}} \right) \\ &\quad + \frac{6R}{C_F L^3} \ln^2\left(1 - \frac{L^2 C_F R}{2}\right) \end{aligned} \quad (4.46)$$

Hence, in conclusion we can write that the resummed leading and next-to-leading logarithms for ρ are

$$\begin{aligned} \rho^{DLL}(R) &= \frac{\left(1 + \frac{6}{L}\right) \left(1 - \frac{C_F^2 L^2}{2} R\right) \ln^2\left(1 - \frac{L^2 C_F R}{2}\right)}{C_F^2 L^4 / 4} \\ &\quad + \frac{6R}{C_F L^3} \left[2 \ln\left(1 - \frac{L^2 C_F R}{2}\right) + \ln^2\left(1 - \frac{L^2 C_F R}{2}\right) \right] \end{aligned} \quad (4.47)$$

Now we are in a position to calculate an expression for $\Delta\rho_0^{DLL}$, using equation (4.31). To do this we shall firstly calculate $\Delta\rho_0^{LL}$ analytically and then add the result for $\Delta\rho_0^{NLL}$ which was calculated numerically. The leading logarithm contribution to $\Delta\rho_0$ is given by

$$\Delta\rho_0^{LL}(R) = \int_0^R \left(-\frac{1}{\rho^{LL}(x)} + \frac{1}{x^2} \right) dx \quad (4.48)$$

where $\rho^{LL}(x)$ is given in equation(4.45). We can rewrite the latter equation in the following form

$$\Delta\rho_0^{LL}(R) = \lim_{\epsilon \rightarrow 0} \left(\int_{\epsilon}^R -\frac{1}{\rho^{LL}(x)} dx + \int_{\epsilon}^R \frac{1}{x^2} dx \right). \quad (4.49)$$

If we now make a change of variables by letting $u = \ln(1 - L^2 C_F x/2)$, then we can write

$$\begin{aligned} \int_{\epsilon}^R -\frac{1}{\rho^{LL}(x)} dx + \int_{\epsilon}^R \frac{1}{x^2} dx &= \frac{L^2 C_F}{2} \int_{\ln(1-L^2 C_F \epsilon/2)}^{\ln(1-L^2 C_F R/2)} \frac{du}{u^2} - \frac{1}{R} + \frac{1}{\epsilon} \\ &= \frac{L^2 C_F}{2} \left[-\frac{1}{u} \right]_{\ln(1-L^2 C_F \epsilon/2)}^{\ln(1-L^2 C_F R/2)} - \frac{1}{R} + \frac{1}{\epsilon} \\ &= -\frac{L^2 C_F}{2} \frac{1}{\ln(1 - L^2 C_F R/2)} + \frac{L^2 C_F}{2} \frac{1}{\ln(1 - L^2 C_F \epsilon/2)} - \frac{1}{R} + \frac{1}{\epsilon} \\ &= -\frac{L^2 C_F}{2} \frac{1}{\ln(1 - L^2 C_F R/2)} - \frac{L^2 C_F}{2} \frac{1}{\frac{L^2 C_F \epsilon}{2} \left(1 + \frac{L^2 C_F \epsilon}{4} + \dots \right)} - \frac{1}{R} + \frac{1}{\epsilon} \\ &= -\frac{L^2 C_F}{2} \frac{1}{\ln(1 - L^2 C_F R/2)} - \frac{1}{R} + \frac{C_F L^2}{4} + O(\epsilon). \end{aligned} \quad (4.50)$$

Setting $\epsilon \rightarrow 0$ allows us to deduce that

$$\Delta\rho_0^{LL}(R) = -\frac{L^2 C_F}{2} \frac{1}{\ln(1 - L^2 C_F R/2)} - \frac{1}{R} + \frac{C_F L^2}{4} \quad (4.51)$$

Taking $R = R_{exp}$ from the OPAL data of reference [5], uncorrected for hadronization effects, we obtain the plot shown in Figure 4.1. As can be seen the curve becomes more negative as $y_c \rightarrow 0$.

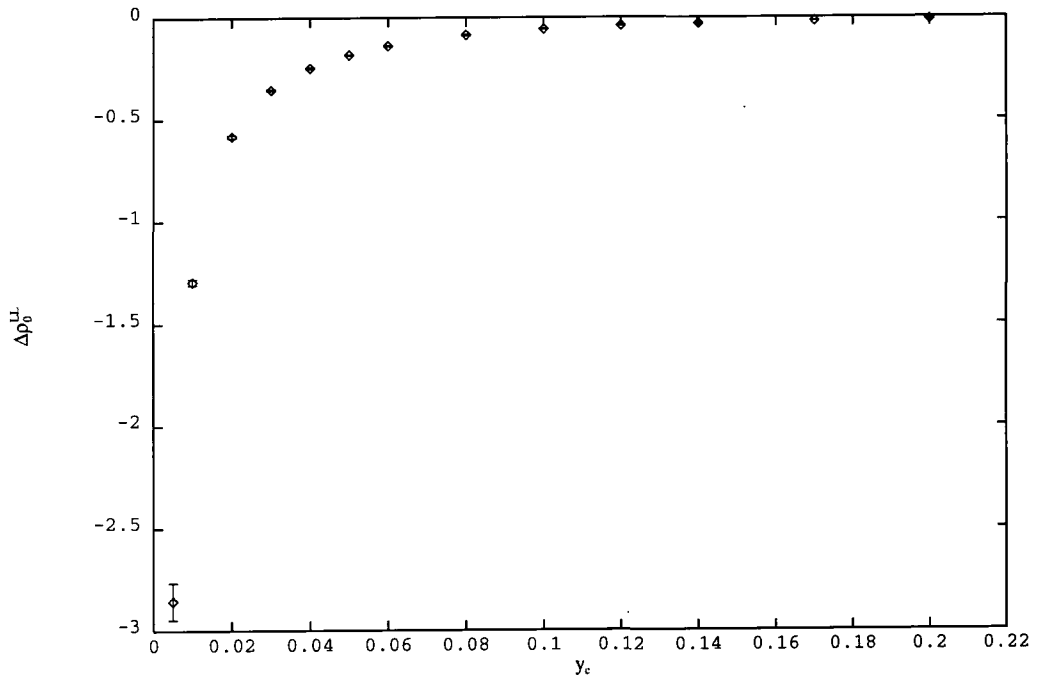


Figure 4.1: The graph to show the leading logarithm contribution $\Delta\rho_0^{LL}$ as a function of y_c for $R_2(D)$

We now need to integrate numerically to obtain $\Delta\rho_0^{NLL}(R)$

$$\Delta\rho_0^{NLL}(R) = \int_0^R \frac{\rho^{NLL}(x)}{(\rho^{LL}(x))^2} dx \quad (4.52)$$

A plot of this is given in Figure 4.2. As can be seen it has the opposite behaviour to $\Delta\rho_0^{LL}(R)$ which is rather disquieting. If we add these latter two graphs together, then we obtain the graph shown in Figure 4.3. In Figure 4.4 we have also plotted $\Delta\rho_0^{exp}$ with $\tilde{\Lambda}_{\overline{MS}}$ set equal to 184.3 MeV so that the two graphs intercept for $y_c = 0.04$.

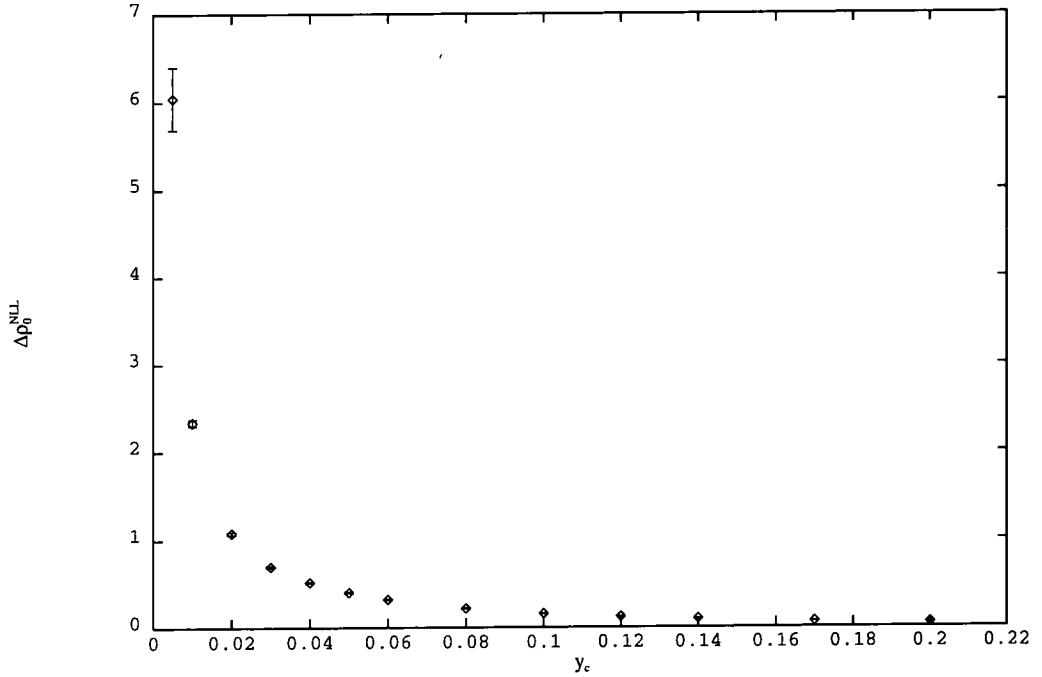


Figure 4.2: The graph to show the next-to-leading logarithm contribution $\Delta\rho_0^{NLL}$ as a function of y_c for $R_2(D)$

The main message that should be learnt from these three graphs is that the next-to-leading logarithm contribution dominates the leading logarithm contribution. This implies that the next-to-next-to-leading logarithm contribution could at least be as large

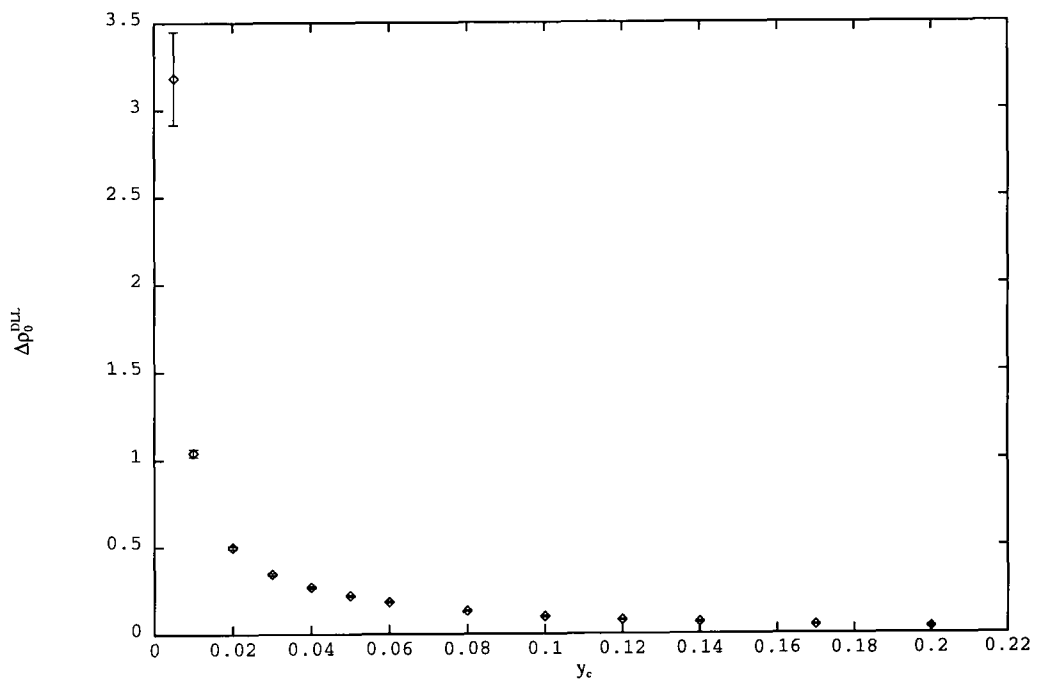


Figure 4.3: The graph to show the resummed double leading logarithm approximation $\Delta\rho_0^{DLL}$ as a function of y_c for $R_2(D)$

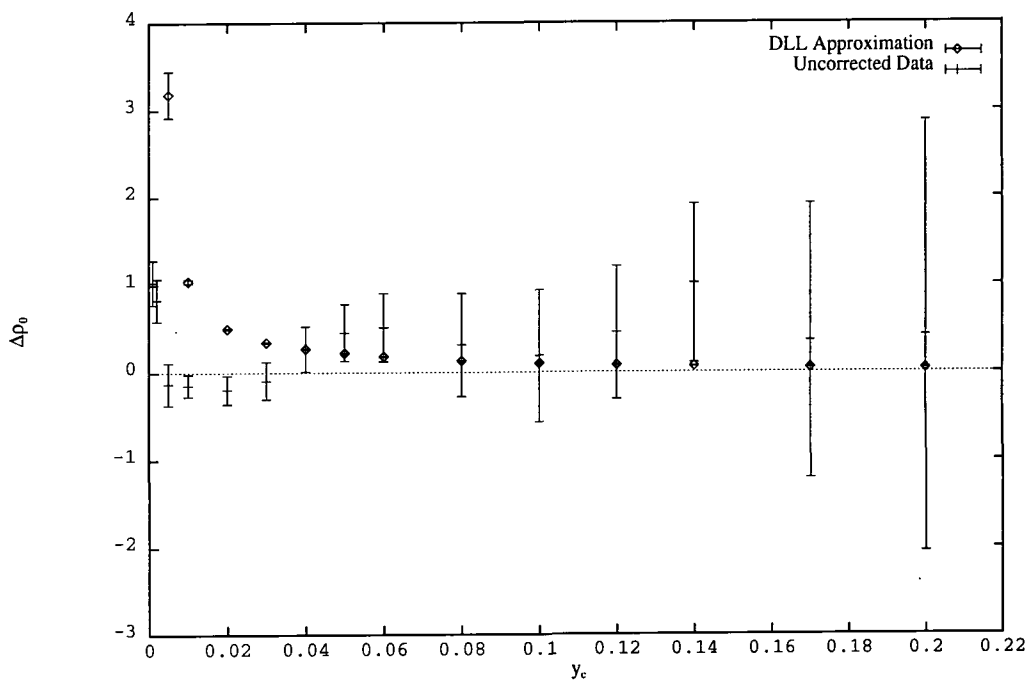


Figure 4.4: For the observable $R_2(D)$ the DLL approximation $\Delta\rho_0^{DLL}$ of equation (4.31) versus y_c is compared with $\Delta\rho_0^{exp}$ with $\tilde{\Lambda}_{MS}^{(5)}$ adjusted. OPAL data of reference [6] uncorrected for hadronization effects is used.

as the next-to-leading logarithm contribution and so could completely change the results obtained above. Hence, there appears to be little benefit from resumming the next-to-leading logarithms, and that the bits that we are neglecting are apparently very important in the region where the experimental data lie.

The simplicity of the exponentiation for $R_2(D)$ means that we can almost solve the entire problem analytically. However, for thrust, the energy-energy correlation function, and $R_3(D)$ the exponentiation is not quite as simple and so any analytical approach is hopeless. Therefore, for these three observables the results obtained will just be outlined.

4.8 Thrust

For thrust it can be shown using the results of Catani et. al. [36], that the leading logarithm contribution is

$$f(a) = ae^{-L^2 C_F a} \quad (4.53)$$

and the next-to-leading logarithm contribution is

$$g(a) = \frac{3}{2} C_F a^2 L e^{-C_F L^2 a}. \quad (4.54)$$

Thus, the leading logarithm contribution to $a(R)$ is given by

$$R = F(R) e^{-L^2 C_F F(R)}. \quad (4.55)$$

As can be seen from the latter equation $F(R)$ is in fact double valued. Therefore, the value for $F(R)$ in the range $[0, 1/L^2 C_F]$ was taken, where the maximum in R occurs at $F(R) = 1/L^2 C_F$. This is the correct choice because it leads to the perturbative solution, whereas the alternative possibility would lead to a contradiction.

If we follow the procedure outlined above, then we will obtain the plots $\Delta\rho_0^{DLL}(R)$ and $\Delta\rho_0^{DLL}(R)$ as shown in Figures 4.5 and 4.6 respectively. As can be seen both

these plots have similar shapes to those obtained for R_2 . That is, for small $\lambda = 1 - T$ the leading logarithm component, $\Delta\rho_0^{LL}$, becomes more negative, whereas the double logarithm contribution, $\Delta\rho_0^{DLL}$, becomes more positive. By comparison between the two graphs, it would again appear that the next-to-leading logarithms are dominating the picture.

The data have been plotted with $\tilde{\Lambda}_{\overline{MS}} = 90.0$ MeV in Figure 4.7 so that a direct comparison with $\Delta\rho_0^{DLL}(R)$, which is also plotted on the same axes, can be made. This particular choice of $\tilde{\Lambda}_{\overline{MS}}$ means that the two graphs intercept at $T = 0.795$. As can easily be seen the resummed double leading logarithm approximation is not a very good prediction of the data.

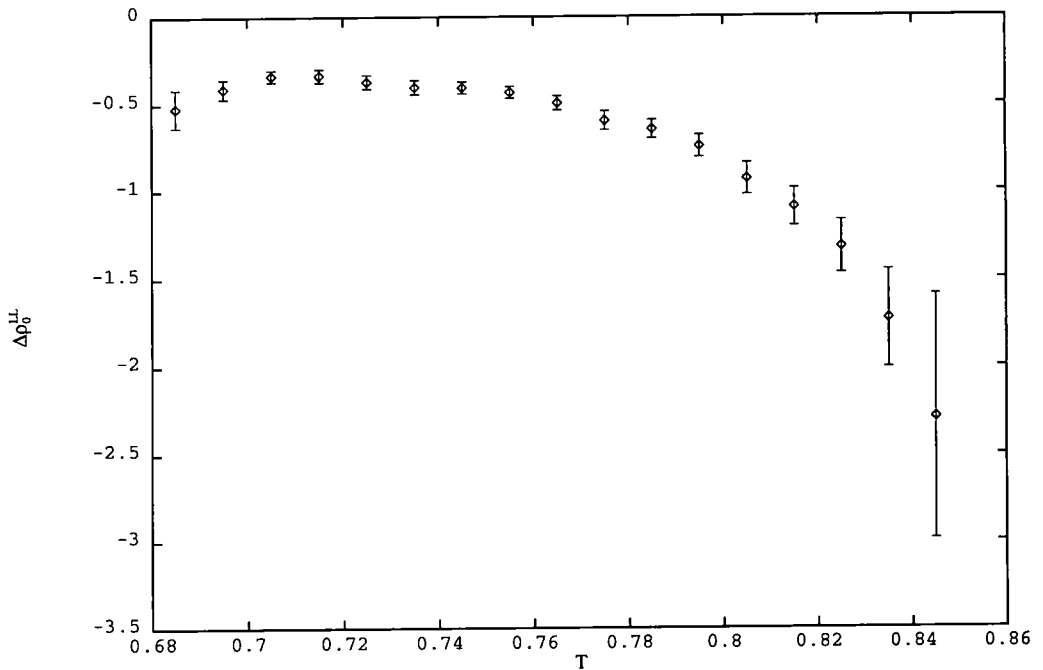


Figure 4.5: The graph to show the leading logarithm contribution $\Delta\rho_0^{LL}$ as a function of T.

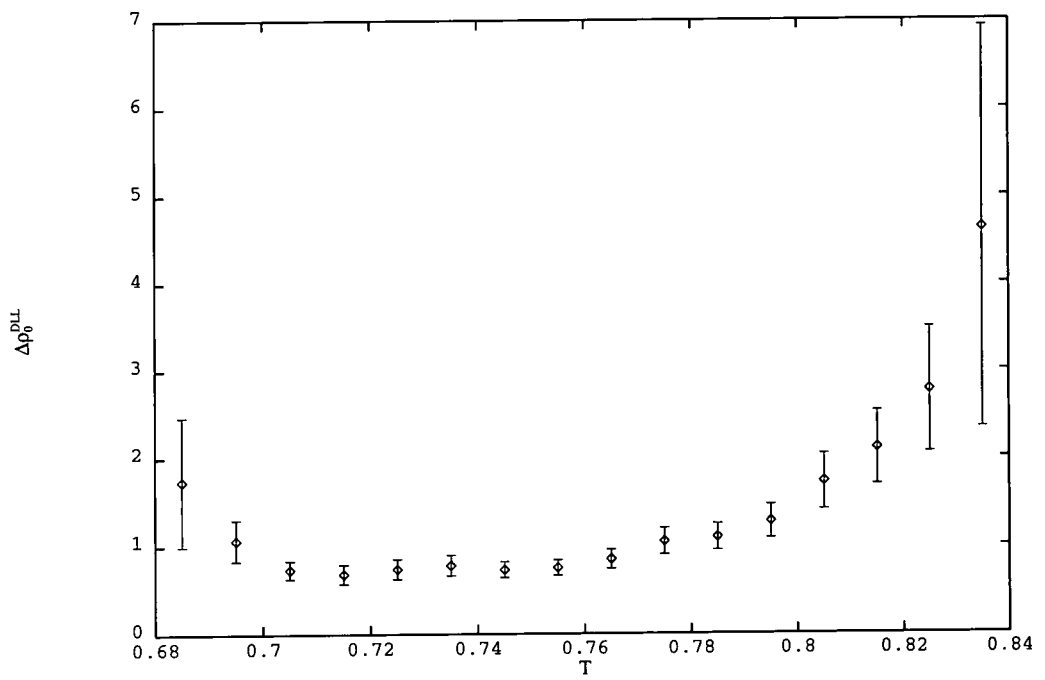


Figure 4.6: The graph to show the resummed double leading logarithm approximation of $\Delta\rho_0^{DLL}$ as a function of T for thrust.

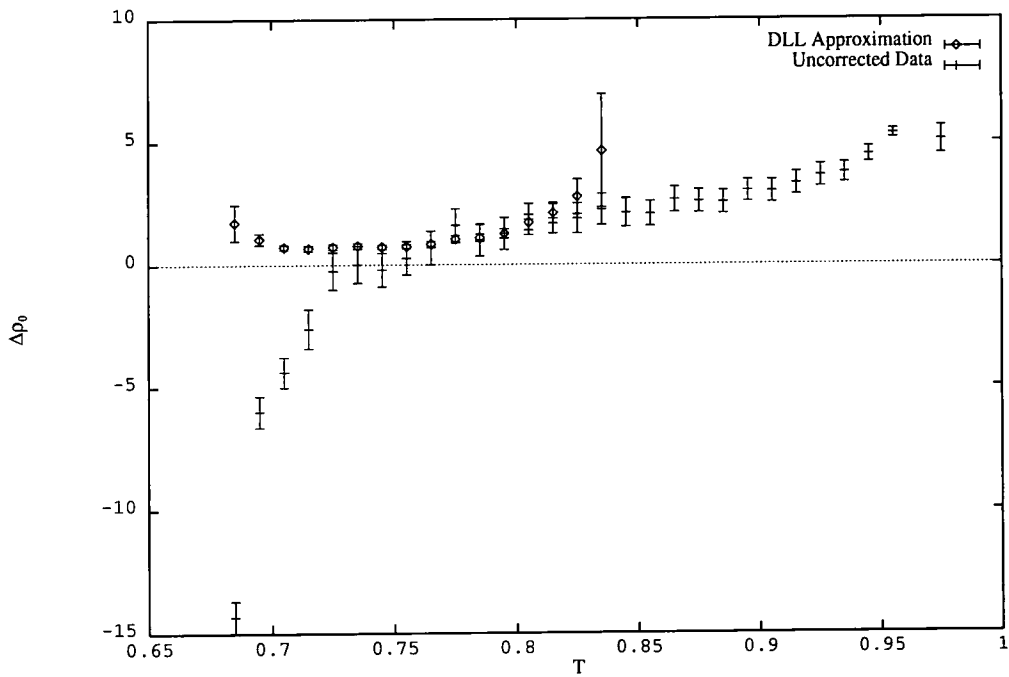


Figure 4.7: For the observable thrust the DLL approximation $\Delta\rho_0^{DLL}$ of equation (3.31) versus T is compared with $\Delta\rho_0^{exp}$ with $\tilde{\Lambda}_{\overline{MS}}^{(5)}$ adjusted. OPAL data of reference [6] uncorrected for hadronization effects is used.

4.9 Energy-Energy Correlation

For the energy-energy correlation function it can be shown using the results of Turnock [59], that the leading logarithm contribution is given by

$$f(a) = a \exp(-C_F L^2 a/2) \quad (4.56)$$

and that the next-to-leading logarithm contribution is

$$g(a) = \frac{3}{2} C_F L a^2 \exp(-C_F L^2 a/2). \quad (4.57)$$

Therefore, we can write that

$$R = F(R) \exp(-C_F L^2 F(R)/2) \quad (4.58)$$

Again $F(R)$ is double valued and so, in order to preserve the perturbative nature of our analysis, we must restrict $F(R)$ to fall within the range $[0, 2/C_F L^2]$.

The results for $\Delta\rho_0^{NLL}(R)$ and $\Delta\rho_0^{DLL}(R)$ are plotted in Figures 4.8 and 4.9 respectively. Both graphs are much the same as the corresponding figures for thrust and $R_2(D)$. That is, for $\chi \rightarrow 180^\circ$ (i.e. the back to back region) $\Delta\rho_0^{LL}(R)$ becomes more positive. Comparison between these two graphs, again, allows us to conclude that the next-to-leading logarithms are controlling our approximation.

The data (i.e $\Delta\rho_0^{exp}(R_{exp})$) have been plotted with $\tilde{\Lambda}_{\overline{MS}} = 201$ MeV in Figure 4.10 so that a comparison with $\Delta\rho_0^{DLL}(R)$, which is also plotted on the same axes, can be made. This particular choice of $\tilde{\Lambda}_{\overline{MS}}$ means that the two graphs intercept at $\chi = 100^\circ$. Again we can see that the resummed double logarithm approximation is not modelling the data at all well.

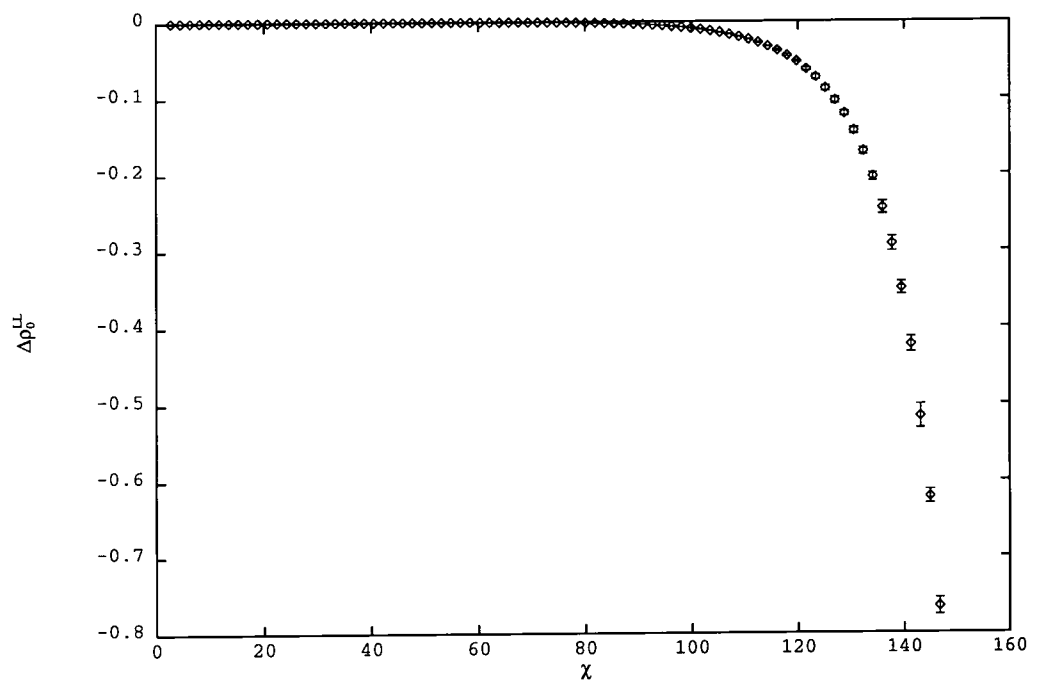


Figure 4.8: The graph to show the leading logarithm contribution $\Delta\rho_0^{LL}$ as a function of χ for the energy-energy correlation function.



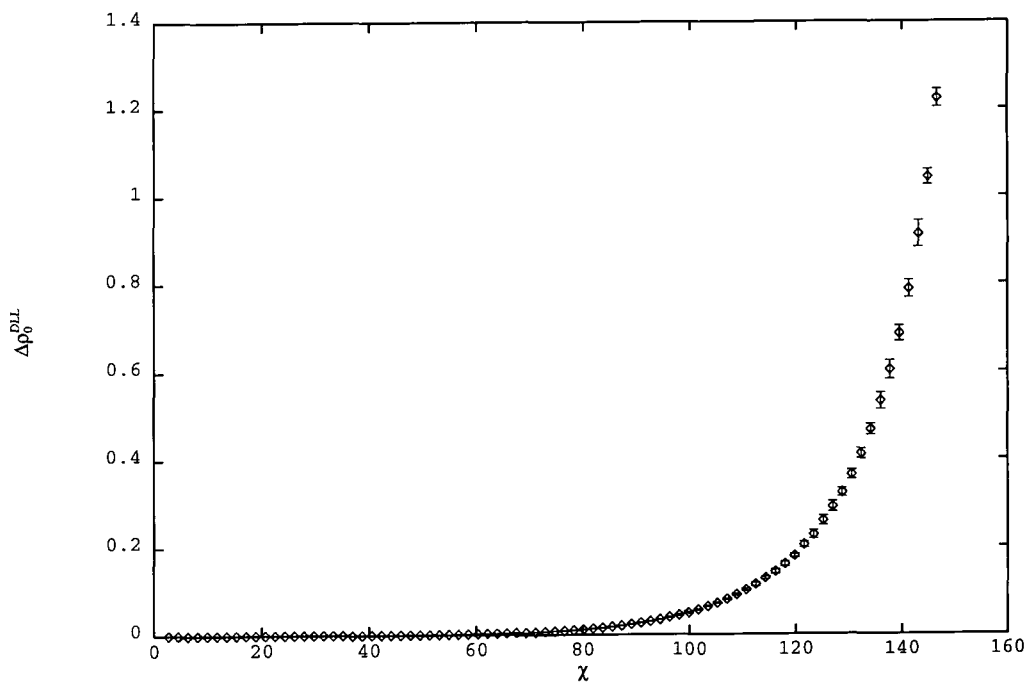


Figure 4.9: The graph to show the resummed double logarithm approximation $\Delta\rho_0^{DLL}$ as a function of χ for the energy-energy correlation function.

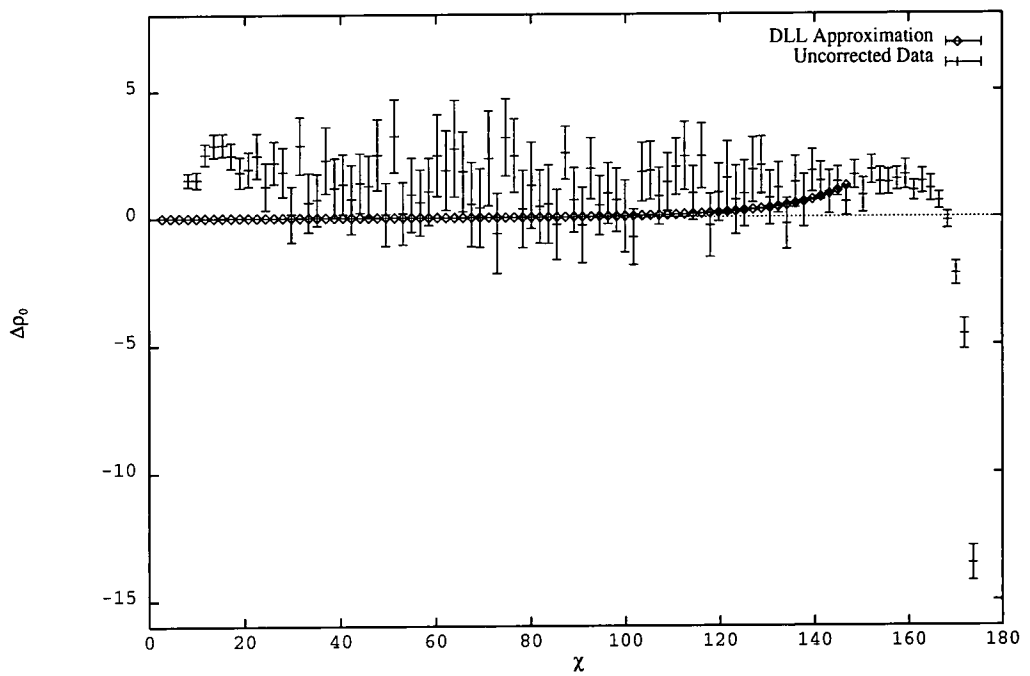


Figure 4.10: For the observable energy-energy correlation the DLL approximation $\Delta\rho_0^{DLL}$ of equation (3.31) versus χ is compared with $\Delta\rho_0^{exp}$ with $\tilde{\Lambda}_{MS}^{(5)}$ adjusted. OPAL data of reference [6] uncorrected for hadronization effects is used.

4.10 The 3-jet Fraction In The Durham Algorithm, $R_3(D)$

For the 3-jet fraction, R_3 , Lovett-Turner [60] has obtained the resummed double leading logarithm contribution. He found that

$$f(a) = -\frac{C_F a L}{2} \exp\left(\frac{-C_F a L^2}{2}\right) \left[-L \sqrt{\frac{4\pi}{C_A a L^2}} \operatorname{erf}\left(\sqrt{\frac{C_A a L^2}{4}}\right) + \frac{1}{C_A} \left(\exp\left(-\frac{C_A a L^2}{4}\right) - 1 \right) \left(-\frac{4}{aL}\right) \right] \frac{3}{2} \frac{1}{L^2} \quad (4.59)$$

and

$$g(a) = \frac{3}{2L^2} \left\{ -\frac{C_F a L}{2} \exp\left(-\frac{C_F a L^2}{2}\right) \left[-\frac{1}{2} \sqrt{\frac{4\pi}{C_A a L^2}} \operatorname{erf}\left(\sqrt{\frac{C_A a L^2}{4}}\right) \times \left(3 + aL^2 b \left(\frac{C_F a L^2}{3} - \frac{1}{2} \right) - 3C_F a L^2 + \frac{b}{C_A} \right) + \frac{1}{C_A} \left(\exp\left(-\frac{C_A a L^2}{4}\right) - 1 \right) \left(\frac{2C_F b L^2}{3} - \frac{b}{3} - 6C_F \right) - \frac{b}{C_A} \right] + \frac{3}{L} f(a) \right\} \quad (4.60)$$

where $\operatorname{erf}(x)$ is known as the error function and is defined in the following way

$$\operatorname{erf}(x) \equiv \frac{2}{\sqrt{\pi}} \int_0^x e^{-t^2} dt. \quad (4.61)$$

Compared to the previous observables, $f(a)$ is a relatively complicated function. Hence, so that we can understand the behaviour of this function $f(a)$ has been plotted as a function of a in Figure 4.11. As can be seen from this plot the function is double valued and so when we solve the equation $f(F(R)) = R$ to obtain $F(R)$, we must again take the smaller solution since this is our perturbatively correct solution.

Again, following the above procedure allows us to obtain the plots for the resummed leading logarithm contribution, $\Delta\rho_0^{LL}$, as shown in Figure 4.12. The resummed double leading logarithm contribution, $\Delta\rho_0^{DLL}(R)$, is shown in Figure 4.13. As can be seen from these two graphs, it appears, once again, that the next-to-leading logarithm contribution is dominating our picture.

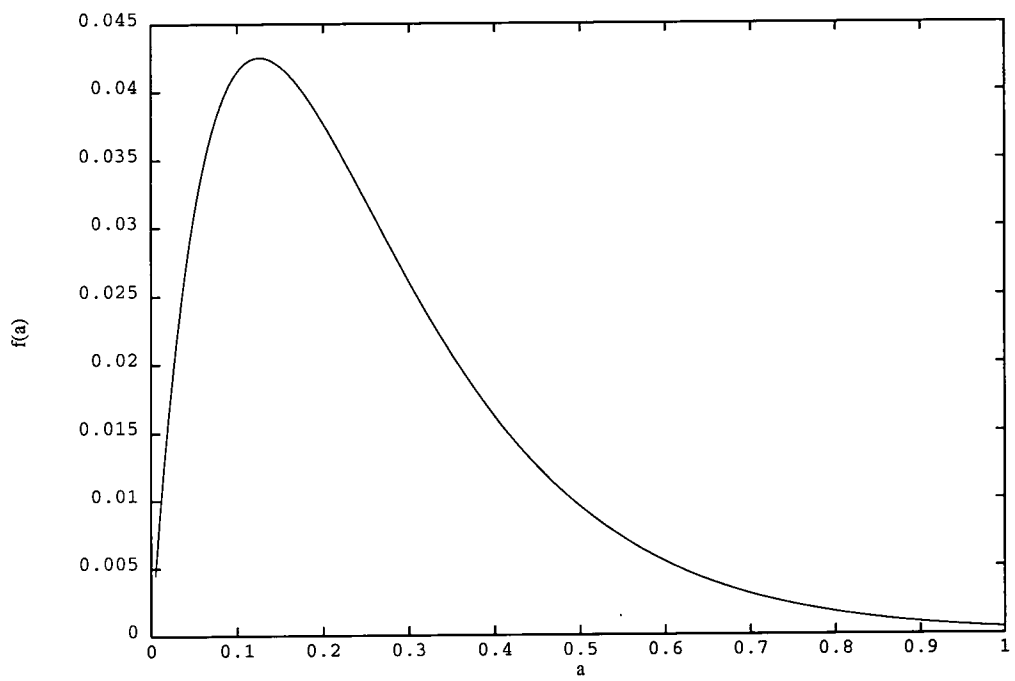


Figure 4.11: This Figure shows how $f(a)$ of equation (4.59) behaves as a function of a for $y_c = 0.04$

If we plot the double leading logarithm contribution on the same axes as $\Delta\rho_0^{exp}$ with $\tilde{\Lambda}_{\overline{MS}}$ set equal to 85.6 MeV, as shown in Figure 4.14, then we again find that there is no similarity between the data and the double logarithm prediction.

Therefore, we again have to conclude that it is unwise to believe that the leading and next-to-leading logarithms are the dominant contributions for the range of data that we are considering.

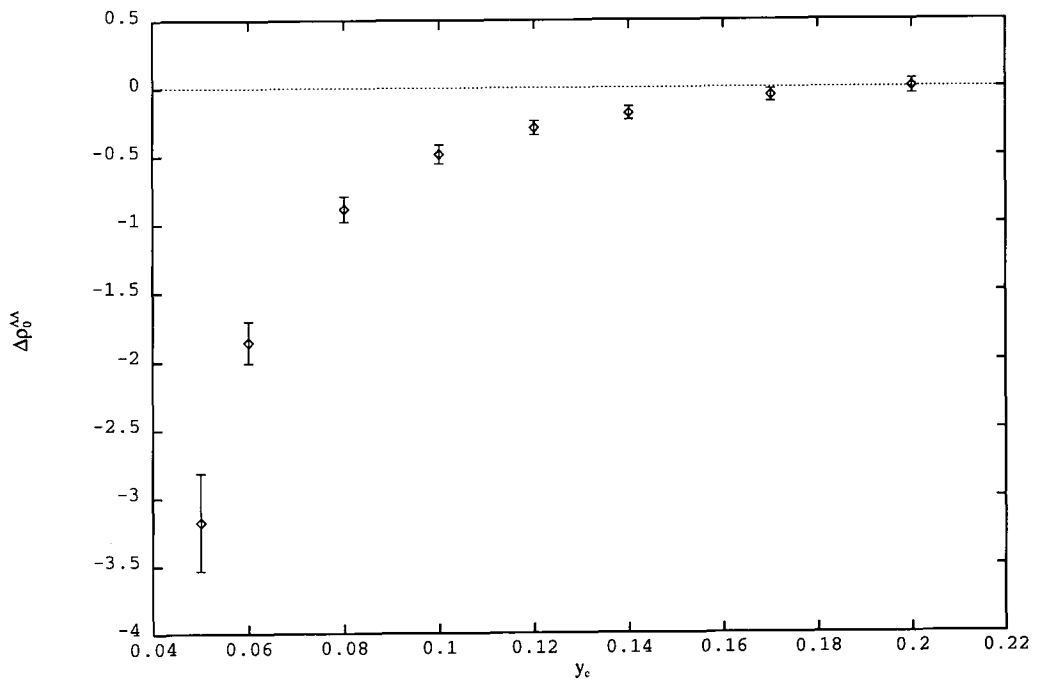


Figure 4.12: The graph to show the resummed leading logarithm approximation $\Delta\rho_0^{LL}$ as a function of y_c for $R_3(D)$

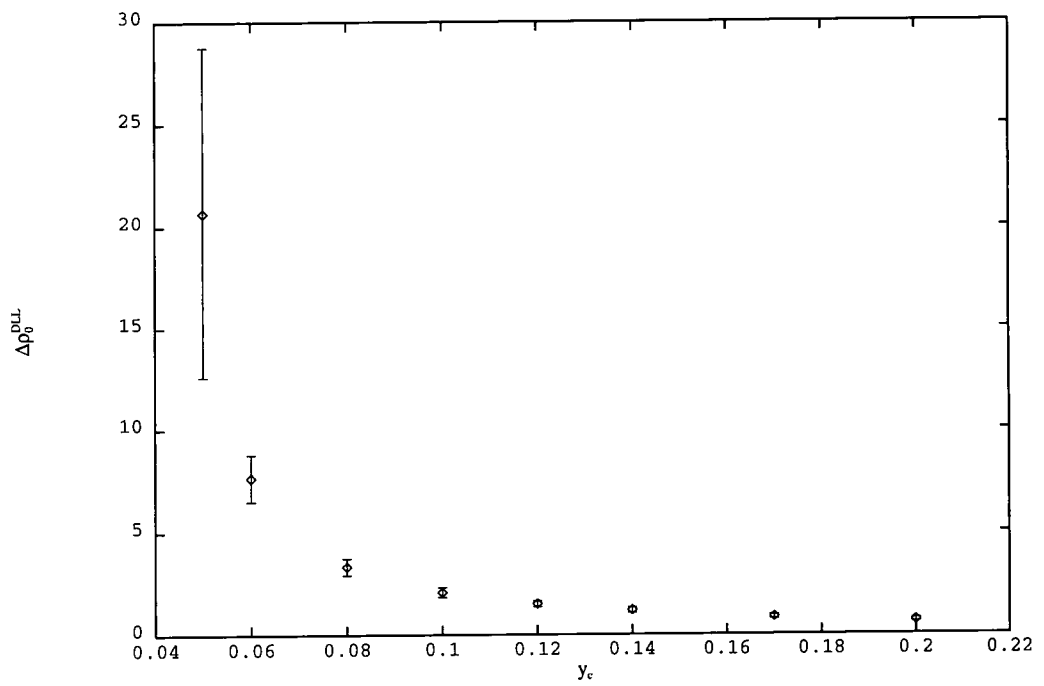


Figure 4.13: The graph to show the double leading logarithm contribution $\Delta\rho_0^{DLL}$ as a function of y_c for $R_3(D)$

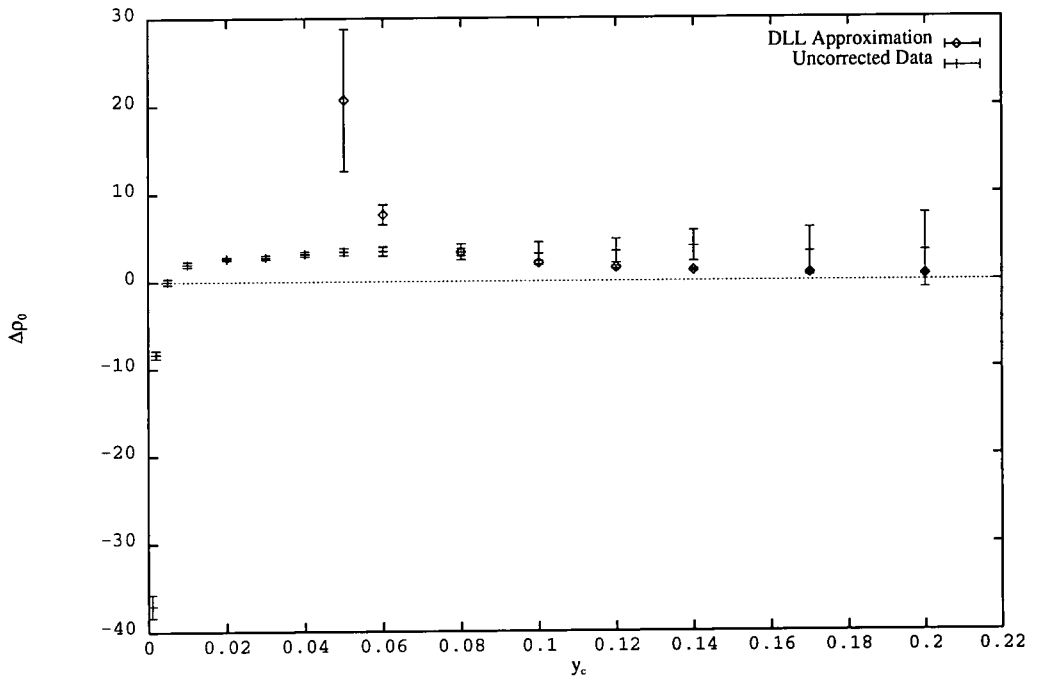


Figure 4.14: For the observable $R_3(D)$ the DLL approximation $\Delta\rho_0^{DLL}$ of equation (4.31) versus y_c is compared with $\Delta\rho_0^{exp}$ with $\tilde{\Lambda}_{MS}^{(5)}$ adjusted. OPAL data of reference [6] uncorrected for hadronization effects is used.

4.11 The Breakdown of the Resummation

It was found, for very small λ , that the resummation broke down. This manifested itself in the fact that for certain λ the equation

$$R_{exp} = f(a) \tag{4.62}$$

has no solution. For $R_2(D)$ this equation only has a solution for $R_{exp} < 2/(L^2 C_F)$, and this condition is only satisfied for $y_c \gtrsim 0.005$. For the energy-energy correlation function the same condition must be satisfied and this only occurs for $\chi \lesssim 140^\circ$. For thrust the condition $R_{exp} < 1/((L^2 C_F))$ must be satisfied for the convergence of our resummation and this only occurs for $T \lesssim 0.835$. For the 3-jet fraction, $R_3(D)$, the condition is far more complicated but again the resummation only converges for $y_c \gtrsim 0.05$.

Hence, it appears that this resummation procedure breaks down, in general, for small λ . This is a little unfortunate since this is exactly the region where the leading and next-to-leading logarithm contributions are supposed to dominate our picture. We conclude that whilst we can resum leading logarithm and next-to-leading logarithm contributions to $\Delta\rho_0$ to all-orders, these terms are not sufficient to represent the actual behaviour of $\Delta\rho_0$. We note that the measured effective charges R_{exp} and the corresponding $\Delta\rho_0^{exp}$ are smooth and essentially λ -independent right down to smaller λ than the region where the resummation breaks down. Therefore, the behaviour of the resummation, as shown in this chapter, is not due to the data we have to hand, but, instead, reflects the inadequacy of the limited resummation that has been performed.

Chapter 5

The Renormalization Group Equation Estimates of Perturbative Coefficients

5.1 Introduction

The calculation of perturbation theory coefficients in renormalizable field theories involves much labour intensive effort. For instance to complete the eighth order QED calculation of the anomalous magnetic moment of the electron has necessitated the evaluation of 891 Feynman diagrams and has so far taken some ten years of intensive numerical calculation using high powered electronic computers, to achieve a result for the $O(\alpha^4)$ coefficient still only accurate to 10% [61]. Similarly, to calculate the QCD coefficient of the total hadronic e^+e^- cross section to $O(\alpha_s^3)$ [62] has necessitated at least five years of effort and the original published results [63] were incorrect due to a computer programming error.

Clearly what is required is a way of plausibly estimating the next perturbative coefficient in the series given more or less exact calculations of the first few [64]. In the past several attempts to do this for QED [65] and QCD [66] have appeared based on Padé approximants and other methods of ‘improving’ power series. A major disadvantage of such approaches is that the particular form of the series one chooses to

improve depends on which renormalization scheme is used to perform the calculation, and in any case the reliable application of such improvement methods needs some knowledge of the large-order behaviour of the series coefficients, which is lacking for the physical quantities of interest.

In Section 5.2 we shall demonstrate that the renormalization group is capable of providing such estimates of uncalculated coefficients when supplemented with certain extra assumptions. We suggest that these assumptions are probably satisfied for the anomalous magnetic moment of the electron, enabling us to give an estimate for the, as yet, uncalculated tenth order coefficient, and to reproduce the calculated eighth order coefficient at the 20% level, based on the known sixth and lower order coefficients. Unfortunately, for the QCD calculations of the total hadronic cross section we find that the extra assumptions are not satisfied and we cannot reliably make similar estimates.

However, we can estimate the $O(a^3)$ for the total hadronic cross section if we examine the behaviour around the $N_f = 33/2$ pole in the QCD Beta-function. This will be demonstrated in section 5.3.

5.2 The First Attempt

The basic idea is very simple. Again we consider the generic physical quantity R calculated as a power series in the renormalization improved coupling $a \equiv \alpha_s/\pi$

$$R = a + r_1 a^2 + r_2 a^3 + \dots \quad (5.1)$$

The importance of the RS invariants ρ_k defined in Chapter 3 is that on rearranging equations (3.46) we can obtain

$$r_n = \frac{1}{(n-1)}(\rho_n - c_n) + \tilde{r}_n \quad (n > 1) \quad (5.2)$$

where

$$\begin{aligned}
\tilde{r}_2 &= r_1 c + r_1^2 \\
\tilde{r}_3 &= 2r_1 r_2 + r_1 \rho_2 + \frac{1}{2} r_1^2 c - r_1^3 \\
&\vdots \quad \quad \quad \vdots
\end{aligned} \tag{5.3}$$

Equation (5.2) tells us that r_n calculated in an RS labelled by c_2, c_3, \dots, c_n and r_1 , can be split into two terms. The first involving $(\rho_n - c_n)$ requires an n -loop calculation for its determination whereas the second, \tilde{r}_n , involves only r_{n-1}, c_{n-1} and lower coefficients and so is specified by an $(n-1)$ -loop calculation. Thus r_n is partitioned into a genuinely new piece of n -loop information, and a term involving old information assembled by the renormalization group from $(n-1)$ -loop and lower orders. The hope is that for some quantities calculated in particular RS's, over a limited range of n , the first term may be much less important than the second so that $r_n \simeq \tilde{r}_n$ serves as an adequate estimate. This will be true provided that for the particular RS and quantity in question $(\rho_n - c_n)$ remains $\lesssim Kn$ where K is of order unity. Let us now apply these considerations to the anomalous magnetic moment of the electron.

$$a_e = \frac{(g_e - 2)}{2} = \frac{a}{2}(1 + r_1 a + r_2 a^2 + \dots) \tag{5.4}$$

All of the perturbative calculations of this quantity have been carried out in the 'on-shell' RS in which $a = a_{fs}$, the QED fine structure constant, so that the on-shell c_r^{OS} are just the invariants ρ_r^{fs} for the fine structure constant. We shall assume in what follows that r_i and c_i are always evaluated in the 'on-shell' scheme unless otherwise stated. The (on-shell) coefficients r_i and c_i up to four-loops are all known with varying degrees of accuracy:

$$\begin{aligned}
r_1 &= -0.6569579311 \dots \\
r_2 &= 2.35222 \pm 0.00084
\end{aligned}$$

$$\begin{aligned}
r_3 &= -2.868 \pm 0.276 & (5.5) \\
c &= \frac{3}{4} = 0.75 \\
c_2 &= -\frac{121}{96} = -1.2604\dots \\
c_3 &= 0.3397
\end{aligned}$$

The quoted errors in the above are the numerical errors from the loop integrations which cannot be performed analytically. r_1 is known analytically and can hence be expressed to an arbitrary number of significant figures.

Using equations (3.46) and (5.3) one finds from the above coefficients $\tilde{r}_2 = -0.061$, $\tilde{r}_3 = -3.40$, $\tilde{r}_4 = 7.62 \pm 0.81$, $\rho_2 = 1.154$, $\rho_3 = 1.408 \pm 0.56$. Clearly r_2 is dominated by the $(\rho_2 - c_2)$ term and so \tilde{r}_2 cannot be used as an estimate. For r_3 , however, we see that \tilde{r}_3 is within 20% of the exact result. The conditions necessary for r_3 and r_4 to be well estimated by \tilde{r}_3, \tilde{r}_4 are $(\rho_3 - c_3) \ll 7$, $(\rho_4 - c_4) \ll 25$, so provided that the ρ_4 and c_4 remain quantities of order 1, as for the lower ρ_r 's and c_r 's, we may anticipate that $r_4 \simeq \tilde{r}_4 = 7.62 \pm 0.81$, should be within 10% of the exact tenth order coefficient.

Another way of looking at this dominance of \tilde{r}_n is to see how dependent r_4, r_5, r_6 are on the as yet unknown $\rho_4, \rho_5, \rho_6, c_4, c_5, c_6$.

To this end we will assume that the c_r continue to alternate in sign with positive ρ_k , as suggested by the known coefficients up to four loops. We then randomly generate sets of $\rho_4, \rho_5, \rho_6, c_4, c_5, c_6$ on a computer so that the $|\rho_k|, |c_k|$ are uniform on the interval $[0, \lambda]$, and we allow the parameter λ to vary from 0 – 10. For each set of randomly generated beta-function coefficients we evaluate r_4, r_5, r_6 using the known exact r_i, c_i $i \leq 3$ and equations (5.2) and (5.3) (we take the central value for the r_3 ignoring the additional numerical error). For each value of λ we then extract the maximum and minimum r_4, r_5, r_6 obtained over a large number ($\sim 10^5$) of trials. The results are tabulated in Table 5.1.

λ	r_4	r_5	r_6
0	7.62	-10.46	14.14
1	8.24	-10.47	19.81
	7.64	-12.17	13.96
2	8.93	-10.24	26.61
	7.65	-14.42	13.66
3	9.59	-10.13	32.84
	7.67	-16.10	13.41
5	10.91	-9.91	45.30
	7.70	-19.86	12.93
10	14.20	-9.37	76.47
	7.79	-29.26	11.72

Table 5.1

The key feature illustrated by the table is the insensitivity of the coefficients to the details of the unknown beta function coefficients, that is changes in the parameter λ . This stability is most evident in the lowest coefficient r_4 , with increasing sensitivity for r_5 and r_6 which, of course, depend on more unknown parameters.

The pattern of signs and magnitudes would seem to be well-established, however. Notice that just the assumptions of positive ρ_k and alternating c_k ensures that $(\rho_k - c_k) > 0$ and hence gives a bound on the tenth order coefficient $r_4 > 7.62 \pm 0.81$.

The coefficients c_k will be polynomials in N , the number of fermions, of degree $k-1$,

$$c_k = c_k^{[k-1]} N^{k-1} + c_k^{[k-2]} N^{k-2} + \dots + c_k^{[0]} \quad (5.6)$$

For the anomalous magnetic moment of the electron $N = 1$ is appropriate and these are the values for c_2, c_3 given in equation (5.5). It is possible to calculate $c_k^{[k-1]}$ to all

orders [71] and study the growth of at least this part of the beta function coefficients. This was first attempted in [72] using an approximation where photon propagators are set to their asymptotic form. In this approximation there was rapid growth of the $c_k^{[k-1]}$. More recently an exact calculation [71] has been performed indicating that there are substantial corrections to the approximation, and a much slower rate of growth. These $c_k^{[k-1]}$ are given in Table 5.2. They remain small quantities of order 1 right up to $k = 9$ where more rapid growth seems to set in. This provides some evidence that the full c_k will not exhibit rapid growth, and the hope is that this is also true of the ρ_k for a_e . The c_k are of course just the ρ_k for a_{fs} .

k	$c_k^{[k-1]}$
2	-1.17
3	-0.37
4	-0.29
5	-0.35
6	-0.55
7	-1.05
8	-2.39
9	-6.45

Table 5.2

We should mention that the approach discussed here is closely connected with the discussions of optimized perturbation theory in QED of [73]. In this work the PMS [18] and fastest apparent convergence (FAC, equivalent to EC) criteria were used to fix the RS. The discrepancy between the ‘optimized’ sixth order and the on-shell result

was then expressed as a multiple of a^4 . The relevant coefficient given by equation (5.4) of [73] for the FAC criterion is just our \tilde{r}_3 . At the time of the publication of [73] only a very preliminary value for r_3 was available, $r_3 = -1.6 \pm 5$ [74] but the reasonable agreement between this coefficient and $\tilde{r}_3 = -3.4$ was noted.

Unfortunately, our estimate of the tenth order coefficient is probably not of too much phenomenological relevance since the discrepancy [61] between the eighth order theoretical prediction using the best measured value of the fine structure constant and the measured a_e is of the order of the eighth order correction. To account for the 1.7σ difference would require $r_4 \sim 10^3$. The estimated coefficient does at least have the positive sign required by the data.

We finally turn to the e^+e^- total hadronic cross section and ask whether similar estimates of higher coefficients are possible. We have

$$R_{e^+e^-} = \frac{\sigma(e^+e^- \rightarrow \text{hadrons})}{\sigma(e^+e^- \rightarrow \mu^+\mu^-)} = \sum_f Q_f^2 (1 + \delta_{QCD}) \quad (5.7)$$

where

$$\delta_{QCD} = a + r_1 a^2 + r_2 a^3 + \dots$$

In the \overline{MS} scheme (with $\mu = Q$ the e^+e^- cm energy) with five flavours of massless quark we have [62, 75, 43] $r_1 = 1.41$, $r_2 = -12.8$; $c = 1.26$, $c_2 = 1.48$ and using equations (3.46) and (5.3) we have $\tilde{r}_2 = 3.77$, $\tilde{r}_3 = -58.91$, $\rho_2 = -15.08$. Evidently, r_2 is dominated by $(\rho_2 - c_2)$ and cannot be estimated from \tilde{r}_2 .

5.3 The Pole Approximation

As discussed in Chapter 3 a next-to-next-to-leading order calculation of the total hadronic cross-section is now available [70],

$$R_{e^+e^-}(s) = \frac{11}{3} \left[1 + a(\sqrt{s}) + r_1 a(\sqrt{s})^2 + r_2 a(\sqrt{s})^3 + \dots \right] \quad (5.8)$$

where, r_1 and r_2 , are given by the two expressions

$$\begin{aligned} r_1 &= 1.9857 - 0.1153N_f = 1.4092 \quad \text{for } N_f = 5 \\ r_2 &= -6.6368 - 1.2001N_f - 0.0052N_f^2 = -12.77 \quad \text{for } N_f = 5 \end{aligned} \quad (5.9)$$

From equation (3.46) we have that

$$\overline{\rho}_2 = r_2 + c_2 - r_1 c - r_1^2 \quad (5.10)$$

and so if we can estimate $\overline{\rho}_2$, then we implicitly have also made an estimate of r_2 .

In a scheme such as \overline{MS} which can be operationally implemented with actual Feynman diagram calculations the r_n coefficients will be polynomials in N_f of degree n . The coefficients of different powers of N_f reflecting diagrams with different numbers of quark loops. For the beta-function coefficients, however, the c_i can be written

$$\begin{aligned} c &= -\left(-\frac{51}{4} + \frac{19}{12}N_f\right) \frac{6}{33 - 2N_f} \\ c_2 &= -\frac{1}{64} \left(-2857 + \frac{5033}{9}N_f - \frac{325}{27}N_f^2\right) \frac{6}{33 - 2N_f} \\ \vdots & \quad \vdots \end{aligned} \quad (5.11)$$

and have single poles at $N_f = \frac{33}{2}$. Allowing a general number of colours, N , we can expand all our coefficients as a series in N and δ where

$$\delta = 1 - \frac{2N_f}{11N} = \frac{6b}{11N}. \quad (5.12)$$

The non-trivial fixed point of QCD where $b = 0$ corresponds to $\delta = 0$, and a pure gauge theory ($N_f = 0$) corresponds to $\delta = 1$. We want to expand around the non-trivial fixed point of QCD, $\delta = 0$, and in $\frac{1}{N}$, N large.

We will have

$$c = \left[-\frac{75 N}{88 \delta} + \frac{3}{8\delta N} + \frac{13N}{8} - \frac{3}{8N} \right], \quad (5.13)$$

$$\begin{aligned} \frac{c_2^{MS}}{c_2} &= \left[-\frac{701 N^2}{704 \delta} + \frac{3}{128\delta N^2} + \frac{11}{64\delta} + \frac{53}{64} N^2 \right. \\ &\quad \left. - \frac{3}{128N^2} - \frac{121}{384}\delta + \frac{77}{72}\delta^2 + \frac{55}{384} \right] \end{aligned} \quad (5.14)$$

and

$$\rho_2 = A_0 \frac{N^2}{\delta} \left[\left(1 + \frac{A_1}{N} + \frac{A_2}{N^2} + \dots\right) + \delta \left(B_0 + \frac{B_1}{N} + \dots\right) + \delta^2 \left(C_0 + \frac{C_1}{N} + \dots\right) + \dots \right] \quad (5.15)$$

The δ^{-1} pole term in ρ_2 comes only from c_2 and $r_1^* c$, where the asterix denotes the $b = 0$ fixed point. It is hence known exactly without requiring knowledge of r_2 . If $\delta \ll 1$ then this term will dominate and ρ_2 should be well estimated by just this term. Similarly, for ρ_3 the δ^{-1} term only involves the δ^{-1} term in c_3 and r_1^* . In general, the ρ_k only have *single* poles in δ . Of course for $N_f = 5$, $N = 3$ $\delta = 0.697$ which is not particularly small.

By substituting the known values of c , c_2 , r_2 and r_1 , where r_2 and r_1 are expressed in terms of Riemann zeta functions [70], we obtain that ρ_2 is given by

$$\begin{aligned} \rho_2 &= -\frac{1377 N^2}{1408 \delta} \left[\left(1 - \frac{153 \cdot 1408}{704 \cdot 1377} \frac{1}{N^2}\right) \right. \\ &\quad + \delta \frac{1408}{1377} \left(\left(\frac{13}{768} + \frac{11}{8} \zeta_3\right) + \left(\frac{11}{8} \zeta_3 - \frac{257}{384}\right) \frac{1}{N^2} + \frac{47}{256} \frac{1}{N^4} \right) \\ &\quad + \delta^2 \frac{1408}{1377} \left(\left(\frac{407}{72} \zeta_3 - \frac{55}{9} \zeta_5 - \frac{3421}{1152}\right) + \left(\frac{55}{6} \zeta_5 - \frac{187}{24} \zeta_3 - \frac{11}{96}\right) \frac{1}{N^2} \right) \\ &\quad \left. + \delta^3 \frac{1408}{1377} \left(\frac{121}{432} \pi^2 + \frac{121}{9} \zeta_3^2 - \frac{847}{54} \zeta_3 - \frac{14399}{5184} \right) \right] \end{aligned} \quad (5.16)$$

If we evaluate these zeta functions, then we are left with the following expression for ρ_2

$$\rho_2 = -\frac{1377 N^2}{1408 \delta} \left[\left(1 - \frac{2}{9} \frac{1}{N^2}\right) + \delta(1.70735 + 1.00570 \frac{1}{N^2} + \frac{517}{2754} \frac{1}{N^4}) \right]$$

$$+ \delta^2(-2.56798 + .0251140 \frac{1}{N^2}) + 0.5713386 \delta^3 \quad (5.17)$$

If we now vary δ between one and zero (i.e. vary N_f between zero and $11N/2$), then we should be able to see a general pattern in the behaviour of this latter function. We can also vary N between zero and any number that we feel is suitable. When this is done we obtain the graph shown in Figure 5.1.

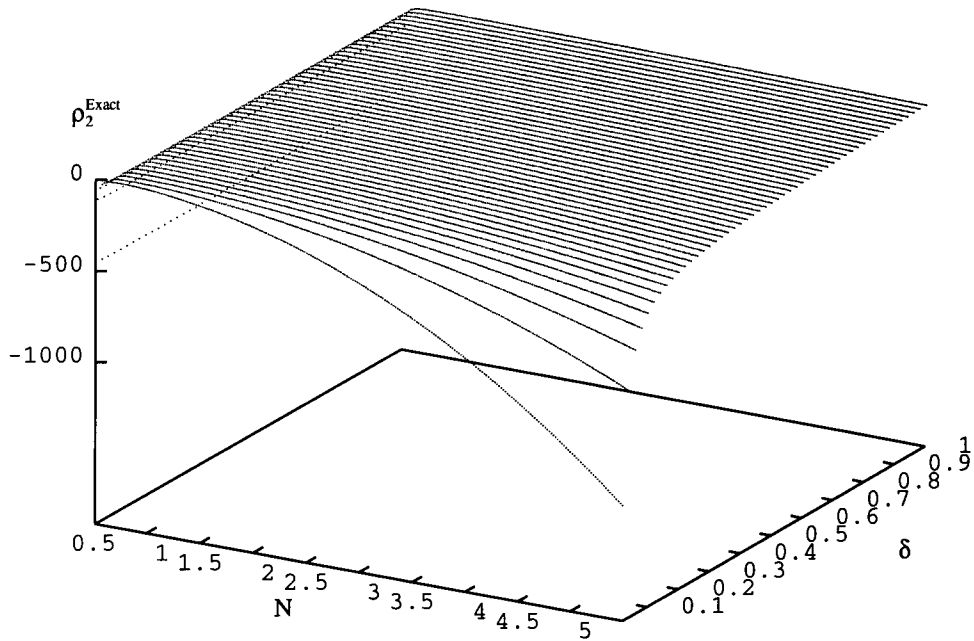


Figure 5.1: A graph to show how ρ_2 , as calculated using equation (5.16), varies with N and δ

Now when we evaluate the coefficient $-\frac{1377 N^2}{1408 \delta}$ we find that it is equal to -12.63 for $N_f = 5$ and $N = 3$. This is very surprising since there is only a 20% discrepancy between this value, which we shall call the pole term, and the exact value of ρ_2 .

Hence, if we plot

$$\rho_2^{Pole} = -\frac{1377 N^2}{1408 \delta} \quad (5.18)$$

as a function of both N and δ , as shown in Figure 5.2, then we find that the pole term is a good approximation to the exact value of ρ_2 . Infact overall there is no more than a 30% discrepancy between the two. This is more easily seen in Table 5.3 in which we have tabulated the values of ρ_2 , calculated using equation (5.16), and the values of ρ_2^{Pole} , as calculated in equation (5.18), for various values of N and δ . Thus, we are able to conclude that it is possible to estimate r_2 using the pole term for the total hadronic cross section.

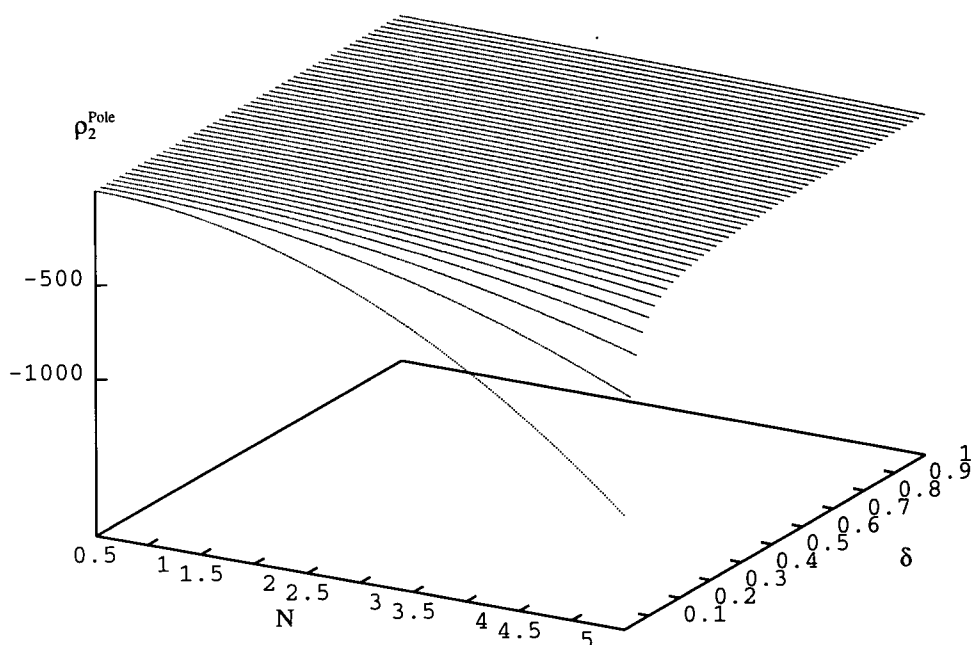


Figure 5.2: A graph to show how ρ_2^{Pole} , as calculated using equation (5.18), varies with N and δ

N δ	0.5	1.0	1.5	2.0	3.0	4.0	5.0
0.1	-2.35 (-2.44)	-10.20 (-9.78)	-24.10 (-22.00)	-43.67 (-39.12)	-99.67 (-88.02)	-178.09 (-156.48)	-278.92 (-244.50)
0.2	-2.16 (-1.22)	-6.17 (-4.89)	-13.66 (-11.00)	-24.27 (-19.56)	-54.64 (-44.01)	-97.19 (-78.24)	-151.90 (-122.25)
0.3	-2.06 (-.81)	-4.68 (-3.26)	-9.86 (-7.33)	-17.22 (-13.04)	-38.33 (-29.34)	-67.90 (-52.16)	-105.94 (-81.50)
0.4	-1.98 (-.61)	-3.83 (-2.44)	-7.73 (-5.50)	-13.29 (-9.78)	-29.27 (-22.00)	-51.65 (-39.12)	-80.45 (-61.12)
0.5	-1.92 (-.49)	-3.25 (-1.96)	-6.29 (-4.40)	-10.65 (-7.82)	-23.17 (-17.60)	-40.73 (-31.30)	-63.31 (-48.90)
0.6	-1.87 (-.41)	-2.81 (-1.63)	-5.20 (-3.67)	-8.66 (-6.52)	-18.60 (-14.67)	-32.55 (-26.08)	-50.49 (-40.75)
0.7	-1.82 (-.35)	-2.46 (-1.40)	-4.33 (-3.14)	-7.07 (-5.59)	-14.95 (-12.57)	-26.02 (-22.35)	-40.26 (-34.93)
0.8	-1.78 (-.31)	-2.16 (-1.22)	-3.60 (-2.75)	-5.74 (-4.89)	-11.92 (-11.00)	-20.59 (-19.56)	-31.76 (-30.56)
0.9	-1.74 (-.27)	-1.90 (-1.09)	-2.98 (-2.44)	-4.60 (-4.35)	-9.32 (-9.78)	-15.95 (-17.39)	-24.49 (-27.17)
1.0	-1.70 (-.24)	-1.67 (-.98)	-2.44 (-2.20)	-3.62 (-3.91)	-7.07 (-8.80)	-11.92 (-15.65)	-18.17 (-24.45)

Table 5.3: A Table to demonstrate quantitatively how ρ_2 , as calculated in equation (5.16), and $\rho_2^{Pole} = -\frac{1377 N^2}{1408 \delta}$, which is the number in brackets, vary as a function of N and δ .

Unfortunately, this appears to be an algebraic 'fluke'. It relies on the fact that

fortuitously the additional polynomial in δ is rather small over the whole range $0 < \delta < 1$.

It is interesting to note that the δ^{-1} pole terms in c and $c_2^{\overline{MS}}$ are both negative and close to unity in magnitude. If this is also true for the higher c_n 's it might suggest that generally $\rho_k \sim -\frac{N^k}{\delta}$. The uniform negative sign would result in an infra-red fixed point in the effective charge beta-function, $\rho(R^*) = 0$, which in turn would lead to freezing of the effective charges for physical observables so that $R(Q) \rightarrow R^*$, $Q \rightarrow 0$. This behaviour has been suggested by Mattingly and Stevenson, who have examined the low- Q experimental data for the e^+e^- QCD R-ratio [58].

Chapter 6

Summary and Conclusions

Evidently if one has a NLO perturbative QCD calculation available there will be some uncertainty in the NLO perturbative prediction for a QCD observable due to the missing uncalculated higher-order terms in the perturbation series. This has the effect that when one compares the NLO calculation with experimental data one may anticipate that the value of $\tilde{\Lambda}_{\overline{MS}}$ extracted will not be universal but will exhibit some scatter for different observables due to the differing sizes of the uncalculated contributions. The problem is compounded by the fact that the $\tilde{\Lambda}_{\overline{MS}}$ extracted depends also on the choice of RS at NLO, which may be labelled by r_1 the NLO coefficient (or equivalently the renormalisation scale μ), an unphysical parameter. It has been seen in equation(3.84) that the relation between the extracted $\tilde{\Lambda}(NLO, r_1)$ and the actual $\tilde{\Lambda}_{\overline{MS}}$ which one is trying to measure is factorized into two contributions. One, $\Delta F(r_1, R)$, is r_1 -dependent and known exactly from equation (3.85), and the other, $\Delta\rho_0$, is unknown but r_1 -independent. $\Delta\rho_0$ depends only on the observable and NNLO and higher RS-invariants ρ_2, ρ_3, \dots . The predictable r_1 -dependence of $\tilde{\Lambda}(NLO, r_1)$ therefore has nothing to tell us about the importance of uncalculated corrections, the irreducible uncertainty resides in the unknown $\Delta\rho_0$. Some of the r_1 -dependent logarithms in the NNLO and higher corrections can be summed up into $\Delta F(r_1, R)$ and the remainder can be absorbed into RS-invariant combinations contained in $\Delta\rho_0$.

The unknown $\Delta\rho_0$ can be isolated by choosing the particular RS where $r_1 = 0$, $\mu = \mu_{EC}$ the effective charge scale, which sets $\Delta F = 0$. From the scatter in $\tilde{\Lambda}(NLO, 0)$ for different observables one can then infer the scatter in $\Delta\rho_0$, in particular relative differences $\Delta\rho_{0A} - \Delta\rho_{0B}$ for observables A,B can be absolutely measured. Figure 3 indicates that these relative differences cannot be neglected for a range of LEP observables. For at least some of the observables $\Delta\rho_0$ must be sizeable, and so $\Delta\rho_0$ must be estimated before we can determine $\tilde{\Lambda}_{\overline{MS}}$ with any reliability.

In contrast, in the standard LEP determinations of $\alpha_s(M_Z)$ one tries to estimate the importance of uncalculated higher-order corrections by using two different ad hoc scale choices and interpreting the spread in extracted $\alpha_s(M_Z)$ as indicating a ‘theoretical error’. By artificially enlarging uncertainties in this way one obtains a spurious consistency between different observables, the real scale-independent uncertainty due to $\Delta\rho_0$ being buried beneath the supposedly informative scale dependence of ΔF . The global $\alpha_s(M_Z)$ determinations obtained with these sort of analyses should therefore be treated with some scepticism.

Having determined that $\Delta\rho_0$ is not negligible one must try to estimate it to make further progress. Within the effective charge formalism one can write $\tilde{\Lambda}_{\overline{MS}}$ in terms of the measured observable $R(Q)$, $r_1^{\overline{MS}}$ and $\Delta\rho_0$ constructed non-perturbatively from the measured running $dR/d\ln Q = -b\rho(R)$. $\Delta\rho_0$ may also be obtained perturbatively by expanding the effective charge β -function, so that given a NNLO calculation one can estimate $\Delta\rho_0^{NNLO} = \rho_2 R$. By combining NNLO calculations and Q -dependence measurements one can refine ones knowledge of $\Delta\rho_0$ and hence of $\tilde{\Lambda}_{\overline{MS}}$. The perturbative RS-invariants $\rho_0(\overline{\Lambda})$, ρ_2 , ρ_3 , ... are connected with $Q \rightarrow \infty$ evolution of the observable $R(Q)$, and hence provide information about the function $\rho(R)$ in the vicinity of $R = 0$.

The present situation is that a NNLO calculation is available only for the hadronic width of the Z^0 . By estimating $\Delta\rho_0^{NNLO}$ for this observable, and combining PETRA data for jet rates and energy-energy correlations, with LEP data on these observables, to obtain an estimate of $\Delta\rho_0$ from Q -dependence, we found consistency for $\tilde{\Lambda}_{\overline{MS}}^{(5)} = 287 \pm 100$ MeV.

We can conclude that reliable measurements of $\tilde{\Lambda}_{\overline{MS}}$ at e^+e^- machines will require at least NNLO perturbative calculations and/or measurements of observables at more than one energy. Acquiring such information will entail considerable experimental and theoretical effort. The effective charge formalism allows one to efficiently harness this hard won information to refine one's knowledge of $\tilde{\Lambda}_{\overline{MS}}$ and the interplay between perturbative and non-perturbative effects. The insistence on formulating everything in terms of physical quantities allows one to quantify uncertainties in a way which is impossible in approaches which choose the unphysical RS-dependence parameters according to some plausibility argument.

An important remaining problem is to extend the approach to processes with initial state hadrons where there is an additional factorization ambiguity connected with the separation of structure functions from the hard cross-sections.

We have also seen that for observables where leading and next-to-leading logarithms in kinematical variables can be resummed one can unambiguously estimate $\Delta\rho_0^{NLL}$ by resumming leading and next-to-leading logarithms in the RS invariants ρ_k . In the conventional approach one needs to use an ad hoc matching procedure to include the exact NLO perturbative coefficient, and the problem of scale dependence still remains. Performing this analysis for all our observables we found that there is no agreement between the λ -dependence at low λ of $\Delta\rho_0^{DLL}$ and $\Delta\rho_0^{exp}$ using uncorrected data.

Additionally, we argued that it is possible to estimate the higher order coefficients in the QED magnetic moment of the electron. Unfortunately, the procedure could not be extended to QCD. We drew attention to the possibility of an expansion in $\frac{1}{N}$ and δ , where $\delta = 0$ corresponds to the non-trivial fixed point of QCD, $b=0$. Whilst inconclusive this expansion had various interesting features, and the "leading" δ^{-1} term gave a good estimate of the invariant ρ_2 for $R_{e^+e^-}$

Bibliography

- [1] D.Bailin and A.Love, *Introduction To Gauge Field Theory*, Adam Hilger, Bristol, 1986.
- [2] C.Itzykson and J.B.Zuber, *Quantum Field Theory*, McGraw-Hill, 1980.
- [3] L.H.Ryder, *Quantum Field Theory*, Cambridge University Press, 1985.
- [4] P.M.Stevenson, *Ann.Phys.* **132**,383 (1981).
- [5] OPAL Collaboration, P.D.Acton et al., *Z.Phys.* **C58**,523 (1993).
- [6] OPAL Collaboration, M.Z.Akrawy et al., *Z.Phys.* **C55**,1 (1992).
- [7] OPAL Collaboration, M.Z.Akrawy et al., *Z.Phys.* **C49**,375 (1991).
- [8] DELPHI Collaboration, P.Abreu et al., *Z.Phys.* **C54**,55 (1992).
- [9] ALEPH Collaboration, D.Decamp et al., *Phys.Lett.* **B225**,623 (1991).
- [10] L3 Collaboration, P.Adeva et al., *Phys.Lett.* **B248**,464 (1990).
- [11] S.Bethke, invited talk at the workshop on Jet Studies at LEP, Durham 1990, *J.Phys.* **G17**,1455 (1991).
- [12] S.Bethke, proceedings of the XXVI International Conference on High Energy Physics, Dallas (1992), edited by James R.Sanford, p.81.
- [13] LEP Collaborations Joint report, CERN-PPE/93-157 (1993).
- [14] R.K.Ellis, D.A.Ross and A.E.Terrano, *Nucl.Phys.* **B178**,421 (1981).
- [15] Z.Kunszt and P.Nason, in "Z Physics at LEP1" (eds. G.Altarelli, R.Kleiss and C.Verzegnassi), CERN 89-08 (1989).
- [16] S.G.Gorishny, A.L.Kataev and S.A.Larin, *Phys.Lett.* **B259**,144 (1991).
- [17] L.R.Surguladze and M.A.Samuel, *Phys.Rev.Lett.* **66**,560 (1991).
- [18] P.M.Stevenson, *Phys.Rev.* **D23**,2916 (1981).

- [19] G.Grunberg, Phys.Lett **B95**,70 (1980);
G.Grunberg, Phys.Rev. **D29**,2315 (1984).
- [20] A.Dhar and V.Gupta, Phys. Rev. **D29**,2822 (1984).
- [21] R.K.Ellis, summary talk in proceedings of the workshop on “New techniques for Calculating Higher Order QCD Corrections” December 1992. ETH Zurich preprint ETH-TH/93-01 (1993).
- [22] D.T.Barclay and C.J.Maxwell, Durham preprint DTP-92/26 (1992)(unpublished).
- [23] JADE Collaboration, S.Bethke et. al., Phys. Lett. **B213**,325 (1988).
- [24] S.Bethke, J.Phys.**G17**,1455 (1991).
- [25] S.Bethke, Z.Kunszt, D.Soper and W.J.Stirling, Nucl.Phys. **B370**,310 (1992).
- [26] C.J.Maxwell, proceedings of the XXVI International Conference on High Energy Physics, Dallas (1992), edited by James R.Sanford, p.905.
- [27] A. Ali et. al., Nucl. Phys. **B167**,454 (1980);
R.K.Ellis, D.A.Ross and A.E.Terrano, Nucl. Phys. **B178**,421 (1981);
K.Fabricius, G.Kramers, G.Schierholz and I.Schmitt, Z.phys. **C11**,315 (1982);
K.Hagiwara and D.Zeppenfeld, Nucl. Phys. **B313**,560 (1989).
- [28] G.Kramer and B.Lampe, Z.phys. **C39**,101 (1988).
- [29] C.J.Maxwell, Phys. Lett. **B225**,425 (1989).
- [30] A.De.Rujula, J.Ellis, E.G.Floratos and M.K.Gaillard, Nucl. Phys. **B138**,387 (1978).
- [31] A.Ali and T.Barreiro, Nucl. Phys. **236**,269 (1984).
- [32] C.Basham, L.Brown, S.Ellis and S.Love, Phys. Rev. Lett.**41**,1585 (1978) , Phys. Rev. **D19**,2018 (1979) and *ibid.* **D24**,2382 (1981).
- [33] D.Bardin et al., Nucl.Phys. **B351**, 1 (1991).
- [34] K.G.Chetyrkin and J.H.Kuhn, Phys. Lett. **B229**, 359 (1990).
- [35] S.Catani, CERN preprint, CERN-TH-6281-91, (1991).
- [36] S.Catani, Y.L.Dokshitzer, M.Olsson, G.Turnock and B.R.Webber, Phys.Lett. **B269**, 432 (1991).
- [37] S.Catani, G.Turnock and B.R.Webber CERN Preprint CERN-TH.6640/92 (1992).

- [38] R.Coquereaux, Ann.Phys.(N.Y.),**125**,401 (1980).
- [39] E.C.G. Stueckelberg and A.Petermann, Helv.Phys.Acta 26,449 (1953).
- [40] W.Celmaster and R.J.Gonsalves, Phys.Rev, **D20**,1420 (1979).
- [41] W.Celmaster and R.J.Gonsalves, Phys.Rev, **D21**,3112 (1980).
- [42] C.J.Maxwell, Phys.Rev. **D29**,2884 (1984);
P.M.Stevenson, Phys.Rev. **D33**,3130 (1986).
- [43] O.V.Tarasov, A.A.Vladimirov, and A.Yu.Zharkov, Phys.Lett. **B93**,429 (1980).
- [44] S.A.Larin and J.A.M.Vermaseren, Phys.Lett. **B303**,334 (1993).
- [45] J.A.Nicholls, Ph.D. thesis Durham University (1990) (unpublished).
- [46] C.J.Maxwell and J.A.Nicholls, Phys.Lett. **B213**,217 (1988).
- [47] J.Chyla, A.Kataev, and S.Larin, Phys.Lett. **B267**,269 (1991).
- [48] The ‘physical scale’ argument is widespread in the literature. For a recent strong defence of the choice $\mu \simeq Q$ see: Stefano Catani, proceedings of the 17th workshop of the INFN Eloisatron Project, QCD at 200 TeV, Erice, June 1991. Preprint CERN-TH. 6281/91 (1991).
- [49] J.Chyla, Phys.Rev. **D40**,676 (1989).
- [50] G.Grunberg, Phys.Rev. **D40**,680 (1989).
- [51] M.Beneke, Max Planck Institute preprint, MPI-PH-93-6 (1993).
- [52] G.’t Hooft in ‘Deeper pathways in high-energy physics’ (Orbis Scientiae, Coral Gables, 1977) eds. B.Kursunoglu, A.Perlmutter and W.Scott (Plenum, New York, 1977); in ‘The whys of subnuclear physics’ (Erice 1977) ed. A.Zichici (Plenum, New York,1977).
- [53] T.Appelquist and J.Carazzone, Phys.Rev. **D11**, 2856 (1975).
- [54] OPAL Collaboration, P.D.Acton et al.,Phys.Lett. **B276**, 547 (1992).
- [55] A.X.El-Khadra, G.M.Hockney, A.S.Kronfeld, P.B.Mackenzie, Phys.Rev.Lett. **69**,729 (1992).
- [56] JADE Collaboration, W.Bartel et al., Z.Phys **C25**,231 (1984).
- [57] M.Jezabek and J.Kuhn, Phys.Lett. **301**,122 (1993).

- [58] A.C.Mattingly and P.M.Stevenson, Phys.Rev.Lett. **69**,1320 (1992);
 Proceedings of the DPF92 (Fermilab, Nov.1992);
 Rice University preprint DE-FG05-92ER40717-7 (1993).
- [59] G.Turnock, Cavendish Laboratory preprint CAVENDISH-HEP-92-3 (1992).
- [60] C.N.Lovett-Turner, in prparation.
- [61] T. Kinoshita and W.B. Lindquist, Phys.Rev. **D42**, 636 (1990).
- [62] L.R. Surguladze and M.A. Samuel, Phys.Rev.Lett. **66**, 560 (1991);
 S.G. Gorishny, A.L. Kataev and S.A. Larin, Phys.Rev.Lett. **B259**, 144 (1991).
- [63] S.G. Gorishny, A.L. Kataev and S.A. Larin, Phys.Rev.Lett. **212B**, 238 (1988).
- [64] R.P. Feynman, Solvay Conference Talk (1959).
- [65] Marshall Luban and Herman W. Chew Phys.Rev. **D31**, 2634 (1985).
- [66] J. Fleischer et. al., Univ. of Bielefeld preprint BI-TP 05/89 (1989).
- [67] C.J. Maxwell, Phys.Rev. **D29**, 2884 (1984);
 P.M. Stevenson, Phys.Rev. **D33**, 3130 (1986).
- [68] M.J. Levine, H.Y. Park and R.Z. Roskies,Phys.Rev. **D25**, 2205 (1982).
- [69] E.De.Rafael and J.L.Rosner:Ann.Phys. **82**, 369 (1974).
- [70] S.G. Gorishny,A.L. Kataev and S.A. Larin, Phys.Lett. **B273**, 141 (1991);
 ibid **B275**, 512 (1992) (Erratum).
- [71] H. Kawai, T. Kinoshita and Y. Okamoto, Phys.Lett. **B260**, 193 (1991).
- [72] R. Coquereaux, Phys.Rev. **D23**, 2276 (1981).
- [73] J. Kubo and S. Sakakibara, Z.Phys. **C14**, 345 (1982).
- [74] T. Kinoshita and W.B. Lindquist, Phys.Rev.Lett. **47**, 1573 (1981).
- [75] D.R.T. Jones, Nucl.Phys. **B75**, 531 (1974);
 W.E. Caswell, Phys.Rev.Lett. **33**, 244 (1974).

